FINAL REPORT

RESEARCH PROJECT HWY-2005-10

FHWA/NC/2006-03

Traffic Control Design for Portable Concrete Barriers

by

M. B. C. Ulker

M. S. Rahman, Ph.D. Professor

Department of Civil Engineering

North Carolina State University

and

A. Mirmiran, Ph.D. Professor

R. Zheng

Department of Civil Engineering

Florida International University

April 2006

Technical Report Documentation Page

1. Report No. **FHWA/NC/2006-03**	2. Government Accession No.	3. Recipient's Catalog No.
4. Title and Subtitle **Traffic Control Design For Portable Concrete Barriers**		5. Report Date **April 2006**
		6. Performing Organization Code
7. Author(s) **M.B.C Ulker, M. S. Rahman, A. Mirmiran, R. Zheng**		8. Performing Organization Report No.
9. Performing Organization Name and Address **Department of Civil Engineering North Carolina State University Campus Box 7908 Raleigh, NC 27695-7908**		10. Work Unit No. (TRAIS)
		11. Contract or Grant No.
12. Sponsoring Agency Name and Address **NC Department of Transportation Research and Analysis Group 104 Fayetteville Street Raleigh, NC 27601**		13. Type of Report and Period Covered **Final Report July 1, 2004 to Dec. 31, 2005**
		14. Sponsoring Agency Code **2004-05**
15. Supplementary Notes Project Monitor: Mustan Kadibhai, P.E.		

16. Abstract

The highway construction is among the most hazardous construction activities, with 39 deaths per 100,000 U.S. workers, as compared to only 6 deaths per 100,000 U.S. workers in all other industries (U.S. Bureau of Labor Statistics). Of this number, the highest fatality rate, which is approximately 23%, is due to workers being struck by vehicles intruding the work zones. In order to reduce this hazard portable concrete barriers are used to control the traffic and protect the work zones. In accordance with the standards developed by National Cooperative Highway Research Program (NCHRP), the NCDOT has been in the process of developing its own traffic control design manual since the applicability of the existing method of evaluating the displacements of the barriers (NCDOT plans to use F-type and the Oregon Tall F-type), is questionable. This investigation was undertaken to develop design aids for portable concrete barriers (PCB) to be included in the new NCDOT traffic control design manual. In this study the problem of vehicular impact on barriers are thoroughly investigated. The two available crash tests are modeled and impact response simulated through a finite element based program, ANSYS-LSDYNA. On the basis of the insight gained through these detailed numerical analyses and calibration of essential model parameters, a simpler program MSC Working Model is used to perform a comprehensive study of the barriers' response under vehicular impact. This leads to the development of a set of design curves for assessing the barrier displacement and related design variables. The finite element based modeling and simulation has been performed at North Carolina State University (NCSU), and the analyses using MSC Working Model and the development of design curves were carried out at Florida International University (FIU).

17. Key Words Crash test, traffic control, barriers, impact, safe work zone, back distance, F-type, modeling, simulation	18. Distribution Statement

19. Security Classif. (of this report) Unclassified	20. Security Classif. (of this page) Unclassified	21. No. of Pages 142	22. Price

Form DOT F 1700.7 (8-72) **Reproduction of completed page authorized**

Disclaimer

The contents of this report reflect the views and opinions of the author(s) and not necessarily the views of Universities (NCSU and FIU). The authors are responsible for the facts and the accuracy of the data presented herein. The contents do not necessarily reflect the official views or policies of either the North Carolina Department of Transportation or the Federal Highway Administration at the time of publication. This report does not constitute a standard, specification or regulation.

Acknowledgements

The authors extend sincere appreciation to the authorities of the North Carolina Department of Transportation (NCDOT) for funding this project. Thanks to the members of the committee for their support and advice. We wish to thank especially to Mr. Joseph Ishak, Mr. Stuart Bourne, Mr. Muhammed Mulla and Mr. Mustan Kadibhai in coordinating the progress made in every step of this project and answering our queries.

Thanks are due to Jim Day and Erkan Tekeli for their assistance in the use of the finite element software package, ANSYS/LS-DYNA.

Executive Summary

The highway construction is among the most hazardous construction activities, with 39 deaths per 100,000 U.S. workers, as compared to only 6 deaths per 100,000 U.S. workers in all other industries (*U.S. Bureau of Labor Statistics*). Of this number, the highest fatality rate, which is approximately 23%, is due to workers being struck by vehicles intruding the work zones. In order to reduce this hazard portable concrete barriers are used to control the traffic and protect the work zones. In accordance with the standards developed by National Cooperative Highway Research Program (NCHRP), the NCDOT has been in the process of developing its own traffic control design manual since the applicability of the existing method of evaluating the displacements of the barriers (NCDOT plans to use F-type and the Oregon Tall F-type), is questionable. This investigation was undertaken to develop design aids for portable concrete barriers (PCB) to be included in the new NCDOT traffic control design manual.

In this study the problem of vehicular impact on barriers are thoroughly investigated. The two available crash tests are modeled and impact response simulated through a finite element based program, ANSYS-LSDYNA. On the basis of the insight gained through these detailed numerical analyses and calibration of essential model parameters, a simpler program MSC Working Model is used to perform a comprehensive study of the barriers' response under vehicular impact. This leads to the development of a set of design curves for assessing the barrier displacement and related design variables.

The finite element based modeling and simulation has been performed at North Carolina State University (NCSU), and the analyses using MSC Working Model and the development of design curves were carried out at Florida International University (FIU).

Keywords: *Crash test, traffic control, barriers, impact, safe work zone, back distance, F-type, modeling, simulation.*

Table of Contents

List of Figures

List of Abbreviations and Symbols

ASTM	American Society of Testing and Materials
A(t)	Acceleration of the Barrier After the Impact
a	Acceleration of the Impacting Object
α	Deformation Variable
c	Velocity of the Impacting Body After the Impact
c_n	Impact Constant
δ	Time Increment
e	Coefficient of Restitution
E	Elasticity Modulus
ε'_p	Effective Plastic Strain
F	Force Applied to the Impacting Body
FHWA	Federal Highway Administration
f(t)	Reaction force produced at the surface of impact
g	Acceleration of Gravity
I	Impulse
m	Mass of the Object
m_v	Mass of the Simple Vehicle
m_b	Mass of the Barrier
μ	Friction Coefficient
μ_{dc}	Decay Coefficient
μ_d	Dynamic Friction Coefficient
μ_s	Static Friction Coefficient
NCAC	National Crash Analysis Center
NCDOT	North Carolina Depormant of Transportation
NCHRP	National Cooperative Highway Research Program
ODOT	Oregon Deparment of Transportation

ω	Angular Velocity
P	Momentum
PCB	Portable Concrete Barrier
ρ	Unit Weight
t	Time
v	Velocity of the Impacting Body Before the Impact
V	Relative Velocity of the Contacting Parts
V_{b2}	Velocity of the Barrier After the Impact
V_{v0}	Initial Velocity of the Vehicle
V_{v1}	Velocity of the Vehicle Before the Impact
V_{v2}	Velocity of the Vehicle After the Impact
V(t)	Velocity with Respect to Time
X_0	Initial Distance Between the Vehicle and the Barrier
X_d	Final Displacement of the Barrier
x	The Displacement of the Colliding Body
X(t)	Displacement-Time History of the Barrier

1 Background

1.1 Introduction

The NCDOT has been in the process of developing its own traffic control design manual. The existing section on temporary traffic barriers requires calculating deflection of free standing portable concrete barriers (PCB) using an impact severity formula based on the Kinetic Energy principle, as follows:

$$IS = \frac{1}{2} M (V \sin q)^2 \tag{1.1}$$

where *IS* is the impact severity in kilo Jules, *M* is the vehicle mass in kilograms, *V* is the vehicle speed in meters per second, and ? is the impact angle in degrees. The method calls for safe back distances of 1 foot to 6 feet depending on the impact severity, varying between 10 and 100 kilo Jules. The impact severity is determined from an existing table. The design method, although approximate, is neither simple nor user friendly. Moreover, its applicability to the NCDOT and the Oregon Type F barriers, which the NCDOT plans to use, is very much questionable.

Recent crash tests have shown the need for greater safe back distances of up to 9 feet for the NCDOT barriers. The safe back distance is a costly measure in construction projects, especially if more right of way, temporary pavement, detour, or more phases of traffic control sequence are required. The barriers are often placed in a narrow space along the construction area, parallel to the edge of retaining walls, or along a bridge deck under staged construction. The limited area behind the barrier should allow for its displacement under the impact of an errant vehicle. Optimum design of the space behind the barrier is therefore of great importance. On one hand, there is the issue of safety of the construction workers and the public. On the other hand, there is the issue of practicality and economic viability of highway construction projects in the State of North Carolina. Regarding the safety issue, it suffices to note that highway construction is among the most hazardous construction activities, with 39 deaths per 100,000 U.S. workers, as compared to only 6 deaths per 100,000 U.S. workers in all other industries (*U.S. Bureau of Labor Statistics*). Of this number, the highest fatality rate, which is approximately 23%, is due to workers being struck by vehicles intruding the work zones. In order to achieve a uniform level of safety, the National Cooperative Highway Research Program (NCHRP) has developed a comprehensive set of standards and procedures for evaluating the performance of permanent and temporary highway safety features in *Report 350*, "Recommended Procedures for the Safety Performance Evaluation of Highway Features" (Ross, et al. 1993).

The objective of this research is to develop design aids, i.e., design charts and tables, for portable concrete barriers (PCB) based on calibrated numerical analysis and rational design approach to be included in the new NCDOT traffic control design manual. Once the physical impact problem is modeled and calibrated against the recent crash tests on both the NCDOT traffic barriers and the Oregon Type F traffic barriers, it can be used to determine the safe back distance as well as the length of need for free standing portable concrete barriers under different design conditions, including barrier type, design speed, vehicle mass, lane configuration, and roadway geometry, i.e., tangent or curved segments with different radii of curvature.

In this study the problem of vehicular impact on barriers are thoroughly investigated. The two available crash tests are modeled and impact response simulated through a finite element based program, ANSYS-LSDYNA. On the basis of the insight gained through these detailed numerical analyses and calibration of essential model parameters, a simpler program MSC Working Model is used to perform a comprehensive study of the barriers' response under vehicular impact. This leads to the development of a set of design curves for assessing the barrier displacement and related design variables.

In the first chapter, a brief literature review about the current studies related with the impact mechanics and the modeling and analysis of crash simulations is presented. Then the current tools of analysis are introduced and defined in terms of available software and methods.

In the second chapter, the actual full scale crash tests are discussed. The available reports on the two crash tests are summarized in terms of the responses of the vehicle and the barriers. The appropriate tables and the figures of the vehicles and the barriers before and after the collision are also provided.

Chapter Three presents the concepts related to modeling and analysis of the impact of vehicle and barrier. The Finite Element Method and the MSC Working Model are described. Four different studies are performed to understand and verify the ANSYS/LSDYNA. For each study, appropriate analytical solutions are developed and the numerical results obtained from the software are compared with these solutions in terms of displacement, velocity and acceleration time-histories. For the last two verification study, additional graphs of maximum barrier displacement versus impact speed are also provided.

The finite element based modeling and simulation of the two actual full scale crash tests are presented in Chapter Four. The essential elements of the finite element modeling of crash simulations are described and the results for both of the simulations are presented and compared with the results of the crash tests and those obtained by MSC Working Model. The rigid body assumption for the barriers is also examined.

In Chapter Five, MSC Working Model based study is presented. For that, the MSC Models for both crash tests are introduced and the results of the parametric studies for these tests are presented in graphical forms. The essential design parameters along with their tabular summary are presented. In addition, the validation charts for the two crash tests are provided.

Chapter Six presents the design curves for the two types of barriers on two types of pavement. The maximum barrier deflections for different barrier lengths are presented to define the 'needed length'.

The summary, conclusions and recommendations are provided in Chapter Seven.

1.2 Literature Survey

1.2.1 General Impact Mechanics

The classical and simplest methods of impact analysis are based on the laws of conservation of momentum and conservation of energy (Huang, 2002). With the help of these laws, the change of velocity before and after the impact and the exchange of energy during the period of impact can be determined. Other external forces exerted on each body are considered to be negligible with respect to the impact induced forces.

Here, it would be useful to define the basic terms that are used in impact mechanics:

Momentum is a vector quantity pertaining to the motion of an object; its magnitude is the mass of the object times its velocity. The units of momentum are mass times velocity (kg.m/s). The symbol usually used for momentum is “P”. Impulse is a vector pertaining to a force; it is the integral of the force over a specified period of time. Usually, the time period is very short, as in the impact occurring during a crash. The units are the same as for momentum. The symbol used for impulse is usually an “I”.

The effect of an impulse on a body is a change in its momentum (a vector quantity) of the body: $\Delta p=I$. Then, for the momentum before and after an impulse, one can write:

$$p_B + I = p_A \tag{1.2}$$

When we consider the impulse and momentum for a single particle, for a body acted on by several forces, the forces can be summed vectorially, giving one resultant force. This produces an acceleration in the direction of the resultant force. Then, by using Newton’s Second Law:

$$\sum \vec{F}_i = m\vec{a} = m\frac{d\vec{v}}{dt} \tag{1.3}$$

Multiplying through by dt yields,

$$\sum \vec{F}_i\, dt = m\, d\vec{v} \tag{1.4}$$

Integrating: $\Sigma \int_{t_1}^{t_2} \vec{F}_i\, dt = m\int_{v_1}^{v_2} d\vec{v} = m\vec{v}_2 - m\vec{v}_1$, where $\vec{v}_i$ is the velocity at t_i. For a single particle, with an impulse acting on it, we have: $p_1+I=p_2$. This also can be stated as:

$$m\vec{v}_1 + \sum\int_{t_1}^{t_2} \vec{F}_i\, dt = m\vec{v}_2 \tag{1.5}$$

In the case of impulse and momentum for a system of particles, an expression can be stated where the velocity corresponds the velocity of the center of mass of the particles. There are both internal and external forces acting on each particle in the system. Internal forces are those exerted by other particles in the system. External forces are those produced by the elements not part of the system. For a vehicle the external forces are the force of the gravity, frictional forces arising from tires contacting the road, impact forces due to a collision with an obstacle, etc.

The equation of motion for a particle I in the system is:

$$\vec{F}_i + \sum_j \vec{f}_{ij} = m_i \vec{a}_i \tag{1.6}$$

The sum over j is for the internal forces associated with other particles. Summing up over all particles in the system gives:

$$\sum F_i = \sum m_i a_i \tag{1.7}$$

When we consider the two bodies of mass m_1 and m_2, respectively, the law of conservation of momentum requires that the momentum immediately before and after the impact can be written as,

$$m_1 x_1'(t) + m_2 x_2'(t) = m_1 x_1'(t+d) + m_2 x_2'(t+d) \tag{1.8}$$

and the law of conservation of energy requires,

$$\frac{1}{2} m_1 x_1'^2(t) + \frac{1}{2} m_2 x_2'^2(t) = \frac{1}{2} m_1 x_1'^2(t+d) + \frac{1}{2} m_2 x_2'^2(t+d) \tag{1.9}$$

Additionally, since the type of equations used to describe the impact of two or more bodies depend largely on the geometry of the bodies and the type of the impact, suitable simplifications are also needed to state general results. According to Tornambe (1996), impacts can be considered with the following three simplifications. First one assumes a quasi-static behavior during the impact. It means a transmission of all the stresses is said to be occur instantaneously to all points of the bodies involved in the impact. These impacts are called one degree of freedom impacts. This case is valid when the deformation takes place in the neighborhood of the point of impact and the centre of the mass of the deformed body is sufficiently behind the point of impact. In this assumption, a deformed body can be adequately defined as composed of rigid body whose mass is equal to the mass of the deformed body, and a flexible body whose mass is negligible. The second simplification assumes that all the stresses induced by the impact are well below the elastic limit that the plastic deformations are negligible. The third one is that the motion before, during and after the impact is adequately described by the motion of the centre of mass of each body involved in the impact. Before and after the impact of two movable bodies, the equations of motions are,

$$m_1 x_1''(t) = f_1(t) \tag{1.10a}$$

$$m_1 x_2''(t) = -f_2(t) \tag{1.10b}$$

During the period of impact the equations of motions of these two bodies are,

$$m_1 x_1''(t) = -f\,(x_1(t) - x_2(t) + r\,) + f_1(t) \tag{1.11a}$$

$$m_2 x_2''(t) = f\,(x_1(t) - x_2(t) + r\,) - f_2(t) \tag{1.11b}$$

where f(t) represents the reaction force produced at the surface of impact as a function of the deformation $\alpha \geq 0$. Even for perfectly elastic bodies the reaction force f(t) may not be a linear function of $\alpha \geq 0$ (α linear elastic reaction force happens only for a small deformation $\alpha \geq 0$). A general form of the reaction force f(t) as a function of deformation $\alpha \geq 0$ that can be used for the representations of many collisions is,

$$f\,(a\,) = c_n a^{\,n} \tag{1.12}$$

where n and c_n are constants: the linear elastic collisions are well characterized by n=1 and c_1= $E(r/2.46)^{1.5}$, while the Hertz elastic collisions are well characterized by n=1.5 and c_1 where E is the modulus of elasticity.

Glocker (2004), examined the three basic equations (the law of impact, kinematic compatibility and energetic consistency) under which a natural extension of the dynamics at an impact is possible without taking additional impact laws, and which additional assumptions have to be made to solve the impact for the different classes of systems. It was also shown that the Newton's law of impact for two colliding point masses can be derived from the concept of energy conservation and the principle of maximum dissipation. Also, it was assigned to single contact impacts in multibody systems as soon as the classical definition of perfect constraints was being extended to impulsive dynamics and unilateral contacts.

Huygens had been examining completely elastic collisions between two point masses since 1656. He recognized the fact that besides the conservation of momentum and kinetic energy, the relative motion of the two bodies has to be taken into account in order to be able to formulate a universally valid law of impact. His law v-V=C-c, describing the relative velocities during the elastic impact, is extended by Newton in 1687 by the restitution coefficient ε in order to accommodate possible losses of energy during the collision. Here v and V are the initial velocities of the two bodies before the impact, and the c and C are the velocities of the two bodies after the impact. By setting e=1 to the equation,

$$e(v-V)=C-c \quad (1.13)$$

Huygens' impact law for the elastic case is obtained, whereas e=0 describes the limiting case of maximum dissipation possible, such that the bodies do not separate after impact but keep moving with a common velocity. The restitution coefficient ε can be regarded as a measure of dissipated energy during the impact. However, if there would be more than one contact points, then one restitution coefficient won't be enough to clearly determine the post-impact velocities of all degrees of freedom since the distribution of kinetic energy is not known. Another difficulty consists in a widely spread misunderstanding of the restitution coefficients. Other than being material constants, they are the measure of dissipation concerning the chosen spatial discretization level of the mechanical system.

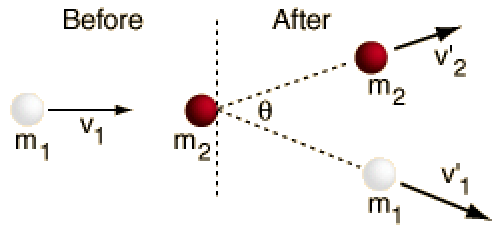

Figure 1-1 Typical elastic impact model

1.2.2 Modeling of Vehicle-Barrier Collision

Finite element models of vehicles have been increasingly used in preliminary design analysis, component design, vehicle crashworthiness evaluation, as well as road side hardware design. And also several studies have been made for the finite element modeling of vehicle-barrier collision. Since the mid-1970's, Lawrence Livermore National Laboratory has been heavily involved in the development and application of non-linear finite element codes for large deformations of structural materials. The results of these studies include DYNA (Logan and Tokarz, 1993), for the study of explicit transient dynamics problems of short duration, NIKE (Logan and Tokarz, 1993), for the study of long duration or quasi-static mechanics and TOPAZ (Logan and Tokarz, 1993), for thermal analysis. Logan and Tokarz (1993), also studied the crash and impact analysis at Lawrence Livermore National Laboratory. Their works resulted in numerous new code features and methodologies for this type of analysis.

Yonten et al., (2002) have used LS-DYNA which is a commercial finite element program for crashworthiness analysis that offers four major constitutive models for concrete. The performance of each of these models is assessed by making comparison between numerical simulations and some benchmark stress-strain data obtained from triaxial experiments conducted on plain concrete. Using the calibrated material models, a vehicular impact-crash scenario was simulated to investigate the prediction of these constitutive models for the concrete barriers subjected to vehicular impact. Different concrete material models produced different impact responses with respect to details. Figure 1-2 shows the finite element simulation of the crash tests by using these material models. The authors conclude that constitutive models of concrete are critical in the numerical simulations of roadside safety tests; the type of concrete material models used can influence the outcome of the analysis.

Yonten et al. (2002) described two crash scenarios and they were generated using the LS-INGRID preprocessor. In each case, the LS-DYNA3D input files of the truck and corresponding barrier models were combined using LS-INGRID for the specified impact configurations. They used the material models like; elastic, Blatz-K0 rubber, rigid, piecewise linear isotropic plastic material types for the detailed model of components of the truck like engine, transmission, mounts and radiator, cabin and rails. Their detailed model simulation results were consistent with the crash tests in terms of different levels of comparison. Furthermore additional simulations need to be performed using the variable time step integration to separate numerical errors from the modeling errors. The model could be further improved by exercising different impact configurations including side impact with the moving deformable barrier (MDB), offset head-on and angle impact with another vehicle, and impact into roadside narrow objects and barriers such as the vertical concrete wall and guardrail.

Another study was made by Merzhievsky and Resnyansky (1995). They analyzed the applicability of some most often used numerical models to describe and solve the high-velocity impact problems. In fact, a distinctive feature of the pioneering works on numerical simulation of high-velocity impact was that the authors tried to search for general physical regularities of the impact process and to validate the physical hypotheses for the determining role of specific parameters.

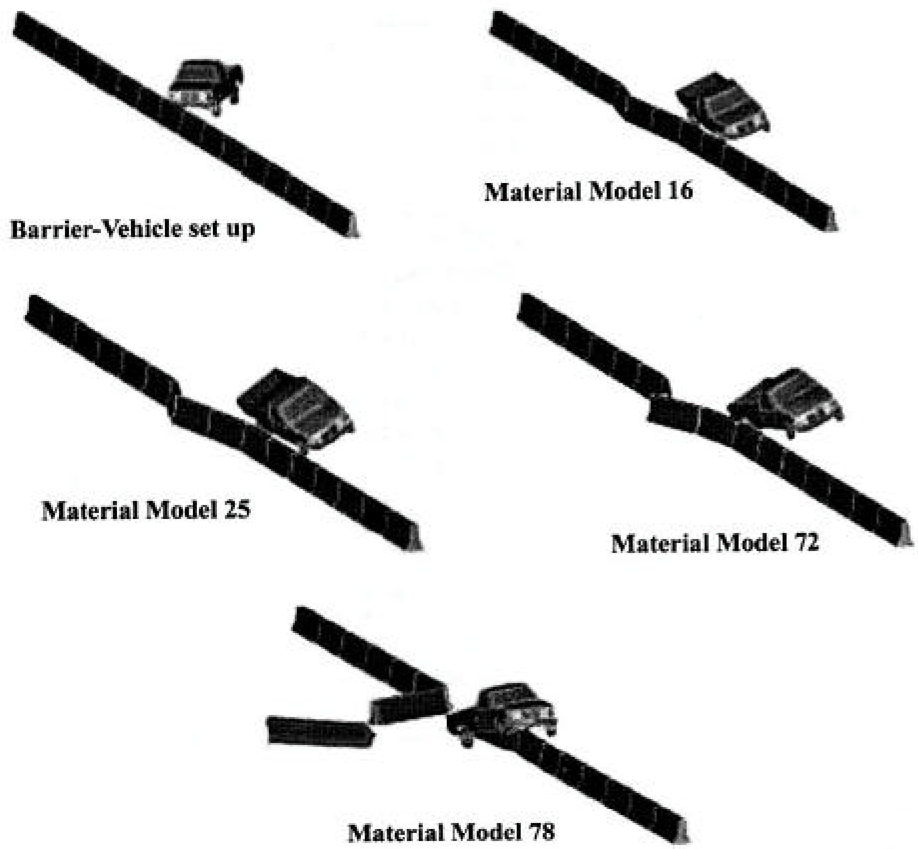

Figure 1-2 Finite element simulation of vehicle-barrier impact (Yonten et al., 2002)

Later, the numerical simulation of high velocity impact was aimed to develop more complicated methods and algorithms. In this way, the computer codes OIL (Dienes and Walsh, 1973), HEMP (Wilkins, 1967), MESA (Cagliostro et al., 1990) and CTH (McGlaun et al., 1990) were developed. Almost in all the methods the mathematical problems, such as, the problems of approximation and stability were well developed. Ultimately, a number of equivalent methods have been developed to calculate the flows of continua under intense loading accompanied by substantial high-velocity deformations. Basically, Merzhievsky and Resnyansky (1995) said that the further numerical investigation of the high-velocity impact processes requires the development of new more accurate models of material behavior to describe the dynamic deformation and displacement processes.

Another study on the simulation and modeling of vehicle-barrier collision was made by Tabiei and Wu, (1997) at the University of Cincinnati. Figure 1-3 shows the typical crash test and the corresponding simulation for a guardrail. The figure clearly shows how close the numerical simulation can predict the actual crash test.

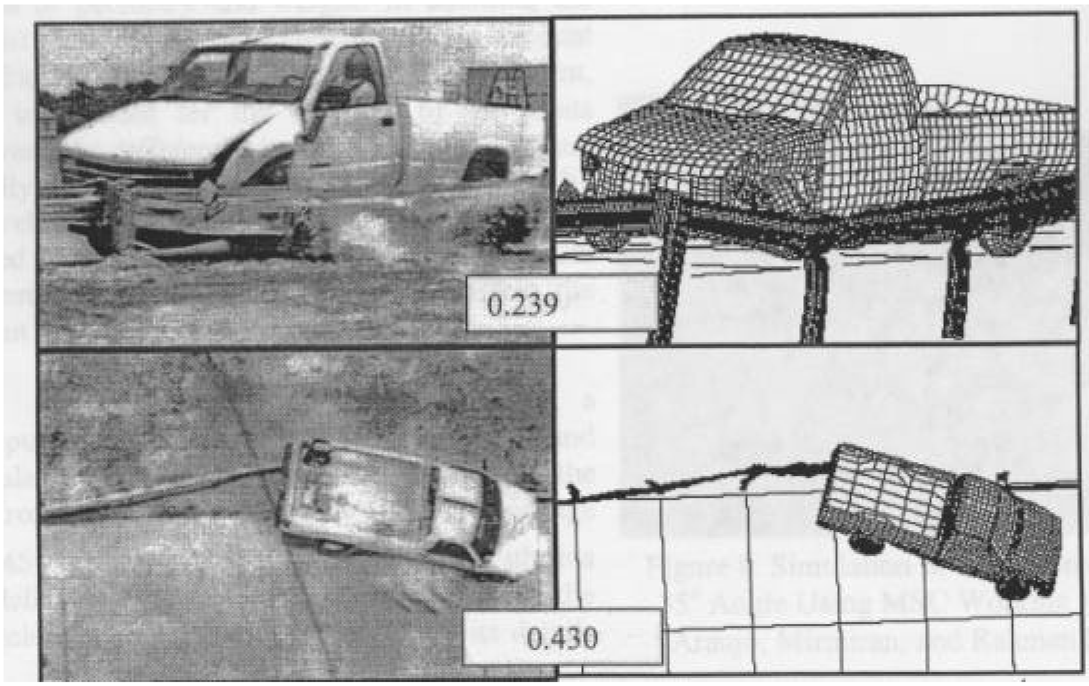

Figure 1-3 Typical comparison of crash test and simulation

A finite element model (FEM) was developed to analyze full frontal, frontal oblique and side impacts (Kirkpatrick, 2000). Mass geometry and physical characteristics of the vehicle and the major sub-components was modeled with a high degree of detail for the portions of the vehicle involved in full frontal impact, frontal oblique impact and side impact of the driver's side. Zaouk et al., (2002), described the results of non-linear FE computer simulations using a detailed multi-purpose FEM of a 1994 Chevrolet C-1500 pick-up truck for frontal full barrier and median highway barrier impacts. This model was developed to specifically address vehicle safety and compatibility issues, including frontal, side performance, new offset barrier tests as well as roadside hardware design and highway/vehicle safety issues.

Mizzi and Jezequel (1992), have proposed a system of rigid bodies to describe the crash behavior of passenger cars. They also used a method of observations by camera based on the introduction of control points. They proposed also a numerical procedure giving the absolute acceleration in a fixed frame from triaxial accelerometer sensor data. A non-parametric identification method using the kinematic data has been used by them to describe the dynamic behavior of vehicles. Regarding the deformability of barriers and vehicles and their initial conditions, current studies that prepare the design guidelines for the analysis by finite elements method, should take into account the possible amount of deflections during and permanent displacements after the impact. In the initial conditions, barriers which are connected to each other with movable joints are at rest and their initial velocity is zero; however, the vehicle has a certain initial velocity that affects the resulting permanent deflection and the damage of vehicle-barrier system. Additionally, the barrier system is subjected to friction at the interface with ground surface. Since the safety is the major concern in the design of the barrier system, evaluation of the post impact response of both the barrier and the pavement requires a design survey regarding this issue. In relation to the design of the barrier system, the important consideration is its deflection due to vehicular impact.

The crash simulations made by several commercial computer programs, are widely preferred methods in understanding the impact phenomenon. Also crash tests are being made but since they are extensive and costly, crash simulation is the appropriate choice. Typical analysis for vehicle-barrier crash test involves dynamic non-linear finite element simulation using a variety of codes such as LS-DYNA, (Logan and Tokarz, 1993), which is now integrated into the ANSYS finite element software package with extended pre and post-processing capabilities. The study regarding the simulation carried out by (Tabiei and Wu, 1997) clearly shows how close the numerical simulation can predict the actual crash test. It will be determined whether the impact problem can be modeled as a rigid body or as a combination of a rigid block and spring dashpot system. With these idealizations, the collision between the vehicle and the barrier will be able to formulated using the physics of impulse and momentum which were discussed before as the conservation of momentum with a definition of coefficient of restitution. Araujo et al. (2003), prepared design charts showing that the change in the deflection of the barrier with respect to the impact speed and impact angle. Consolazio et al. (2001), showed that by making extensive use of non-linear dynamic finite element simulation, several cycles of conceptual design refinement can be achieved by using simulation rather than expensive full scale crash testing. According to the LS-DYNA simulation results, Consolazio et al. (2001) decided to develop a portable concrete work zone barrier that could meet the following criteria;

- Crash Test Validation
- Portable and Modular
- Low Profile
- Minimal Anchorage
- Minimal Work Zone Intrusion

In order to design a barrier system that could achieve these issues with minimal crash testing costs, extensive use was made of the finite element simulation code LS-DYNA. At the end, several cycles of design iteration were performed based on computational simulation reducing the time and the costs associated with development and the testing of the system. Also some modifications to the NCAC C2500 reduced resolution pickup truck model were made to expand its applicability to impacts involving significant movement of the front suspension assemblies.

1.3 Tools of Analysis

1.3.1 ANSYS/LS-DYNA: Finite Element Method

In this study, the finite element based simulations of recent crash tests are made by using ANSYS/LS-DYNA. The simulations followed the guidelines of NCDOT (North Carolina Department of Transportation).

ANSYS/LS-DYNA combines the LS-DYNA explicit finite element program with the powerful pre and post-processing capabilities of the ANSYS program. The explicit method of solution used by LS-DYNA provides fast solutions for short-time, large deformation dynamics, quasi-static problems with large deformations and multiple nonlinearities, and complex contact/impact problems. Using this integrated product, one can model a structure in ANSYS, obtain the explicit dynamic solution via LS-DYNA, and review results using the standard ANSYS post-processing tools. It is also possible to transfer geometry and results information between ANSYS and ANSYS/LS-DYNA to perform sequential implicit-explicit / explicit-implicit analyses, such as those required for droptest, springback and other applications.

ANSYS/LS-DYNA is used predominantly for analyzing nonlinear phenomena found in crash and drop tests, sheet metal forming and catastrophic failures. This code provides extensive contact analysis options. Parallel processing methods are available to minimize the solution time on multiple CPUs.

ANSYS/LS-DYNA has a pre-processor, solution and a post-processor interface. A smart size mesh generation including complex 3-D meshing, a wide range of linear and non-linear material models (a total of 146), static and explicit dynamic solution modules are provided with the software. Some of the material models are piecewise linear plasticity, general visco-plasticity, honeycomb, inelastic spring discrete beam, etc.

ANSYS/LS-DYNA combines the premier software package for explicit non-linear structural simulation with one of the industry's most recognized and respected finite element pre and post-processors. It is the result of a collaborative effort between ANSYS Inc. and Livermore Software Technology Corporation (LSTC).

ANSYS can deal with limited-duration events (such as severe collisions) and large, permanent deformations. It helps engineers understand the elaborate combinations of non-linear phenomena found in crash tests, metal forging, stamping and catastrophic failures. ANSYS/LS-DYNA supports both 2-D and 3-D explicit elements and features an extensive set of single surface, surface to surface and node to surface contact as well as a contact analysis option that automatically creates the contact surfaces.

Explicit dynamics with ANSYS/LS-DYNA is beneficial to engineers who analyze problems involving contact, large deformations, non-linear materials, high frequency response phenomena or problems requiring explicit solutions. The researchers will be able to distinguish between problems that should be solved explicitly versus implicitly, identify and choose element types, materials and commands used in explicit dynamic analyses, perform all procedures for explicit dynamic analyses.

1.3.2 MSC-Working Model: Analytical Method

The MSC Working Model based simulations at FIU complements the work at NCSU, by focusing on developing design aids using the MSC Working Model's dynamic simulation engine that follows the Newtonian mechanics for rigid body impacts. In early 2003, Araujo, Mirmiran and Rahman (2003) simulated crash tests using MSC Model. Both the vehicle and the barriers were modeled accurately in the program in terms of geometry and weight. The models were created and run using MSC Working Model's dynamic simulation engine that applies real world Newtonian mechanics to desktop computer simulation.

A number of dynamics/kinematics applications have been analyzed in the literature and practice using the MSC Working Model. This is a conceptual design tool that allows simulations instead of rough energy calculations. The software has been used to test new design for side tip stability of cranes by varying both the boom load and the platform counter-weight. In another application, NASA has used this software to improve passenger survivability in predicting their crash tests. Since by definition the crash tests are destructive, they are the last tests performed on many prototype aircraft employing new construction techniques or structural materials. Other times, makes of military and commercial aircraft presently in service are tested to re-create conditions from actual crashes to learn how survivability might have been improved. Most relevant applications of the program have been in accident reconstruction simulation as well as crash test simulations with construction equipment.

2 Crash Tests

2.1 Introduction

A full scale crash test, of course, is the most reliable way to study the nature of vehicle-barrier impact. In relation to the problem being studied, several crash tests have been made. In these crash tests, the main elements are the vehicle and the portable concrete barriers connected to each other with a specific joint model. Portable Concrete Barriers (PCB), which are made of precast concrete safety shape sections joined together to form a continuous longitudinal barrier which has greatly improved safety in construction work zone. Because portable concrete barriers are primarily intended to keep errant vehicles from hitting construction workers, the dynamic lateral deflection of these barriers must be kept to minimum.

The Karco Engineering conducted several numbers of crash tests with two types of barriers at test facility in Adelanto, California. The objective of these crash tests was to determine if the tested free-standing, unanchored, concrete median barrier system meets the minimum performance standards of the National Cooperative Highway Research Program Report 350 (NCHRP 350) test level 3 guidelines.

Appel et al. (1994), applied several crash tests to passenger cars and determined the results regarding the impact conditions. They concluded that global crash evaluation techniques must cover and evaluate both self-protection and the compatibility of passenger cars. According to the results a deformable fixed barrier has the potential feature of being able to combine all frontal tests in a single test, in which the compatibility is simultaneously tested. A safe design of barrier requires mainly the following:

(i) No structural failure of the concrete barrier

(ii) No excessive displacement of the barrier

(iii) Occupant impact velocity and ride-down acceleration.

In terms of underlying mechanics the problem at hand involves a collision between two deformable bodies: the vehicle and the barrier system. In their initial conditions, the barrier system is at rest while the vehicle is moving at certain velocity. In addition to the forces of impact, the barrier system is subjected to a friction force between the barrier and the pavement. The evaluation of the post-impact response of both the barrier and the vehicle is needed to ensure a safe design. The parameters that will be considered in the crash simulation and the analysis are:

- Impact angle,
- Impact speed,
- Coefficient of friction between barriers and ground, vehicle and ground,
- Coefficient of restitution of vehicle,
- Weight of vehicle, and
- Spring constants

In relation to the design of the barrier system, one important consideration is its displacement due to vehicular impact. The amount of displacement depends on the velocity of the vehicle, friction force between the structures, the dimensions and weight of the vehicle and the dimensions and the strength of the precast concrete barriers. The deflection should be between certain values and must not exceed a required value that would possibly cause an extra damage to other structure placed close to barrier system. In order to avoid some extra problems that could result from the excessive barrier deflection, this issue will also be taken into account.

In this part of our study, we are focusing on the following two crash tests to be simulated by the available tools mentioned previously. These crash tests have been done on two different types of PCBs which are NCDOT F Type and ODOT Tall F type.

2.2 NCHRP 350: Guidelines For The Crash Tests And The Required Performance Criteria

In order to achieve a uniform level of safety, the National Cooperative Highway Research Program (NCHRP) has developed a comprehensive set of standards and procedures for evaluating the performance of permanent and temporary highway safety features in Report 350, "Recommended Procedures for the Safety Performance Evaluation of Highway Features" (Ross, et al. 1993). The Federal Highway Administration (FHWA) has required that by no later than October 2002, states must confirm that their safety features are acceptable under these new standards.

NCHRP 350 provides the guidelines for the crash tests and the required performance criteria, depending on the feature being evaluated. There are up to six test levels that can be selected. In general, the lower test levels are applicable for evaluating features to be used on lower service level roadways and certain types of work zones while the higher test levels are applicable for evaluating features to be used on higher service level roadways or at locations that demand a special, high performance safety feature (Ross, et al. 1993).

FHWA specified that a Test Level 3 crash test-Test Designation 3-11 must be performed on both the Standard F-shape and the Tall F shape barriers. This test calls for crashing a 2000 kg (4400 lb) pickup truck into the barrier at 100 km/hr (62 mph), at an angle of 25 degrees from parallel. A total length of 61 m (200 ft) of barrier is required for the test with the vehicle impact occurring approximately at the middle of the run. The evaluation criteria for this test can be found in (Ross, et al. 1993). For a temporary barrier, it would not normally be designed for impact conditions greater than test level 3 except under very unusual conditions. It should perform acceptably using the 820C and 2000P type vehicles with all appropriate tests. The evaluation criteria for this test are as follows (Ross, et al. 1993):

“A. Test article should contain and redirect the vehicle; the vehicle should not penetrate, underride or override the installation, although controlled lateral deflection of the test article is acceptable.

D. Detached elements, fragments or other debris from the test article should not penetrate of show potential for penetration the occupant compartment, or present an undue hazard to other traffic, pedestrians of personnel in a work zone. Deformations of, or intrusions into, the occupant compartment that could cause serious injuries should not be permitted.

F. The vehicle should remain upright during and after collision, although moderate roll, pitching and yawing are acceptable.

K. After collision it is preferable that the vehicle’s trajectory not intrude into adjacent traffic lanes.

L. The occupant impact velocity in the longitudinal direction should not exceed 12m/sec, and the occupant ride down acceleration in the longitudinal direction should not exceed 20 Gs.

M. The exit angle from the test article preferably should be less than 60 percent of the test impact angle, measured at time of vehicle loss of contact with test device."

In addition to those criteria, when portable concrete barrier is used in work zones to separate traffic in high-occupancy vehicle lanes, special attention should be paid to lateral deflection it undergoes during a vehicular impact. Because the amount a given installation can deflect without adverse consequences depends on site conditions, it is not feasible to establish limiting deflection values for crash tests of these barriers. Rather, it is important to accurately measure and report barrier displacement that occurs during the test so that a user agency can make an objective assessment of the appropriateness of the barrier for its intended application.

2.3 NCDOT F-Type PCB - Ford F-250 Pickup Truck Crash Test

The North Carolina Department of Transportation (NCDOT) has been using several types of barriers. Recently on the basis of a crash test, a specific barrier was accepted by FHWA. The accepted barrier is a standard 810-mm (32-in) high F-shape portable barrier in segment lengths of 3.0 m (10 ft). The base width is 610 mm (24 in) and the barrier tapers to a 150-mm (6 in) top width. All dimensions and other properties of the NCDOT barrier can be seen in Figure 2-1.

The aim of crash tests is to provide the vehicle manufacturer, the legislative authorities, the public and the customer with evidence on the safety design, determine approval for the market and also enable comparative safety evaluation. Until now, there has been several full scale crash tests made in order to understand the real mechanism of vehicle-barrier impact. California State Transportation Department applied several crash tests at the Caltrans Dynamic Test Facility in West Sacramento. The test area was a large, flat, asphalt concrete surface and according to the technical report (Jewel and Weldon, 1999), there were no obstructions nearby except for a 2 m high earth berm at 40 m downstream from the barrier in test 551. The test vehicles were 1989 Chevrolet 2500 and 1994 Geo Metro which were in good condition, free of major body damage and without missing structural parts. All of them had standard equipment and front-mounted engines and their inertial masses were within recommended limits. The pickups were self-powered and a speed control device limited acceleration once the impact speed had been reached. The

Geo Metro was connected by a steel cable to another vehicle and towed to impact speed. A short distance before the point of impact, each vehicle was released from the guidance rail and the ignition was turned off. A detailed description of the test vehicle equipment and guidance systems is contained in that report.

2.3.1 Crash Test Report

A 1994 Ford F-150 pickup was used for this crash test. Test inertia weight and its gross static weight was 1993 kg. The height to the lower edge of the vehicle bumper was 392 mm and it was 625 mm to the upper edge of the bumper. Additional dimensions and information about the vehicle can be seen in Figure 2-2. The vehicle was directed into the installation using the tow system and was released to be freewheeling and unrestrained just prior to impact. Figure 2-3 shows the initial position of the vehicle.

The test was performed in the morning of January 4, 2002. The pavement was dry. The vehicle traveling at 100.4 km/h impacted the PCB at 25 degrees, 1.2 upstream of the joint between number 7 and 8. At approximately 0.04 sec after impact the vehicle was traveling parallel with the barrier. The rear contacted the barrier at approximately 0.104 sec after impact. The rear extended over the test barriers 1.7 m and returned to the impact side after approximately 18 m. The vehicle later came to rest 68.1 m longitudinally and 12.8 m laterally from the impact point. After the test none of the barrier segments or pin and loop connections appeared to fail. Three of the barrier segments had small pieces of concrete chipped from them during the impact-segment 6 in the center between the lift openings; segment 7 at the upstream, lower corner; and segment 8 upstream from the lift opening. A maximum static deflection of 1.54 m was recorded at the downstream end of segment 7 at joint 7-8. Segment 5 through segment 10 were disturbed with static deflections varying from 0.04 m to 1.5 m. The post impact conditions of the vehicle and the barrier article are shown in Figure 2-4 and 2-5.

The vehicle sustained moderate damage primarily to the right front. Structural damage included deformation to the right frame rail, right rod ends and right side I-Beam suspension components. There has also been damage to the front bumper, grille, right headlight, right front fender, rear right outer body panel and both right side tires and rims. The maximum occupant compartment deformation was 12 mm at the right floorboard.

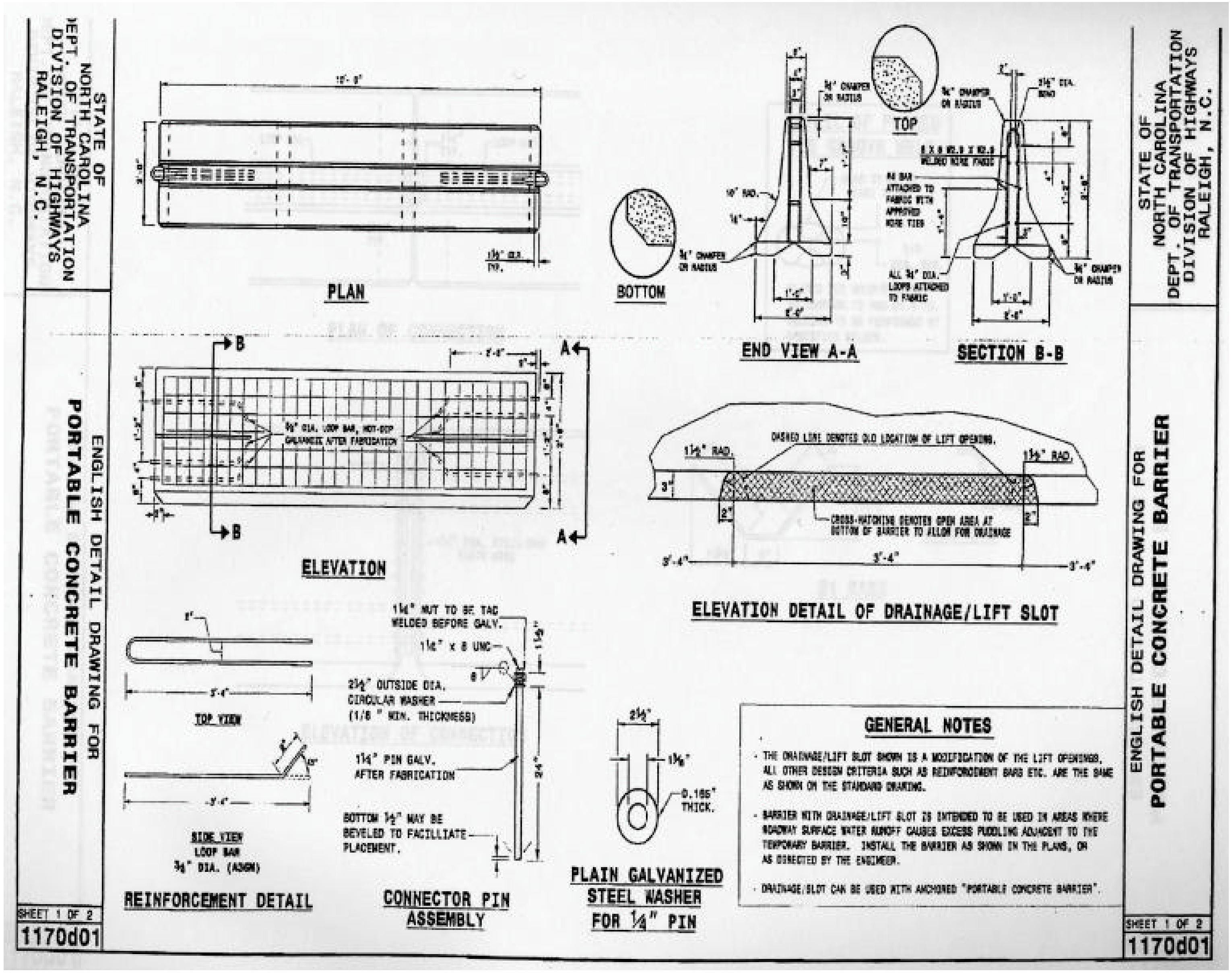

Figure 2-1 Design specifications for the NCDOT Barrier

Date: 01/04/02 **Test No.:** 020104 **VIN No.:** 1FTDF15Y2RNB19494

Year: 1994 **Make:** Ford **Model:** F-150 P/U

Tire Inflation Pressure: FR: 35psi RR: 41 psi **Odometer:** 224,752 **Tire Size:** LT235/75R15

Mass Distribution (kg): **LF:** 502.4; **RF:** 521.2; **LR:** 494.6; **RR:** 474.8

Describe any damage to vehicle prior to test:

Upper center portion of windshield was cracked, tailgate was dented and the body had various scratches and minor dents.

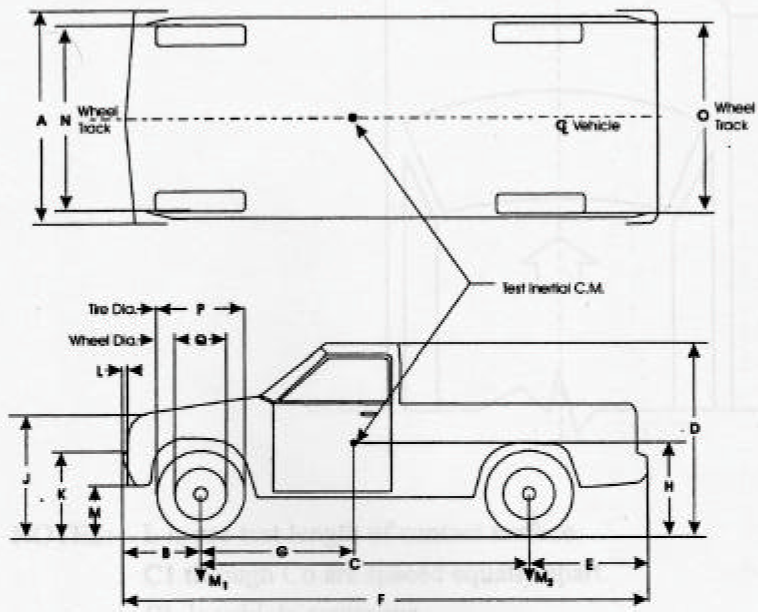

Engine type: 6-cylinder, straight, inline (longitudinal)

Engine CID: 4.9 liter

Transmission Type:

_X_ Auto

___Manual

Optional Equipment:

None

Dummy Data:

Type: N/A

Mass: N/A

Seat Position: N/A

Geometry - (cm)

A	195.1	E	131.0	J	104.0	N	162.8	R	N/A
B	85.6	F	512.2	K	62.5	O	163.9	S	N/A
C	297.5	G	144.7	L	41.0	P	69.5	T	N/A
D	181.4	H	N/A	M	39.2	Q	41.0	U	N/A

Mass - (kg)	Delivered Weight	Test Inertial	Gross Static
M_1	1073.5	1023.6	1023.6
M_2	803.5	969.4	969.4
M_T	1877.0	1993.0	1993.0

Figure 2-2 Vehicle properties for the crash test of NCDOT

Figure 2-3 Vehicle position prior to impact

Figure 2-4 Vehicle condition after impact

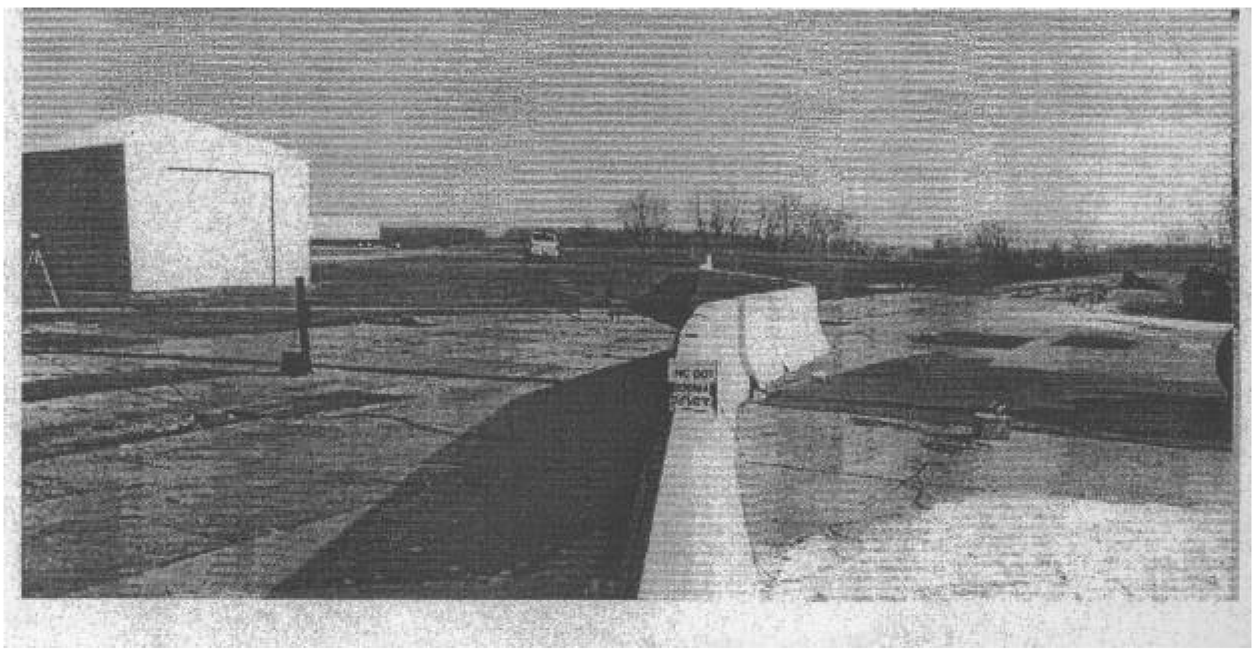

Figure 2-5 Orientation of the barrier segments after the impact

2.4 ODOT F-Type PCB –Chevrolet Pickup Truck Crash Test

The second crash test that we are focusing on is ODOT Tall F-type PCB-Chevrolet pickup truck crash test. For F-shape barriers, Oregon DOT F shape precast concrete barrier has minimum "Maximum Deflection" of 760-mm (30 in.) during NCHRP 350 test 3-11. In general, barrier deflection can be minimized by using longer and heavier barrier segments and by using joints that can develop a bending moment of 6913 kg-m (50 kip-ft) or more. Pulling the barrier segments tight and anchoring the end segments to the ground are also very helpful in reducing the lateral deflection. Anchoring each barrier segment with steel pin driven into the ground is very effective, but it makes the barrier less portable and labor-intensive.

2.4.1 Crash Test Report

This crash test was conducted on June 19, 2001. The test article was the Tall F-shape precast concrete barrier (Figure 2-6, 2-7, 2-8) with bolted "C-shape" connection. Twenty barrier segments, totaling 61 m (200 ft) were placed in a line and connected together. The line of barriers was placed at angle of 25 degrees. There weren't any anchorages used for the connection of the barrier to the ground but the string of barriers was placed directly onto the surface of asphalt concrete. The test vehicle was a 1995 Chevrolet Cheyenne ¾ ton pickup (Figure 2-9, 2-10) with a gross static weight of 2024 kg (4462 lb). This weight was within the allowable range of ± 5 kg as specified in NCHRP Report 350. At the point of impact the vehicle had achieved a 102.38 km/h (63.6 mph) speed. This velocity was within the allowable range of ± 4 km/h as specified in the Report 350. ODOT recently adopted a "Tall F-shape" precast concrete barrier for use on highways which carry large volumes of trucks. The higher barrier – 1065 mm (42 in) in height – is intended to provide more safety on the roadway, by better managing the impact of larger vehicles than the smaller barrier. Each barrier section is 3.0 m (10 ft) in length. The barrier sections are held together with a 25 x 760 mm (1 x 30 in) bolt and perforated C-shape assembly.

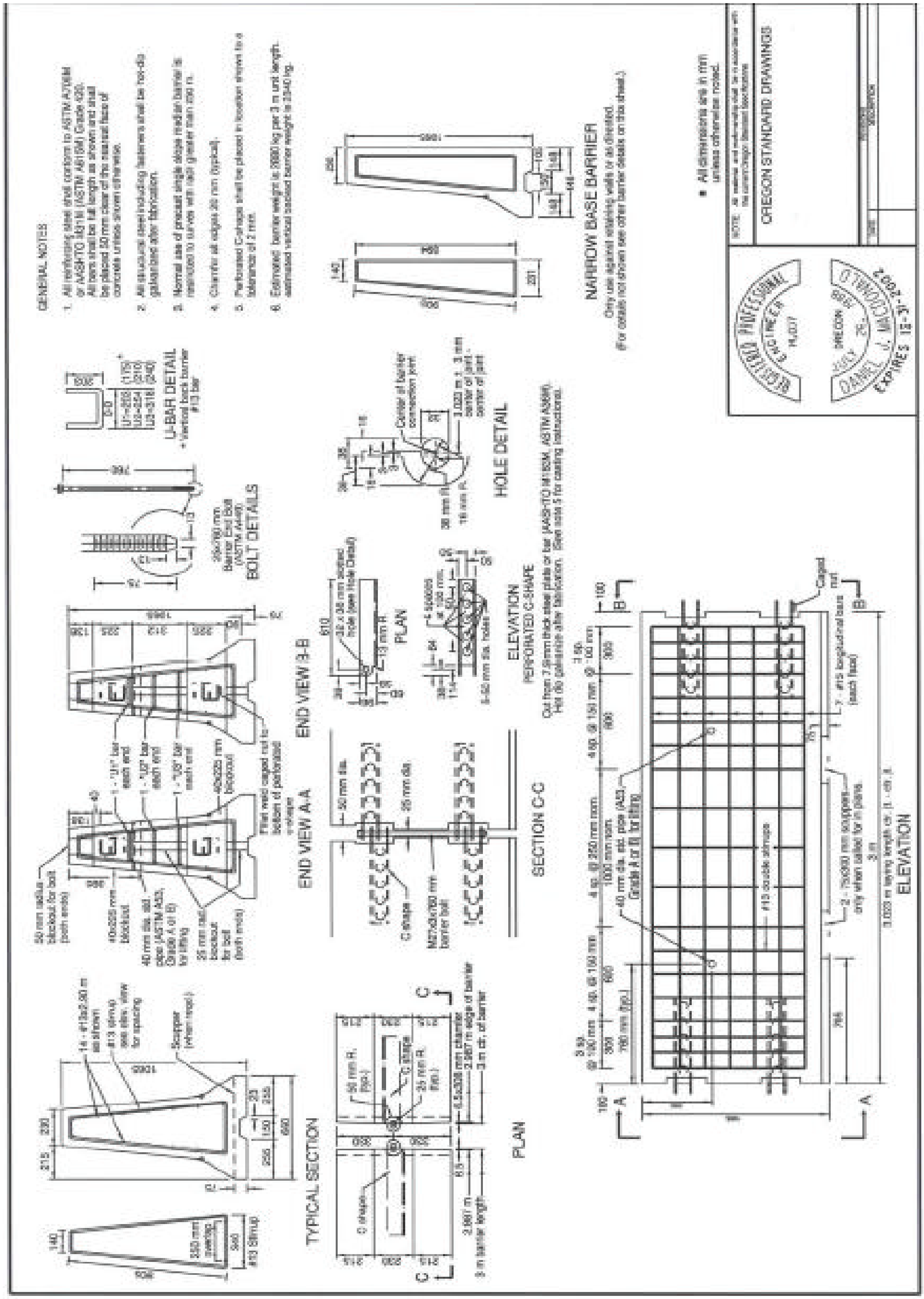

Figure 2-6 Design specifications for the Tall F-Shape Barrier (MacDonald and Kirk, 2001)

Figure 2-7 Tall F-Shape portable concrete barrier 42” high, 10 ft long

Figure 2-8 ODOT Tall F-Shape portable concrete barrier and joints

DATA SHEET NO. 1

VEHICLE PROPERTIES FOR TEST NO. 3-11

DATE	06/18/01	COLOR	WHITE	VIN	1GC6C24K8SE197292
YEAR	1995	MAKE	CHEVROLET	MODEL	CHEYENNE TRUCK
TIRE PRESSURE (psi)	45/80	ODOMETER (mi.)	289044	TIRE SIZE	LT245/75 R16E
ENGINE	FRONT	CYLINDERS	8	DISPLACEMENT	5.7 LITER
TRANSMISSION	4-SPEED	AUTOMATIC	YES	MANUAL	NO
DESCRIBE ANY DAMAGE TO VEHICLE PRIOR TO TEST:			BROKEN REARVIEW MIRROR, DENTS & SCRATCHES IN DOORS,		
BED IS SHIFTED TO RIGHT FROM PREV. CRASH, MINOR DAMAGE TO LEFT REAR FENDER UNDER TAIL LIGHT.					

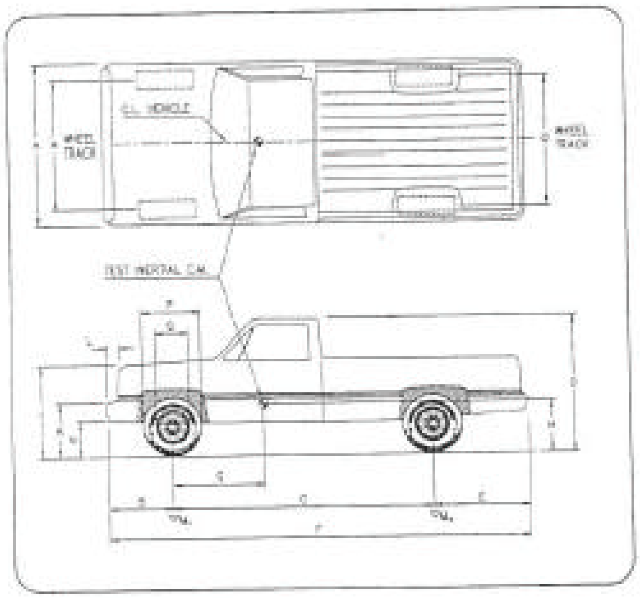

TEST VEHICLE GEOMETRY (mm)							
A	880	E	1330	J	1075	N	620
B	860	F	5518	K	650	O	620
C	3328	G	1963	L	98	P	760
D	1830	H	760	M	500	Q	445

MASS DISTRIBUTION							
LEFT FRONT	539 kg (1188 lb)	RIGHT FRONT	584 kg (1288 lb)	LEFT REAR	480 kg (1058 lb)	RIGHT REAR	421 kg (928 lb)

MASS (kg)	CURB	TEST INERTIAL	GROSS STATIC
FRONT AXLE	1193 kg (2630 lb)	1123 kg (2476 lb)	1123 kg (2476 lb)
REAR AXLE	973 kg (2144 lb)	901 kg (1986 lb)	901 kg (1986 lb)
TOTAL VEHICLE	2165 kg (4774 lb)	2024 (4462 lb)	2024 (4462 lb)

Figure 2-9 Vehicle properties for the crash test of Tall F-Shape PCB (MacDonald and Kirk, 2001)

Figure 2-10 Chevrolet pickup truck

The number of longitudinal barriers that were tested was 20. Each test article was a 1035 mm (3.393 ft) high F-Shape with a 660 mm (2.16 ft) wide base and a 230 mm wide top. Barrier segments were 3023 m (9911 ft) long and were connected with 79 mm (3.11 in.) thick perforated C-chaps that when meshed with opposing ends forms eight points of connection. Connecting the C-shapes was a 27 x 3 x 760 mm (1.06 x 0.118 x 30.0 in.) barrier end bolt confirming to ASTM A449. The allowable gap between matched barrier ends was 25 mm (0.98 in.). The point of impact occurred on barrier segment #10, approximately 150 mm (6 in) upstream of the joint between segments #10 and #11. As shown in Figure 2-11, the barrier segments were deflected from the impact and the maximum deflection was 813 mm (32 inches), with no perceptible rebound.

The test results, as provided by KARCO Engineering, are summarized in Table 2-1. As shown in the table, the Tall F-shape barrier passed all of the NCHRP requirements. Again, the terrace was judged not to have had a material effect on the outcome of the test. Thus the crash test of the Tall F-shape barrier was judged to be successful. The summary of the test can be seen in Figure 2-12.

Figure 2-11 Deflected shape of ODOT barriers

Table 2-1 Crash test results for ODOT Tall F Shape Barrier

Parameter	Result	NCHRP Requirement
Vehicle containment & redirection	Pass	Vehicle redirection in a controlled manner; no underride or override allowed.
Debris from the impact	Pass	No debris from the impact should present a hazard to occupant compartment or others.
Occupant compartment	Pass	No hazardous deformation or intrusion of the occupant compartment
Vehicle attitude	Pass	Vehicle should remain upright; moderate roll, pitch and yaw acceptable
Occupant impact velocity longitudinal direction	X: -6.22 m/sec Y: 5.08 m/sec	Allowable, not to exceed 12 m/sec
Occupant ridedown acceleration longitudinal direction	X: -19.36 G Y: 12.25 G	Allowable, not to exceed 20 G
Vehicle exit trajectory	12 degrees	Preferred not to exceed 60% x 25 = 15 degrees
Maximum barrier deflection	813 mm (32 inches)	No NCHRP requirement; ODOT requirement: 914 mm (36 in)

DATA SHEET NO. 2

SUMMARY OF RESULTS FOR TEST NO. 3-11

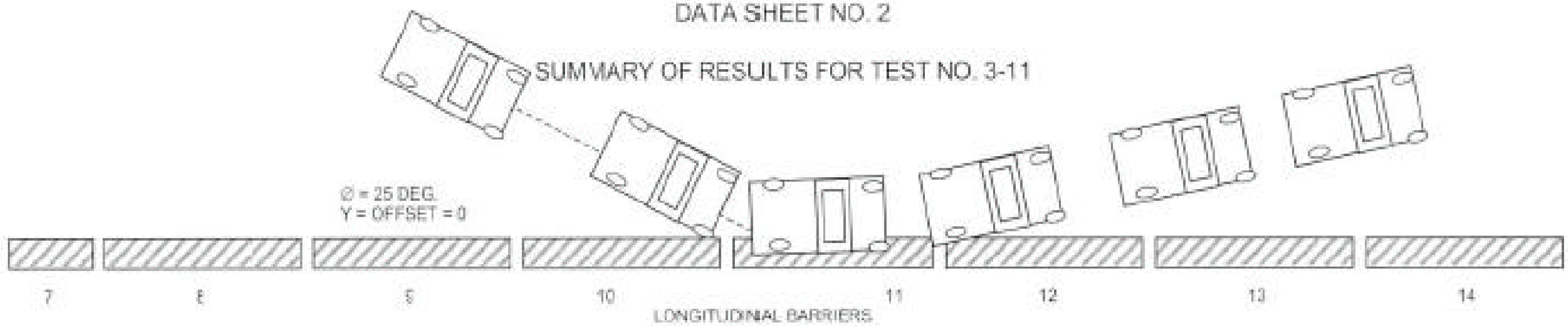

GENERAL INFORMATION	
TEST AGENCY	KARCO ENGINEERING
TEST NO.	3-11
DATE	06/19/01
TEST ARTICLE	
TYPE	LONGITUDINAL BARRIERS
INSTALLATION LENGTH (m)	60.96 m (200 ft.) precast concrete
SIZE AND/OR DIMENSION OF KEY ELEMENTS	3.023 m (9 ft 11 in.)
SOIL TYPE AND CONDITION	N/A
TEST VEHICLE	
TYPE	PRODUCTION
DESIGNATION	2000P
MODEL	1995 CHEVROLET PICKUP TRUCK
MASS (CURB)	2165 kg
MASS (TEST INERTIAL)	2024 kg
DUMMY(s) MASS	N/A
GROSS STATIC WEIGHT	2024 kg
IMPACT CONDITIONS	
SPEED (km/h)	102.38 km/h (63.62 mph)
ANGLE (Deg.)	25°
IMPACT SEVERITY (kJ)	N/A
EXIT CONDITIONS	
SPEED (km/h)	81.00 km/h (50.34 mph)
ANGLE (Deg.)	12°

OCCUPANT RISK VALUES	
IMPACT VELOCITY (m/sec)	
X-DIRECTION	-6.22 m/sec
Y-DIRECTION	5.08 m/sec
THIV (optional)	N/A
RIDEDOWN ACCELERATION (g's)	
X-DIRECTION	+ 10.10 to -19.36
Y-DIRECTION	+ 12.25 to -8.58
PHD (optional)	N/A
ASI (optional)	1.405
TEST ARTICLE DEFLECTIONS (m)	
DYNAMIC	32 in.
PERMANENT	32 in.
VEHICLE DAMAGE	
EXTERIOR	
VDS	n/a
CDC	n/a
INTERIOR	
OCDI	n/a
POST IMPACT VEHICULAR BEHAVIOR	
MAXIMUM ROLL ANGLE (Deg.)	+ 16.04 to -11.49
MAXIMUM PITCH ANGLE (Deg.)	+ 23.07 to –1.12
MAXIMUM YAW ANGLE (Deg.)	+ 0.41 to -32.54

Figure 2-12 Summary of the crash test results of Tall F-Shape Barrier (MacDonald and Kirk, 2001)

It has been noted some minor spalling of concrete at the joint where impact occurred. None of the connecting bolts failed or was bent. The Principal Investigator requested that KARCO make special note in the report of the disassembly of the system, with regard to potential difficulties of bent bolts and their removal. KARCO personnel reported that they had no major problems taking the system apart, only the need to realign some of the segments so that the bolts could be turned easier.

At the end of the test, the vehicle sustained major damage to the passenger side bumper, right front fender and right front wheel as a result of the impact with the redirected longitudinal barriers. It sustained moderate damage to the grill, hood and passenger side door. It received slight damage to the driver side door and driver side front fender, as well as the loss of both front tires and passenger side turn signal and headlights. The windshield suffered slight damage, but did not interfere with the driver's vision. The vehicle sustained negligible deformation to the roof. Maximum vehicle crush at the bumper height was indeterminate.

3 Modeling and Analysis of Vehicle Barrier Collision

3.1 Introduction

Modeling and analysis of vehicle-barrier collision has been an important consideration in relation to the roadside safety. As it was also mentioned previously, the barriers need to be designed such that they can withstand severe impacts from vehicles. In this study, our primary focus is on the displacement of the barrier. Considering the situation of a typical barrier assembly resting directly on the surface of a pavement, we can represent the essential features of the problem by the following sketch:

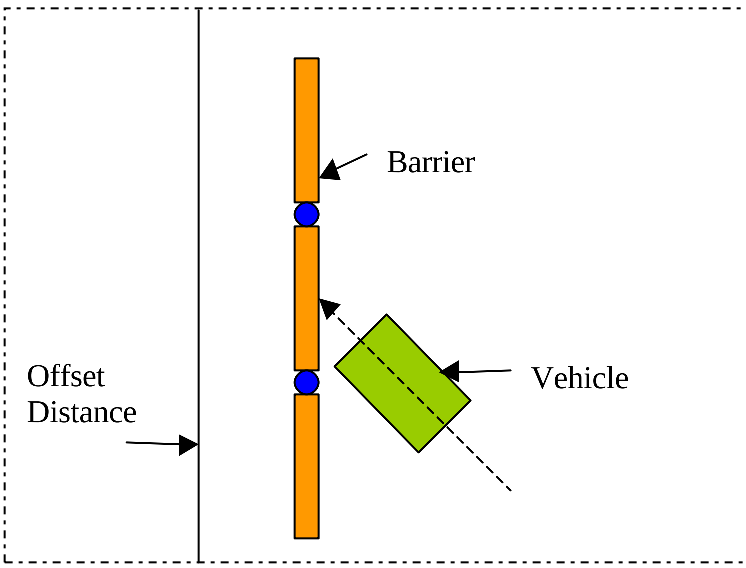

Figure 3-1 Essential features of the problem

3.2 Finite Element Modeling

The finite element modeling procedure for the explicit dynamic analysis consists of three main steps:

1. Building the model,

2. Application of loads and obtaining the solution,

3. Visualization and interpretation of the results.

In this procedure, firstly, we built the solid model that represented the physical system to be analyzed. For that, we used the PREP7 preprocessor of ANSYS/LS-DYNA. In the preprocessor, basically we performed the following tasks step by step:

1. Definition of the element types and real constants

2. Specification of material models

3. Definition of the model geometry

4. Meshing the model

5. Definition of contact surfaces

After defining the geometry, we built the finite element model by discretizing the barrier and vehicle parts. Figure 3-2 shows an illustration of a typical FE model of vehicle and barrier system.

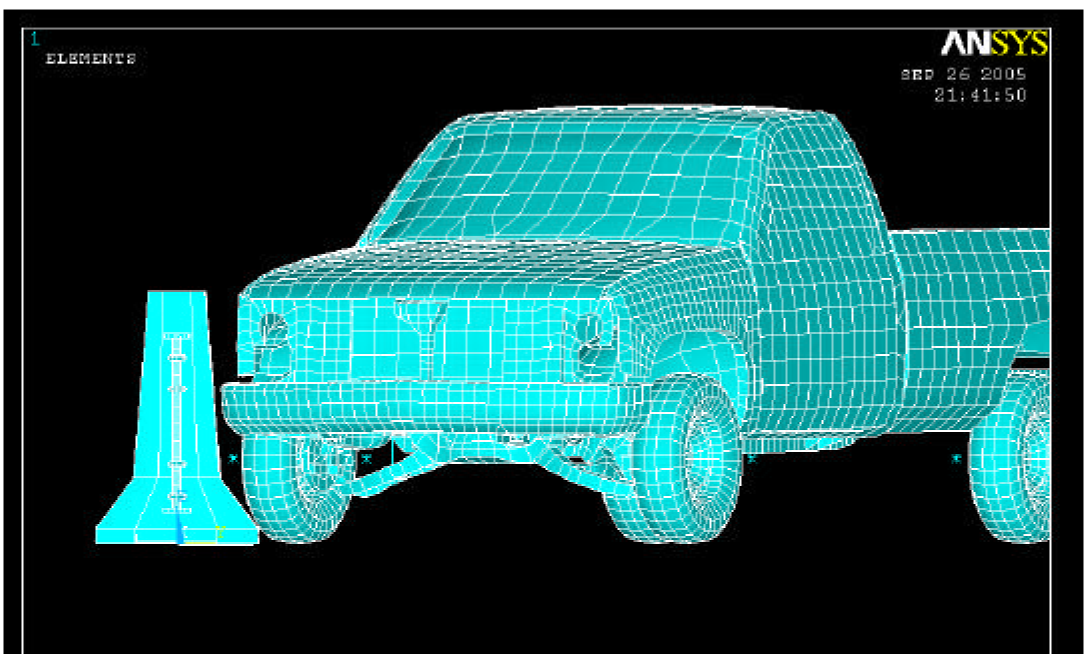

Figure 3-2 FEM of vehicle and barrier

3.3 MSC Working Model

Since our concern is the maximum barrier displacement obtained after the impact, it would be appropriate to model the vehicle as a rigid body which makes the analysis numerically accurate enough and computationally cheap and effective.

The most important factors in modeling the vehicle and the barrier are the geometry and weight, both of which are accurately modeled. In addition, the model requires three coefficients; one to account for friction between the barrier and the pavement, one to account for the stiffness of the joints between the different segments of the barrier, and finally, one to account for the energy absorbed by the vehicle during the impact. The latter, which is called coefficient of restitution, is of great importance, since its magnitude can affect the extent of deflection of the barriers. Figure 3-3 shows the application of MSC Working Model for simulation of the traffic barrier impact. The safe back distance of 6 ft (72 in) is shown as a solid line parallel to the initial line of the barrier chain, only as a guide. Both the vehicle and the barriers are modeled as individual rigid bodies.

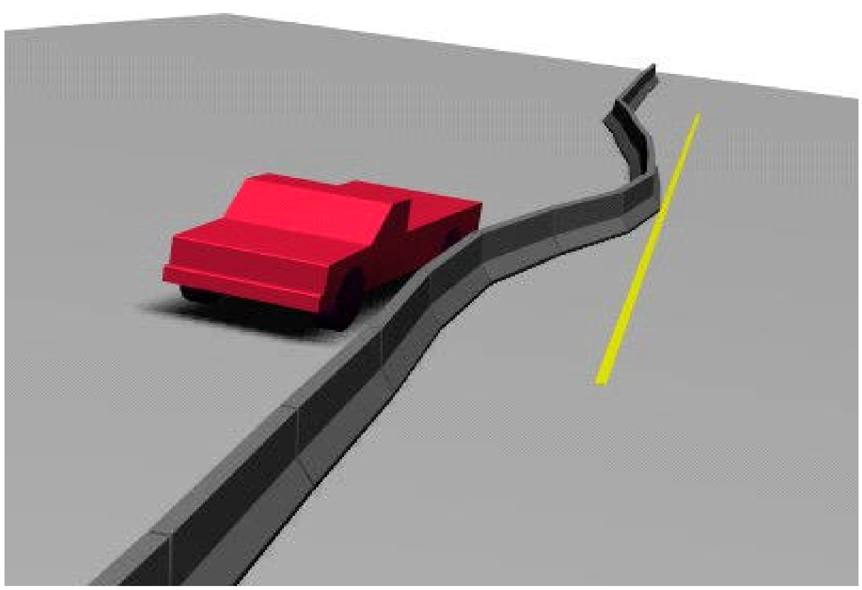

Figure 3-3 Simulation of Barrier Impact at 35^o Angle Using MSC Working Model (Araujo, Mirmiran, and Rahman, 2003)

3.4 Verification Studies

In order to validate our modeling study, we did the following: (i) developed simple analytical solutions for the response of a rigid barrier (resting on frictionless and frictional surfaces) subjected to an impulsive force, (ii) using ANSYS/LS-DYNA, developed the results for the response of the benchmark problems, and (iii) compared the results from analytical and ANSYS/LS-DYNA solutions. These verification studies are presented in the following sections.

The response of the barrier to the applied impulsive impact force is evaluated in terms of the resulting acceleration, velocity, and displacement. All these responses are presented in graphical forms. The results from our finite element based simulation compare very well with those from the analytical solutions. This verifies that the way in which we are incorporating friction is correct and gives us confidence for our subsequent modeling and simulation.

As stated above, the MSC/Working Model is based primarily on rigid body movements, and therefore, is quite sensitive to the selection of the coefficients of friction, stiffness, and restitution. Therefore, the model is used with great caution and in conjunction with more focused and concise finite element model of the vehicle-barrier crash test. Furthermore, the MSC Working Model is calibrated against the available crash tests for the NC and OR barriers. The results of the validation and calibration tests are discussed later in this report.

3.4.1 Study 1: Impulsive Force Applied to Single Barrier (No Friction)

In this first simulation, we modeled an asphalt concrete ground surface and a reinforced concrete barrier staying above that surface using the 3-D simulation property of ANSYS/LS-DYNA. We defined these two materials as part identities and the two contacting surfaces of these parts separately as different components composed of nodes. The horizontal impulsive force was applied to the middle node of the back surface of the barrier which slides above the asphalt concrete ground surface and we didn't account for the friction between the corresponding surfaces for this particular simulation.

Firstly, we selected a solid element named SOLID64 which is used for the 3-D modeling of anisotropic solid structures. The element is defined by eight nodes having three degrees of freedom at each node: translations in the nodal x, y, and z directions. This element has also stress stiffening and large deflection capabilities.

Then, we specified the material models as asphalt concrete for pavement and reinforced concrete for the sliding barrier. The material properties are as follows for the pavement:

ρ (density) = 1600 kg/m^3, E (elasticity modulus) = 6.895*10^9 kg/m^2, μ (Poisson's ratio) = 0.35 and for the barrier these parameters are specified as: ρ = 2500 kg/m^3, E = 3.025*10^7 kg/m^2, μ = 0.20. For the creation of the model geometry, we simply used the solid modeling capabilities of the ANSYS/LS-DYNA program. We created two volumes to model the rigid bodies for both the pavement and the barrier. Figure 3-4 shows the geometry of the model.

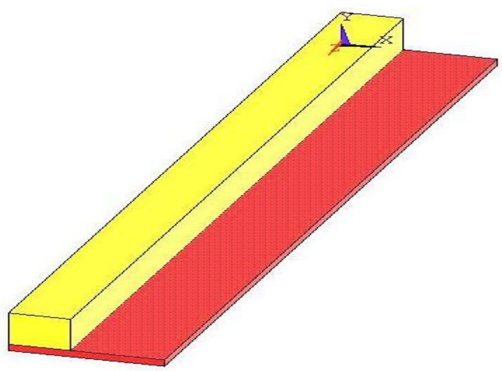

Figure 3-4 Geometry of the first simulation

The barrier model has the dimensions of 0.5 m x 0.5 m x 8.0 m whereas the ground surface has 0.1m x 1.25 m x 8.0m dimensions. After building the solid model, we were able to generate our finite element model using the meshing attributes of ANSYS. We preferred to use a uniform mesh in all directions for all of the simulations in order to decrease the computational cost and avoid the problems that can possibly occur resulting from element generation and unreasonable, high aspect ratios (Wriggers & Miehe, 1994). Figure 3-5 shows the finite elements of the model.

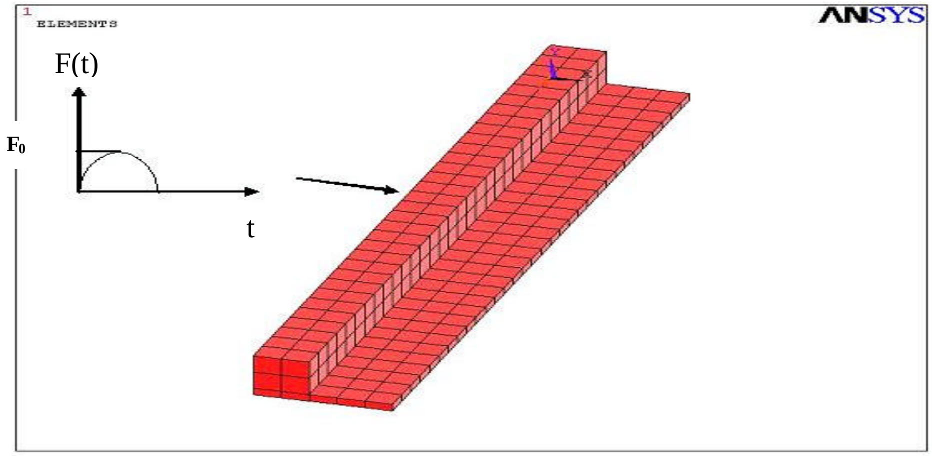

Figure 3-5 Finite elements and the application of the load for the first simulation

The last step of the model generation was the definition of the contact surfaces involved in the simulation. For explicit dynamics, the contact definition is different from the implicit analysis. Other than using any contact and/or target elements, we simply indicated the contact surfaces, the type of contact between them, and other parameters such as friction, related to the contact type. For that, we have taken into account the bottom surface of the sliding barrier which is composed of nodes as the contact (slave) surface, and the upper surface of the pavement as the target (master) surface which is also composed of nodes.

ANSYS/LS-DYNA allows many contact capabilities for different type of problems. In order to adequately describe interaction between complex geometries during large deformation contact and dynamic impact, a large number of contact surface options have been incorporated into the ANSYS/LS-DYNA product. These contact types, which include node-to-surface, surface-to-surface, single surface, single edge, eroding, tied, tiebreak, drawbead, and rigid contact options, are briefly explained in ANSYS Theoretical and User's Manual. In Chapter 4, the definition of contact is also described for the vehicle-barrier collision.

In this simulation, automatic-surface-to-surface contact card has been used. This is the most general type of contact as it is commonly used for bodies that have arbitrary shapes with relatively large contact areas. This type of contact is most efficient for bodies that experience large amounts of relative sliding, such as a block sliding on a plane which describes our problem accurately.

3.4.2 Analytical Solution 1: Impulsive Force Applied to Single Barrier (No Friction)

In the simulation, first we have solved the actual physical problem analytically. The analytical solution involved the representation of the model as one rigid block which is subjected to horizontal impulsive force F(t) within two time regions. Figure 3-6 represents the applied F(t) force versus time relationship. The time regions are 0=t=0.1 sec and t=0.1 sec. The following calculations show the evaluation of the acceleration, velocity and displacement-time histories for frictionless case obtained by time integration for the two regions:

$$\left.\begin{cases} \mathrm{a}\,(\mathrm{t}) = \dfrac{\mathrm{F}_0}{\mathrm{m}} \sin\,(w * t) \\ v(t) = \dfrac{\mathrm{F}_0}{\mathrm{m} * w}(1 - \cos(w * t)) \\ x(t) = \dfrac{\mathrm{F}_0}{\mathrm{m} * w^2}(w * t - \sin\,(w * t)) \end{cases}\right\} \quad 0 \le t \le 0.1 \tag{3.1}$$

$$\left.\begin{cases} \mathrm{a}\,(\mathrm{t}) = 0 \\ v(t) = V_0 \\ x(t) = X_0 + V_0 * (t - t_0) \end{cases}\right\} \quad t \ge 0.1 \tag{3.2}$$

Here, V_0 is the velocity when t is equal to t_0 and t_0 is equal to 0.1 seconds at which the impulsive force is 0. We have substituted the following values for the constant parameters; F_0 as the amplitude of force, m as the mass of the barrier, and ω as the angular frequency;

F_0 = 50000 kg-f

m = 5000 kg

ω = 10*π (1/s)

We analytically obtained the acceleration, velocity and displacement as;

$$
\left\{
\begin{array}{l}
a\ (t) = 10 * \sin\ (10 * p * t) \\
v(t) = \dfrac{1}{p}(1 - \cos(10 * p * t)) \\
x(t) = \dfrac{1}{10 * p^{2}}(10 * p * t - \sin\ (10 * p * t))
\end{array}
\right\} \quad 0 \le t \le 0.1 \qquad (3.3)
$$

$$
\left\{
\begin{array}{l}
a\ (t) = 0 \\
v(t) = 0.637\, m / \sec \\
x(t) = 0.032 + 0.637 * (t - 0.1)
\end{array}
\right\} \quad t \ge 0.1 \qquad (3.4)
$$

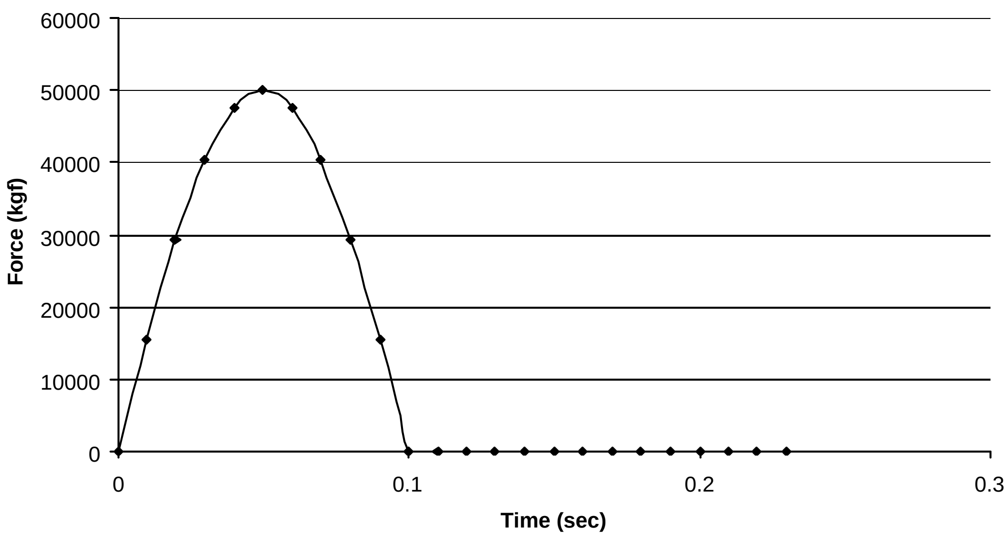

Figure 3-6 Impulsive force

3.4.3 Results of the First Study

In the simulations, we first initiated the acceleration of gravity to the system and then applied the horizontal impulsive force to the barrier in order to avoid excessive displacements and the releasing of the contact. So, a shift of 0.01 sec occurred in the response as a result of the shift in the horizontal impulsive force. The following results were obtained;

Table 3-1 Comparison of maximum values of the responses obtained from analytical and LS-DYNA solutions for frictionless case

μ=0	LS-DYNA	Analytical
Max. Acc. (m/s^2)	9.99	10
Max. Velocity (m/s)	0.631	0.637
Max. Disp. (m)	0.185	0.185

Figures 3-7, 3-8 and 3-9 show the results obtained from analytical and LS-DYNA solutions at the same graphs for acceleration, velocity and displacement, respectively.

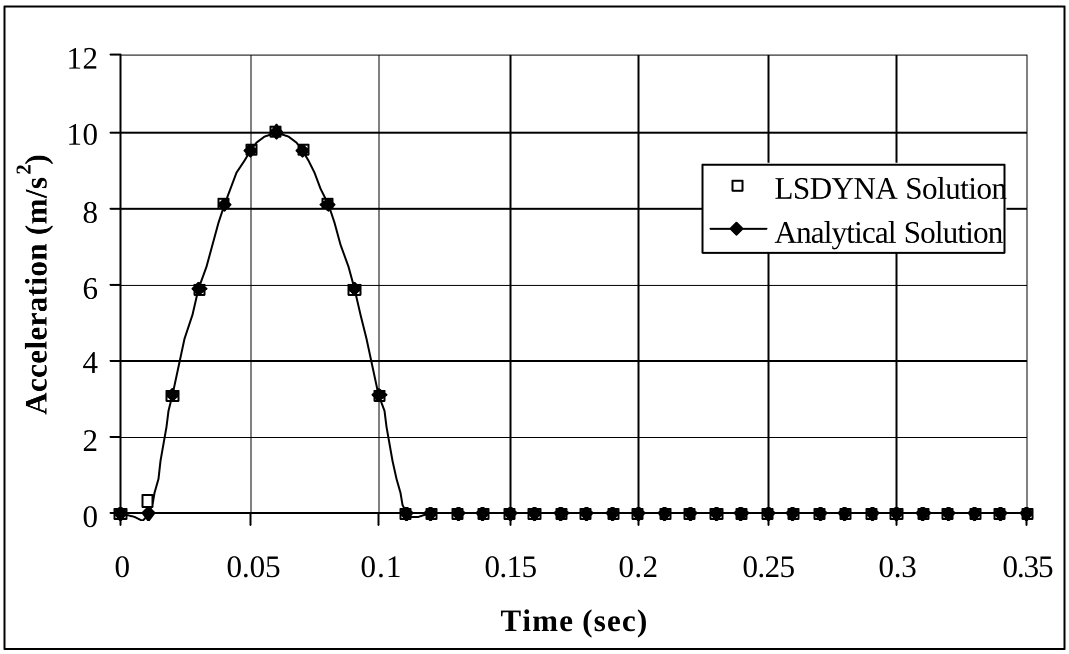

Figure 3-7 Comparison of the acceleration-time history of the response of the barrier

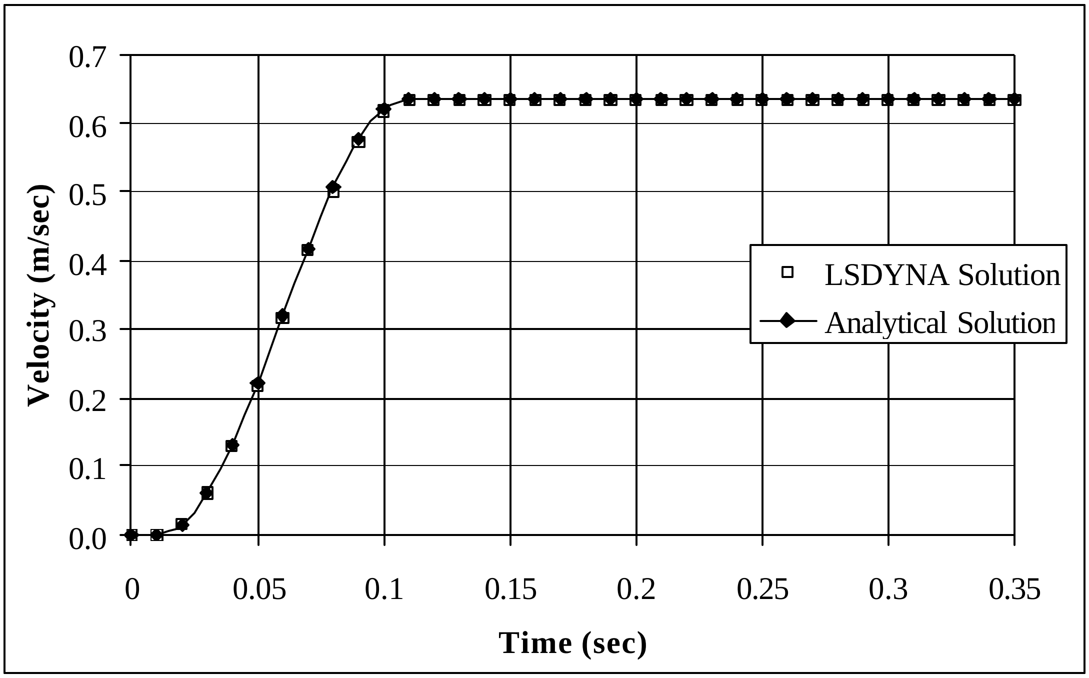

Figure 3-8 Comparison of the velocity-time history of the response of the barrier

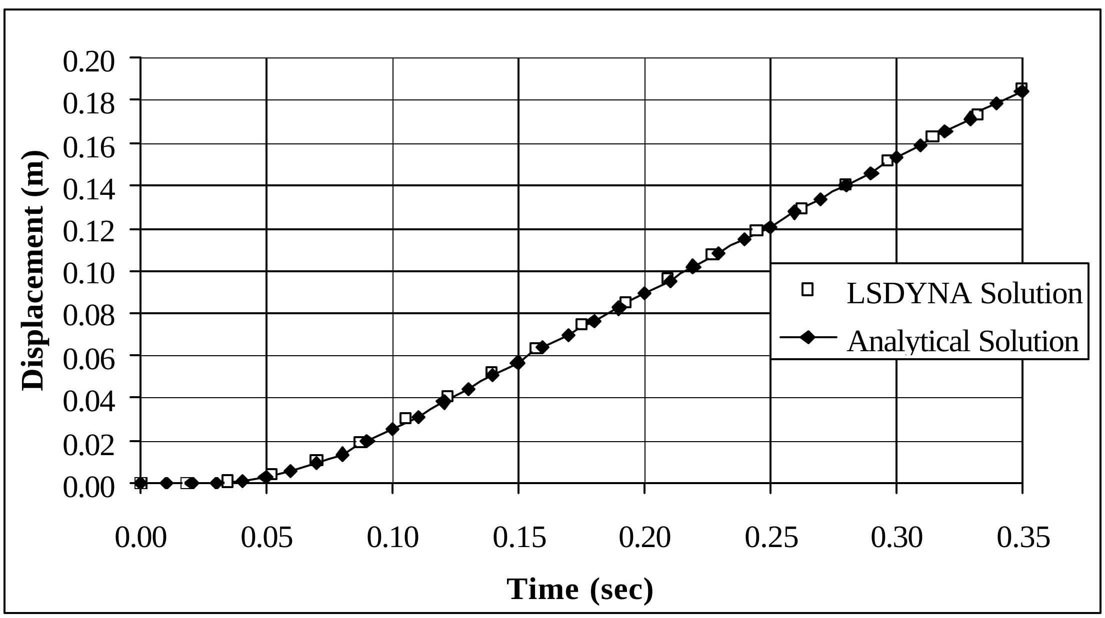

Figure 3-9 Comparison of the displacement-time history of the response of the barrier

For this first simulation, we haven't taken into account the coefficient of friction. So, the contact was defined between the surfaces with a specified Coulomb static coefficient of friction (μ=0). As we can see from the result plots, there isn't much difference between the responses of the barrier. The death time of the contact between the surfaces was chosen as 0.35 sec which will also be seen in the responses obtained when friction is defined.

3.4.4 Study 2: Impulsive Force Applied to Single Barrier (With Friction)

In this second model, the static friction coefficient of 0.2 was added to the input file deck of the first model. Additionally, we used the new pre- and post-processor of LS-DYNA called LS-PREPOST to define the surface to surface contact accurately including all of the parameters such as stiffness, penalty, constraint, penetration etc. LS-PREPOST was also used to check every step of the input file and the analytical solution using the graphical representation.

3.4.5 Analytical Solution 2: Impulsive Force Applied to Single Barrier (With Friction)

Since this second simulation involved the static coefficient of friction, we integrated our actual impulsive force regarding also the friction force acting between surfaces. The evaluation of time histories analytically can be seen in the following formulas for the same time regions;

$$\left\{\begin{array}{l} \mathrm{a}\,(\mathrm{t}) = \dfrac{\mathrm{F}_0}{\mathrm{m}} \sin\,(w*t) - m*g \\ v(t) = \dfrac{\mathrm{F}_0}{\mathrm{m}*w}(1-\cos(w*t) - m*g*t \\ x(t) = \dfrac{\mathrm{F}_0}{\mathrm{m}*w^2}(w*t-\sin\,(w*t) - \dfrac{m*g*t^2}{2} \end{array}\right\} 0 \le t \le 0.1 \qquad (3.5)$$

$$\left\{\begin{array}{l} \mathrm{a}\,(\mathrm{t}) = -\,m*\mathrm{g} \\ v(t) = V_0 - m*\mathrm{g}*(\mathrm{t}-t_0) \\ x(t) = X_0 + V_0*(t-t_0) - \dfrac{m*\mathrm{g}*(\mathrm{t}-t_0)^2}{2} \end{array}\right\} \; t \ge 0.1 \qquad (3.6)$$

If we substitute the same parameters and additionally the gravitational acceleration (g) as 9.81 m/s^2, and coefficient of friction (μ) as 0.2, we would find the responses as:

$$\left\{\begin{array}{l} a\,(t) = 10 * \sin\,(10 * p * t) - 1.962 \\ v(t) = \dfrac{1}{p}(1 - \cos(10 * p * t)) - 1.962 * t \\ x(t) = \dfrac{1}{10 * p^{2}}(10 * p * t - \sin\,(10 * p * t)) - 0.981 * t^{2} \end{array}\right\} \quad 0 \le t \le 0.1 \tag{3.7}$$

$$\left\{\begin{array}{l} a\,(t) = -1.962\ \mathrm{m/s}^{2} \\ v(t) = 0.449 - 1.962 * (t - 0.1) \\ x(t) = 0.0182 + 0.449 * (t - 0.1) - 0.981 * (t - 0.1)^{2} \end{array}\right\} \quad t \ge 0.1 \tag{3.8}$$

3.4.6 Results of the Second Study

Table 3-2 summarizes the results obtained from both LS-DYNA and analytical calculations.

Table 3-2 Comparison of maximum values of the responses obtained from analytical and LS-DYNA solutions for m=0.2.

μ=0.2	LS-DYNA	Analytical
Max. Acc. (m/s^2)	7.961	8.038
Max. Velocity (m/s)	0.449	0.449
Max. Disp. (m)	0.073	0.073

The acceleration response can be seen in Figure 3-10. Although there is some difference between the maximum accelerations (Table 3-2), we can see from the Figure 3-11 and 3-12 that, this difference hasn't affected the actual velocity and displacement response. We think that this difference in the acceleration response occurred because of the little amount of oscillations during the motion.

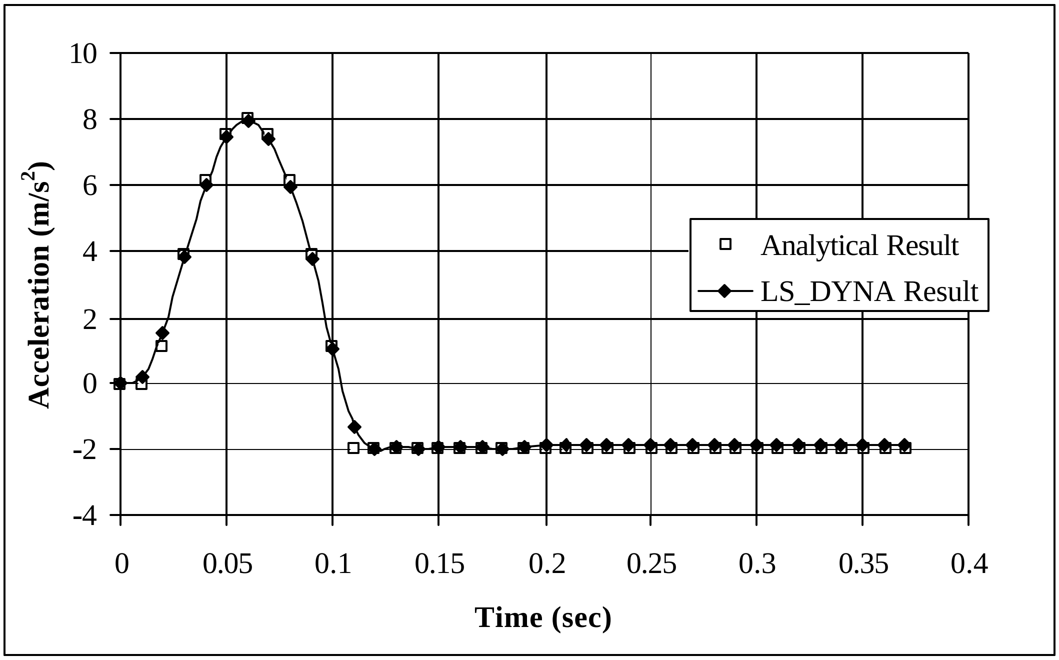

Figure 3-10 Acceleration-time history for μ=0.2

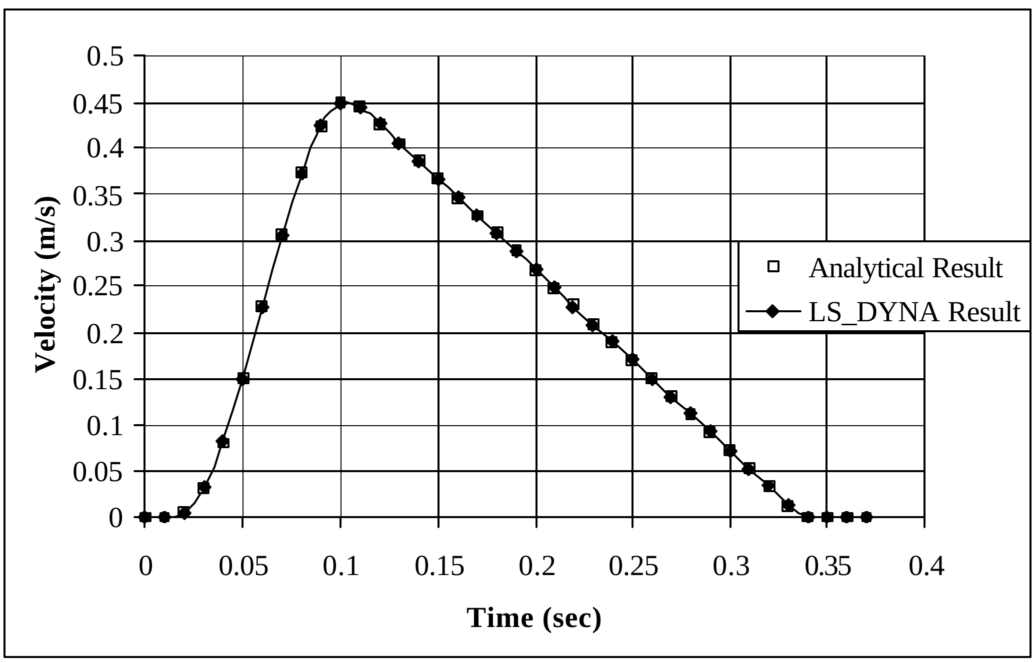

Figure 3-11 Comparison of velocity-time history of the response of the barrier for μ=0.2

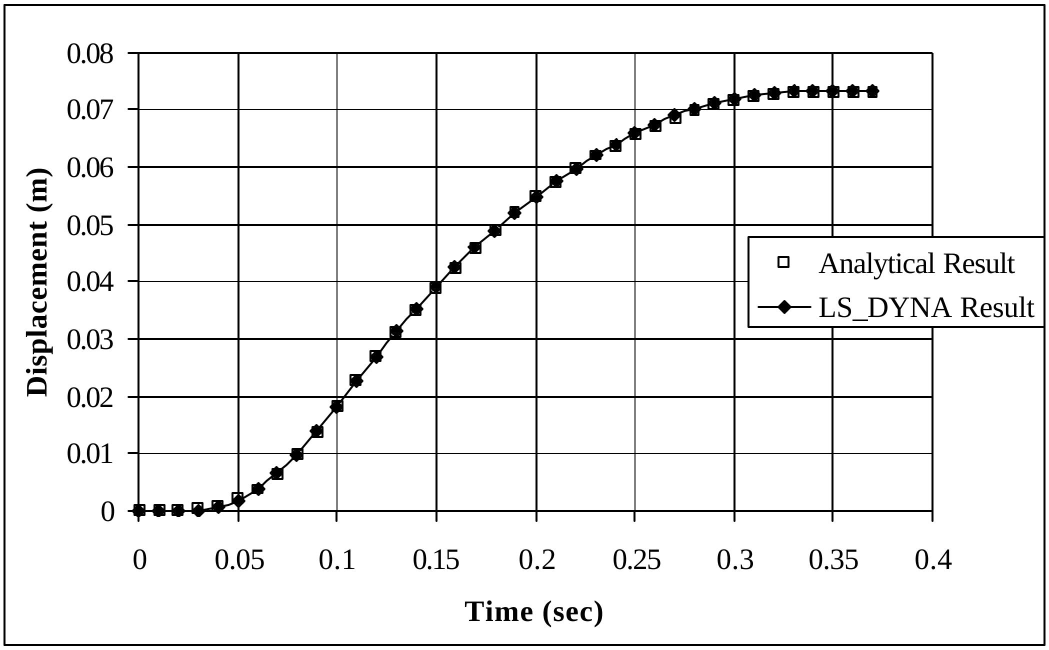

Figure 3-12 Comparison of displacement-time history of the response of the barrier for m=0.2

3.4.7 Study 3: Finite Element Simulation of a Single Barrier-Rigid Block Collision

In this third simulation, we analyzed the vehicle-barrier frontal and angular impact. For that, we assigned an initial velocity to the simple vehicle model and defined a frontal impact condition between the barrier and the vehicle. Then we obtained the responses of both the barrier and the vehicle for different initial velocities of the vehicle under the same static coefficient of friction between vehicle and the pavement; barrier and the pavement and vehicle and the barrier. And finally we changed the friction coefficient between these surfaces under the same initial velocity of the vehicle and recorded the results. For the first simulation, we used a solid element named SOLID64 for the barrier, pavement and the vehicle which is used for the 3-D modeling of anisotropic solid structures. The element is defined by eight nodes having three degrees of freedom at each node: translations in the nodal x, y, and z directions. This element has also stress stiffening and large deflection capabilities.

Then, we specified the material models as rigid asphalt concrete for pavement, reinforced concrete for the barrier and linear elastic aluminum material properties for the vehicle. The material properties and the sizes are defined in Table 3-3 for all of the parts.

For the creation of the model geometry, we simply used the solid modeling capabilities of the ANSYS/LS-DYNA program. We created three volumes to model the rigid bodies for both the pavement and the barrier. After building the solid model, we generated the finite element model using the meshing attributes of ANSYS. We preferred to use a uniform mesh in all directions for all of the simulations in order to decrease the computational cost and avoid stability problems. Figure 3-13 shows the geometry and the finite element model of this first simulation.

Table 3-3 Material properties of the simulation

Part ID	Dimensions (m)			Material Properties			Mass		
	X	Y	Z	E (Pa)	ρ (kg/m^3)	ν	kg	Element #	Node #
Vehicle	0.75	0.75	0.5	2.00E+11	7500	0.29	2109.4	18	48
Barrier	0.5	0.5	8	2.00E+10	2500	0.2	5000	128	297
Pevement	16	0.15	16	3.40E+10	2400	0.35	92160	4096	8450

The last step of this simulation was the definition of the contact type between the interacting parts of the model. In this simulation, automatic-surface-to-surface and automatic single surface contact cards have been used separately. These are the most general type of contacts as they are commonly used for bodies that have arbitrary shapes with relatively large contact areas. As we mentioned before, surface to surface type of contact is more efficient for bodies that experience large amounts of relative sliding, such as a block sliding or crash analyses. Besides, in single surface contact, ANSYS/LS-DYNA automatically determines which surfaces within a model may come into contact. Therefore, single surface contact is the simplest type to define because no contact or target surface definitions are required. When it is defined, single surface contact allows all external surfaces within a model to come into contact. This option can be very powerful for self-contact or large deformation problems when general areas of contact are not known beforehand (priori unknown).

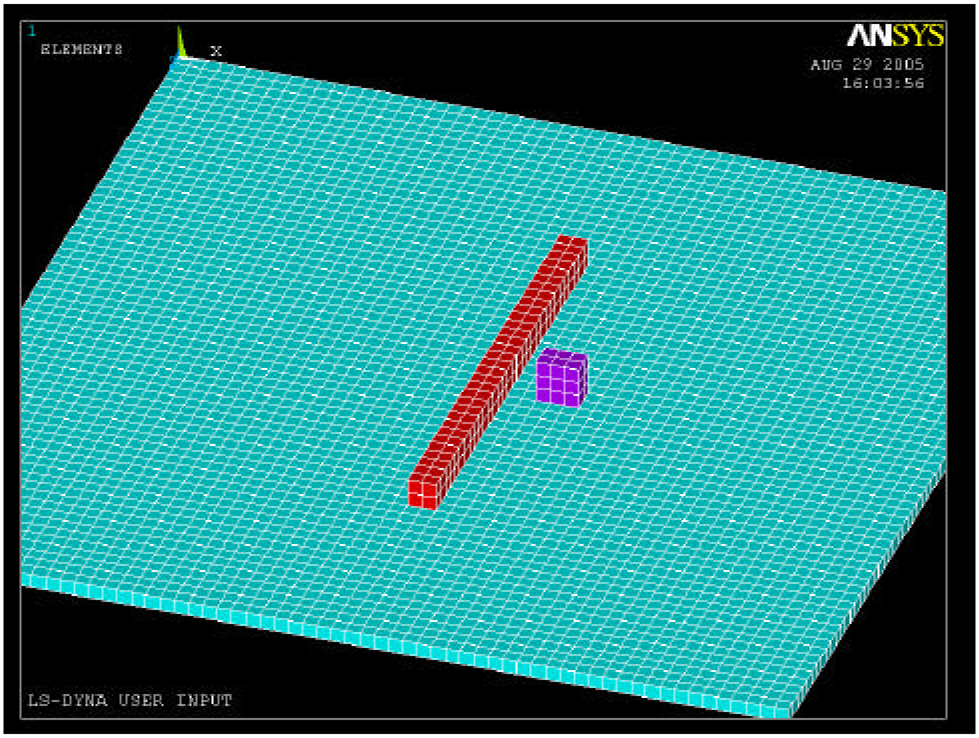

Figure 3-13 Finite element model of this simulation study

We first defined the single surface contact for all contact surfaces between the part ids keeping the coefficient of friction constant between them. Good results were obtained from this definition. However, more realistically, the effect of the friction coefficient between the barrier and the vehicle during the impact was concerned and the definition of contact was changed into automatic surface to surface and different friction coefficients were assigned for different contacting surfaces as a result of this contact definition. Results have been more accurate when compared to analytical solutions regarding the conservation of energy and momentum.

3.4.8 Analytical Solution for Single Barrier-Rigid Block Collision

In the simulation, considering the conservation of energy of the vehicle before the impact, when the vehicle moves towards the barrier, it loses some energy resulting in the decrease in velocity. The velocity of the vehicle just before the impact can be evaluated using the equation,

$$\frac{1}{2}m_1 * Vv_0{}^2 - m * m_1 * g * X_0 = \frac{1}{2}m_1 * Vv_1{}^2 \tag{3.9}$$

as,

$$V_{v1} = \sqrt{V_{v0}^{2} - 2mgX_{0}} \tag{3.10}$$

Here, m_1 corresponds to the mass of the simple vehicle; g is the acceleration of gravity, μ is the friction coefficient, V_{v0} is the initial velocity of the vehicle and X_0 is the distance between the vehicle and the barrier, initially.

Considering the conservation of momentum and energy between the vehicle and the barrier, the velocity of the barrier, V_{b2}, and the velocity of the vehicle just after the impact, V_{v2}, can be evaluated as follows;

$$m_v Vv_1 = m_v Vv_2 + m_b Vb_2 \tag{3.11}$$

$$\frac{1}{2} m_v Vv_1^{2} = \frac{1}{2} m_v Vv_2^{2} + \frac{1}{2} m_b Vb_2^{2} \tag{3.12}$$

$$\rightarrow \ V_{v2} = \frac{\left(\dfrac{m_v}{m_b} - 1\right)}{\left(1 + \dfrac{m_v}{m_b}\right)} V_{v1} \tag{3.13}$$

$$\rightarrow V_{b2} = \frac{\left(m_v - \dfrac{m_v\left(\dfrac{m_v}{m_b} - 1\right)}{\left(1 + \dfrac{m_v}{m_b}\right)}\right)}{m_b} V_{v1} \tag{3.14}$$

Here, m_v and m_b correspond to the mass of the simple vehicle and the barrier, respectively. Since the barrier is at rest initially, its initial velocity is zero, so the initial momentum of the barrier does not appear in the equation 3.11 above. The final displacement of the barrier, X_d, after the impact can be calculated from the energy equation,

$$\frac{1}{2} m_b * V_{b2}{}^2 = m * m_b * g * X_d \tag{3.15}$$

as;

$$X_d = \frac{Vb_2{}^2}{2mg} \tag{3.16}$$

Following these formulas, we have determined the time history responses of the barrier after the impact from the equations below;

$$\begin{aligned} A(t) &= -mg \\ V(t) &= -mgt + c_1 \\ X(t) &= -\frac{1}{2} mgt^2 + c_1 t + c_2 \end{aligned} \tag{3.17}$$

Here, A(t) is the acceleration of the barrier after the impact, V(t) is the velocity with respect to time and X(t) is the displacement-time history of the barrier. The integral constants c_1 and c_2 can be evaluated from the values of velocity and displacement when t=0.05 sec which is the time passes before the vehicle hits the barrier. In this report, we compare the horizontal X-displacement of the barrier after the impact and these equations have been solved considering this displacement; however, they can also be solved considering the Y-displacement of the barrier in X-Y plane.

3.4.9 Results for Single Barrier-Rigid Block Collision

In this simulation, we used 3 different initial velocities for the vehicle, 2 different friction coefficients and two impact angles. For both frontal and angular impacts, we compared the results obtained from the series of analyses with the analytical solutions and determined the effect of the initial velocity, friction coefficient and the impact angle to the response of the barrier after the impact. Some of the finite element analysis results and their comparison with the theoretical solutions are summarized in the figures below. The displacement–time histories of the barrier obtained from both analytical solutions and various LS-DYNA analyses agreed well and are shown in Figures 3-14, 3-15 and 3-16. From the plots the effect of the impact angle, friction coefficient and the initial velocity can easily be seen. The analyses lasted till 2.5 sec termination time.

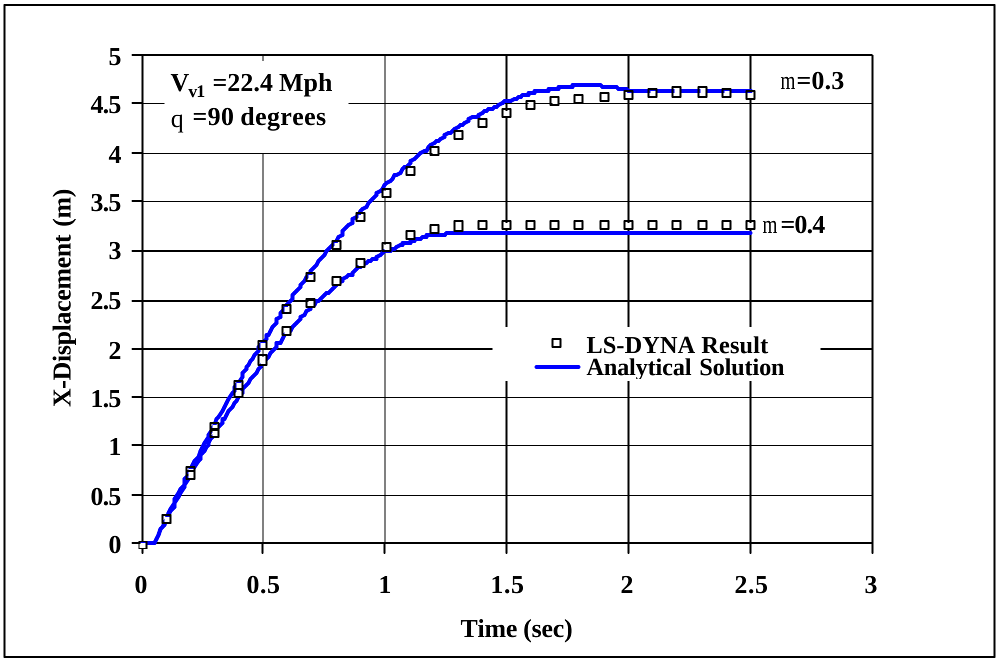

Figure 3-14 The effect of friction to the impact behavior of the concrete barrier

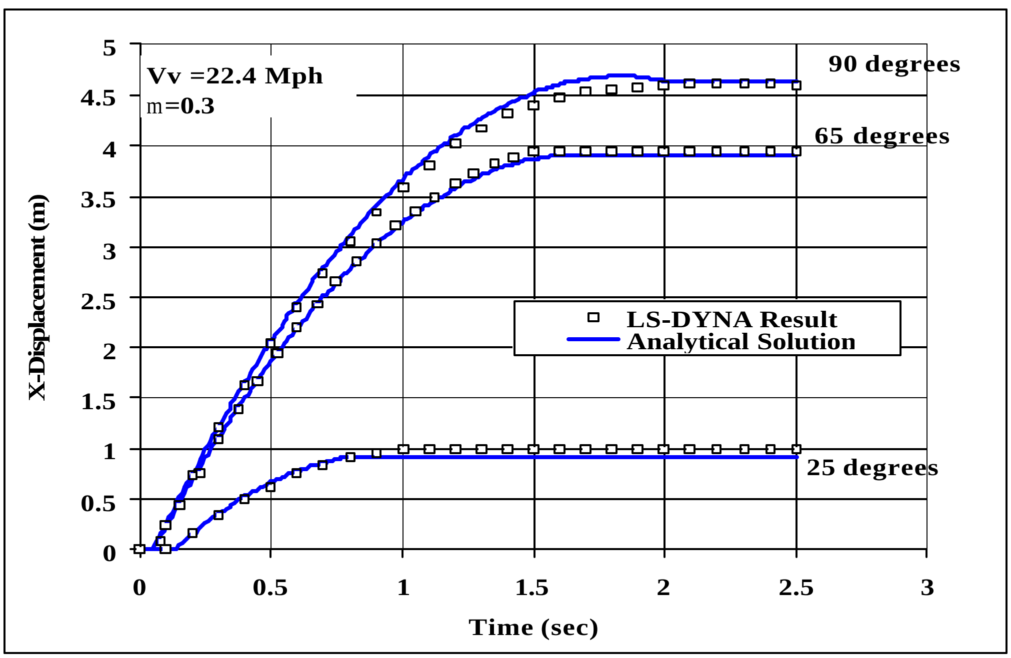

Figure 3-15 The effect of impact angle to the response behavior of the concrete barrier

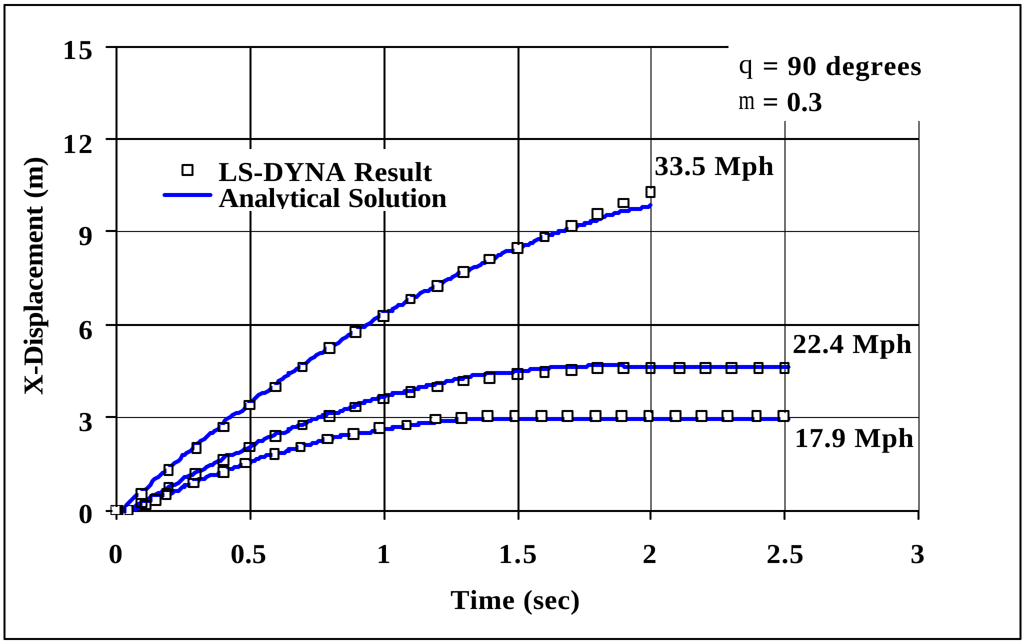

Figure 3-16 The effect of initial velocity to the response behavior of the concrete barrier

Figures 3-17, 3-18 and 3-19 show the maximum amount of horizontal displacement of the barrier with respect to the initial vehicle velocity depending on the friction coefficient and impact angle. These results summarize the response of one segment of the concrete barrier after the impact.

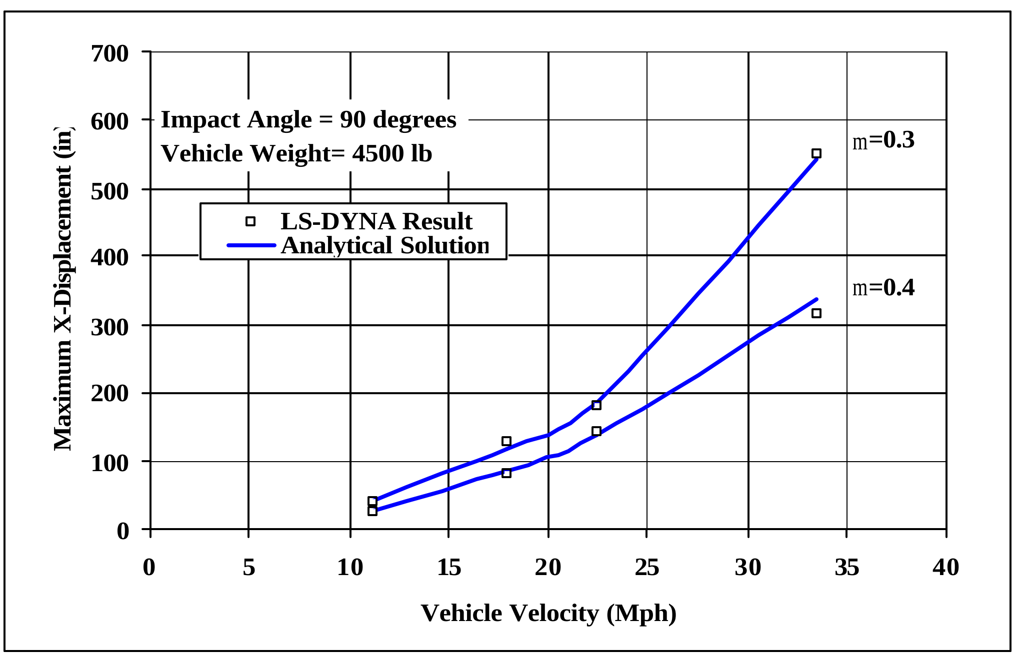

Figure 3-17 Barrier response for the impact angle of 90 degrees

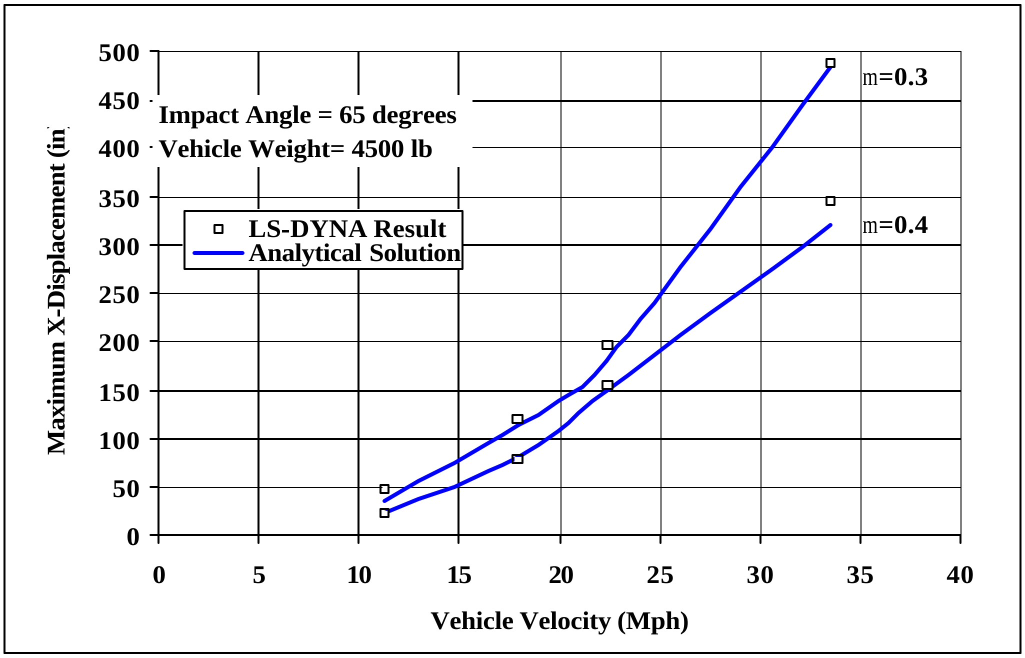

Figure 3-18 Barrier response for the impact angle of 65 degrees

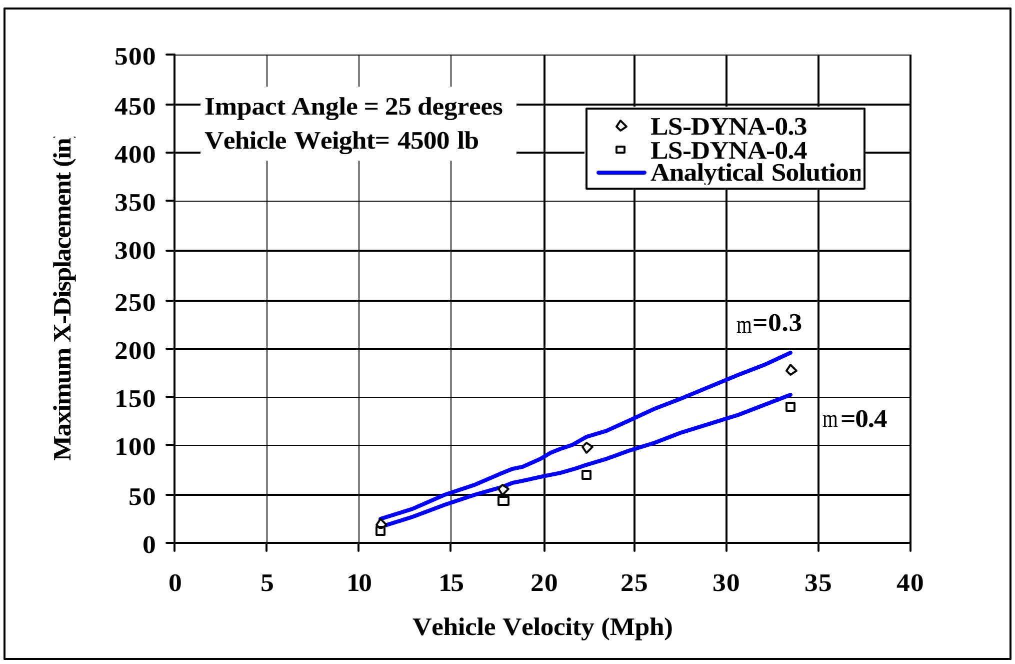

Figure 3-19 Barrier response for the impact angle of 25 degrees

3.4.10 Study 4: Finite Element Simulation of a System of Barriers

The aim of this simulation was to define and understand the behavior of joints between the barrier segments. For this reason, we used the original 18 segment F type PCB model prepared by National Crash Analysis Center (NCAC) in which the joints consisted of loops, pins and bolts which were analyzed by the LS-DYNA finite element software. The model has 18 segments with a total length of the barriers is 61 m.

The vehicle was primarily as a simple cubic solid model that reflects the material properties of the original vehicle itself. The block has a weight of 2109 kg and volume of 1 m^3.

In the simulations, four different vehicle velocities (35, 45, 62.4, 75 Mph); one impact angle (25 degrees) and two friction coefficients (0.2, 0.35) were used. Depending on the initial velocity of the vehicle model, at most 5 segments of the barrier article were influenced by the impact and displaced both in x and y directions. The overall model, the barrier cross section and the joint model can be seen in Figures 3-20, 3-21a and 3-21b.

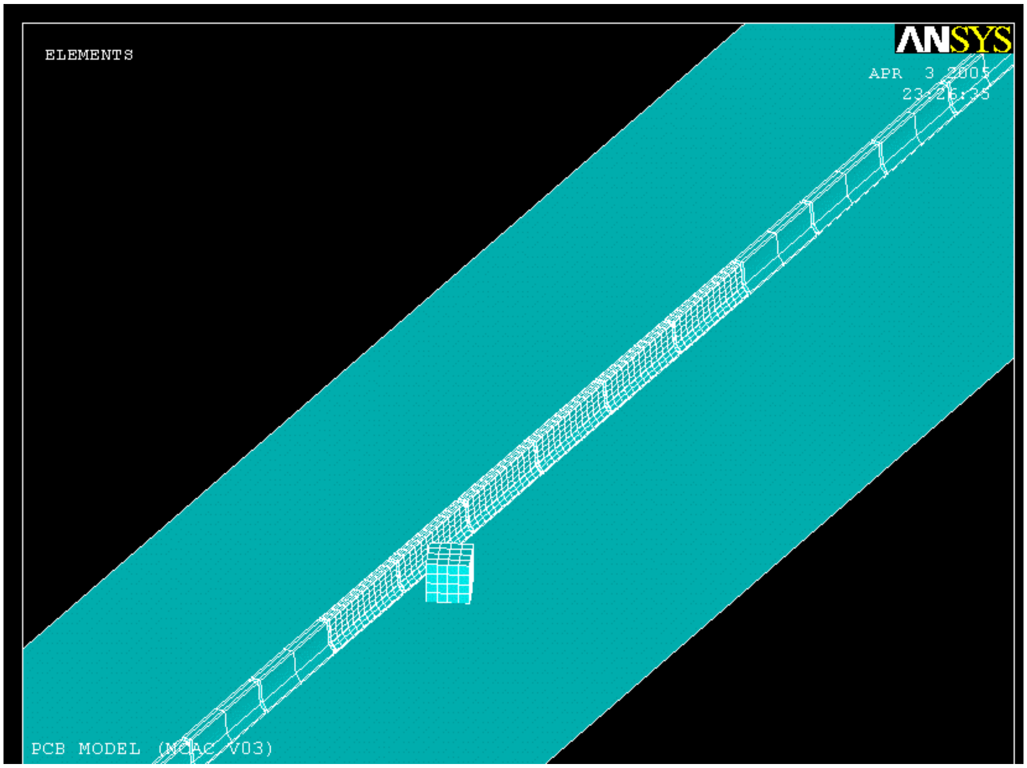

Figure 3-20 Finite element model of the PCB simulation

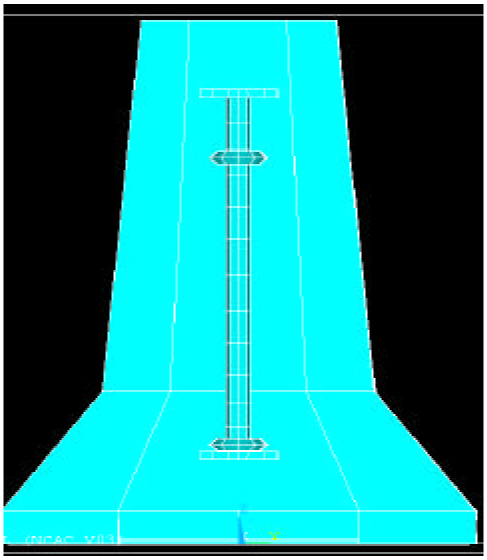

a)

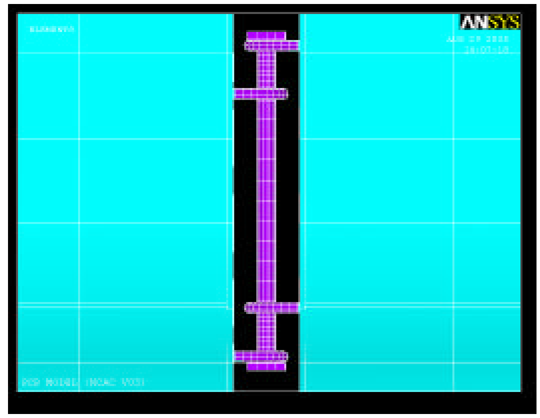

b)

Figure 3-21 Finite element model of, a) barrier cross section, b) joints

3.4.11 Results of Study 4

The parameters that play the major role in the response of the barrier segments have been determined as the initial velocity of the vehicle, coefficient of friction and the impact angle. The results obtained from this study have been compared with the ones calculated by MSC Working Model (Mirmiran et al., 2002). It has been determined that the behavior of the barrier segments during the impact significantly depends on the modeling of the joints between the barriers. In MSC model, the high strength ASTM 449 25 x 760 mm galvanized pins and A36 steel loops were replaced by sets of four linear springs with their elastic constant k being proportional to the maximum elastic force of the weakest point of failure between top and the bottom side of barriers at heights equivalent to the actual connections. The coefficient of restitution has also been controlled by the MSC model prior to the analyses.

In this study, the actual joints used in the field crash tests were modeled having the same geometry as well as material properties by using finite elements. Additionally, the friction involved non-linear behavior of the impact modeling handled by the explicit dynamic analysis capability of the LS-DYNA. The comparison between the results showed that the handling the response behavior of the pre-cast concrete barriers using finite elements can give more accurate results. Figure 3-22 and 3-23 show the maximum horizontal displacement of the barrier segment versus the initial velocity of the vehicle. Since the behavior of the joints were modeled closer to the crash tests, the maximum displacements of the barrier segments were obtained lower than the MSC model for both of the friction coefficients. The maximum displacement obtained from the full scale crash test having the same vehicle and barrier properties was 60.6 inches. This study resulted in a maximum displacement of 58 inches which is closer than the MSC model. The reason for this is the more accurate modeling of the barrier joints using finite elements.

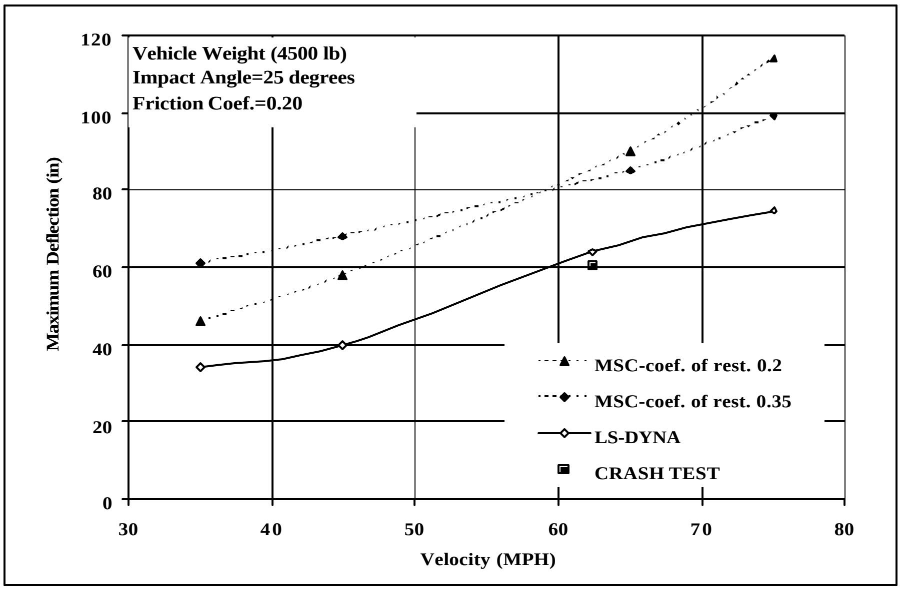

Figure 3-22 Comparison of the MSC Working Model and LS-DYNA analysis, m=0.2

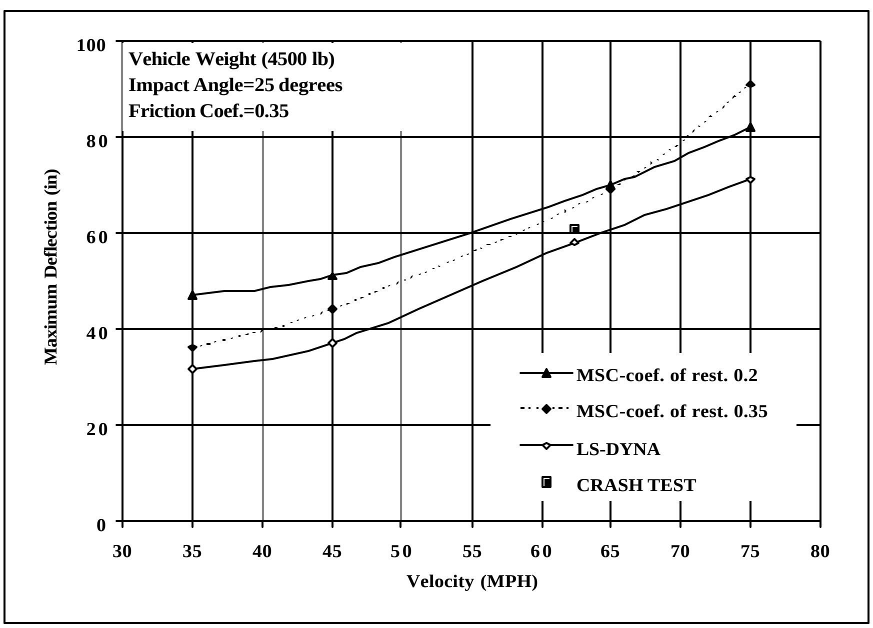

Figure 3-23 Comparison of the MSC Working Model and LS-DYNA analysis, m=0.35

3.5 Summary

The results presented in this chapter demonstrate the effectiveness of both finite element model and MSC Working Model in predicting the displacement of barriers. The finite element modeling, however, requires much larger effort, while the MSC Model can also make reasonably good predictions with much less effort if the parameters used in the model are selected correctly. Therefore, we take the position that after calibration of the MSC Working Model with the results from crash tests as well as FEM simulation, we will use MSC Model to develop the design curves.

4 Finite Element Based Simulation of Crash Tests

4.1 Introduction

In the previous chapter, we presented some preliminary verification studies by using ANSYS/LS-DYNA. These studies form a basis for the actual modeling and simulation of crash tests. In this chapter, we are presenting the finite element based simulation of the actual full scale crash tests. Firstly, the elements of the FEM based simulation such as the models incorporated in the analysis, the contact type defined between the parts of the model including the joints are introduced and described briefly. Then the modeling aspects of the two full scale crash tests are presented in the following last two sections.

4.2 Elements of FEM Based Simulation

The finite element based simulation of crash tests involves some major elements which have special modeling features. These elements are;

- Vehicle Model
- Portable Concrete Barrier Model
- Joints
- Contact Type and Friction

4.2.1 Vehicle Model

The vehicle models used in this study were obtained from National Crash Analysis Center (NCAC). The detailed models consist of shell, solid and beam elements. The number and type of elements used can be seen in Tables 4-2 and 4-4.

In the models it is possible to find many details of the original vehicles used in the crash test. The cabin and seats, hood, bumper, engine, rail, doors, windows, tires and many other parts of the vehicle have been drawn in 3-D, discretized and meshed with the preprocessing tool of LS-DYNA and uploaded to website of NCAC by its researchers. In NCAC's “Vehicle Modeling Laboratory”, researchers inspect vehicles to develop models that virtually recreate automobiles and trucks. With these accurate models, the researchers are able to simulate several different crash scenarios and predict vehicle and occupant response to incidents. Such foresight leads to more efficient research time and more effective and useful data for making safety decisions. Developing accurate and comprehensive FE models is a complex task that requires precise detail work and a tremendous amount of mathematical computation. Researchers:

- Apply tape over an entire vehicle to get an accurate representation of the geometries
- Digitize every component using a seven-degree-of-freedom coordinate measuring machine
- Disassemble all vehicle components
- Collect mass and material thickness data for vehicle and individual parts
- Identify all parts and connections
- Conduct center-of-gravity calculations
- Execute material property tests for component strength
- Create a computerized "mesh" grid of the vehicle using advanced computer codes
- Reconnect all parts accurately, including spot welds, rigid body constraints, joints, springs and dampers, (www.ncac.gwu.edu).

The vehicle models that we used in this study involve special material types that can be chosen from the preprocessing tool of LS-DYNA. Each material model is used in different parts of the vehicle. For example, since the behavior of the front side of the vehicle is more important than the back due to the nature of the impact response observed from the crash tests, piecewise linear plastic model was used for the frontal elements whereas rigid elements were used for modeling the back of the vehicle. The types of material models are:

- Elastic
- Blatz-K0 Rubber
- Damper Viscous
- Honeycomb
- Piecewise Linear Plastic
- Rigid
- Spring Elastic

These material models are generally being used in most of the other vehicle FE models as well, (NCAC).

4.2.2 Barrier Model

There are two basic barrier model types used in this study. These are NCDOT F-type and ODOT Tall F-type barriers. After some modifications, the FE models of these barriers obtained from NCAC reflect the actual dimensions and properties of the drawings of NCDOT. The detailed models consist of shell and solid elements. The number of elements used for barrier models can also be seen in Table 4-1 and 4-3.

Elastic, rigid and piecewise linear plastic material models were used in the FE model of the barriers. The barrier mass consists of elastic and rigid materials whereas the joints are made up of piecewise linear plastic materials which is discussed in the following section. Figure 4-1 shows a typical FE model of ODOT Tall F type barrier model.

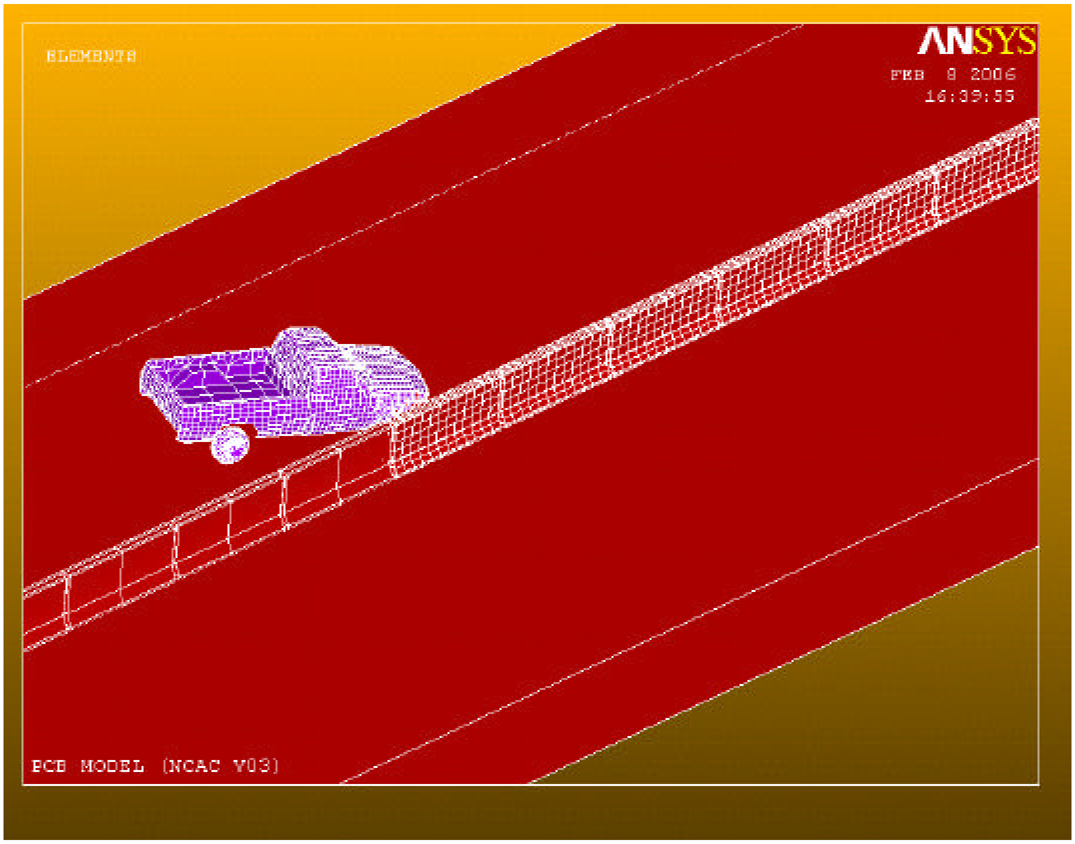

Figure 4-1 Finite element model of portable concrete barriers

4.2.3 Joint Model

Modeling of joints is considered as one of the most important components of the finite element based simulation of this study. It is also clear that the behavior of the barrier segments during the impact significantly depends on the accurate and comprehensive modeling of the joints between the barrier segments.

Pin and loop connections are widely used as joints to connect adjacent segments because they can readily accommodate horizontal curvature and changes in vertical grade. However, only after the joint has undergone a significant amount of rotation, the pin and loop connections can develop bending-moment capacity. Loops made of reinforcing bars are better than wire loops because they can resist torsional rotations of the barriers at the joints. A washer or cotter pin at the bottom end of the steel pin is necessary to prevent the pin from jumping vertically out of the loops upon impact, (McDevitt and Charles 2000).

In both NCDOT and ODOT barrier models, the high strength ASTM 449 25 x 760 mm galvanized pins and A36 steel loops were used between each barrier segment to connect them. Reinforcing consists of two longitudinal 13M (#4) bars in the barrier system and a u-shaped section of 6 x 6 x w2.9 welded wire fabric throughout the barrier length. For NCDOT model the loop connection between segments is comprised of round 19-mm (0.75-in) diameter steel bars bent to an inside radius of 51 mm (2.0 in). There are two such loops at the top of each segment on one end and a single loop on the opposite end. The bottom loops are reversed with a single bottom loop on the end with a double top loop and a double bottom loop on the opposite end. Barrier segments are connected by positioning the single loops between the double loops at each end and inserting a galvanized 32-mm (1.25-in) diameter high-strength bolt, 660-mm (26-in) long through the all six loops. A flat washer and nut are welded to the pin 610 mm (24 inches) up from the bottom. No nut or other type of retention device is used on the pins. In ODOT barrier model, additionally one more loop was placed on the bottom of the single loop on one end which makes the number of the loops on the top and the bottom as two.

The actual joints used in the field crash tests were modeled having the same geometry as well as material properties. The material type used to model the actual behavior of joints is piecewise linear plasticity. In this elasto-plastic material type, it is possible to define an arbitrary stress-strain curve and an arbitrary strain rate dependency. Also, failure based on a plastic strain or a minimum time step size can be defined. All the details about this type can be found in (LS-DYNA Keyword User's Manual, Version 970). A typical joint model can be seen in Figure 4-2.

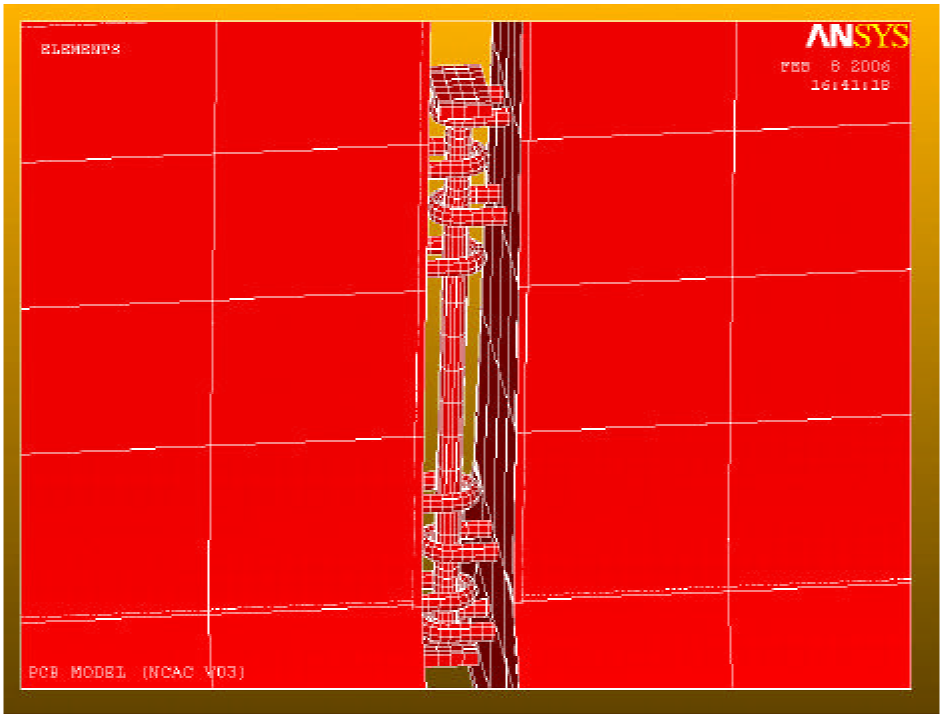

Figure 4-2 Finite element model of joints connecting NCDOT portable concrete barriers

4.2.4 Contact Types and Friction

Finite element modeling of vehicle-barrier collision is a highly nonlinear and dynamic analysis. Due to this complicated large deformation dynamics, during an explicit analysis, determining contact between components in a model can be extremely difficult. For this reason, special features have been included in the ANSYS/LS-DYNA program to define the contact between surfaces as efficiently as possible. In order to do that, there are some steps that should be followed during this process, which are:

1. Determination of the type of contact which best defines the physical model,
2. Identification of the contact entities such as master and slave parts,
3. Specification of friction coefficient parameters,
4. Specification of any additional input which is required for a given contact type,
5. Specification of birth and death times for the contact definition.

In order to adequately characterize the complex interaction between surfaces in this kind of explicit dynamic analysis, 85 different contact types have been incorporated in the program and it is required to have an understanding of these contact types for the selection of the most proper type for a specific analysis. Basically, the interaction between the FE models depends on three different algorithms (LS-DYNA Theoretical Manual, 1998):

1. Kinematic constraint method,
2. Penalty method,
3. Distributed parameter method.

In this study, the penalty method has been used for the definition of contact-impact algorithm which consists of placing the normal interface springs between all penetrating nodes and the contact surface. The reason is because by using this method, we can say that the momentum is exactly conserved during the motion. In this respect, penalty method has some features which should be taken into account when the nonlinear dynamic analysis happens to be the major concern. If there is some amount of initial penetration of contacting nodes that is considered in the finite element model, then the numerical problems caused by the instability of the solution could be prevented. We can say that, the amount of penetration between contact and target surfaces depends on the normal stiffness and the amount of slip in contact depends on the tangential stiffness. Higher stiffness values decrease the amount of penetration/slip, but can lead to ill-conditioning of the global stiffness matrix and to convergence difficulties. Lower stiffness values can lead to a certain amount of penetration/slip and produce an inaccurate solution (LS-DYNA Theoretical Manual, 1998). Ideally, a high enough stiffness is required that the penetration/slip is acceptably small, but a low enough stiffness should take place to make the problem numerically behave well in terms of convergence.

Furthermore, no special treatment of intersecting interfaces is required, greatly simplifying the implementation. In this method, also the interface stiffness is chosen to be approximately the same order of magnitude as the stiffness of the interface element normal to the interface. Consequently, the computed time step size is unaffected by the existence of the interfaces. Basically, in the penalty method, the contact pressure is assumed to be proportional to the amount of penetration by introducing a penalty parameter. In static problems such as (Nour-Omid & Wriggers, 1986) and (Felippa, 1978), it was mentioned that the penalty parameter should be, in principle, an arbitrarily large number (Hunek, 1993). However, for a computer with a finite number of digits, it should be large enough to enforce the constraint condition, but not so large that the governing equations become ill-conditioned. On the other hand, too small a penetration parameter results in an unacceptable penetration of one body into the other and the overall response is distorted (Hunek, 1993). This is generally not applicable to contact-impact problems for dynamic case because of the inertial term. When penalty parameter is too large, noisy solutions or great oscillations are obtained which we encountered in some of our trial simulations. Also, large contact force can cause unrealistic separation immediately or a few time steps after detecting contact. We have also come across unreasonable separation of contact in some of our trial analyses.

From the mathematical point of view, since general contact problems are inherently nonlinear, it is not so easy to obtain the accurate results by means of velocity and displacement values (Wriggers et. al., 1990). This non-linearity, results from the contact area being a priori unknown and the boundary conditions determined as part of the solution. During last 20 years, various numerical techniques on the basis of FE modeling were developed for contact and contact-impact simulation. They allow the solution of these problems in their complexity with a high degree of nonlinearity due to various accompanying factors such as large deformations, friction effects and material nonlinearities. The results obtained from the first part of this study for frictional contact show that ANSYS/LS-DYNA is one of the most effective finite element programs available to simulate the contact problems under dynamic effects.

In the two crash test simulations, “Contact Nodes to Surface”, “Automatic Single Surface”, “Automatic Contact Surface to Surface” contact types have been selected. These types have different properties and are used to define the contact between different types of surfaces. Specifically, the use of these types is mentioned in section 4.3 and 4.4.

Regardless of the contact type, a friction definition which depends on the relative velocity of the contacting parts was used between all interacting surfaces which are:

- Vehicle and pavement contact
- Vehicle and barrier contact
- Barrier and pavement contact

However, the values of the parameters used to calculate the friction between the surfaces have been different. The formula below reflects that the friction that is mobilized when the vehicle starts to move, is calculated in a relatively smooth manner (LS-DYNA Theoretical Manual, 1998). So, the change in the friction from static to dynamic depends on the change in the velocity of the vehicle during the motion. The definition of the friction in all of the contacts has been adjusted and this definition was used in the overall analysis between the contacting parts as;

$$m = m_d + \left(m_s - m_d\right)e^{-m_{dc}|V|} \tag{4.1}$$

where V is the relative velocity of the contacting parts in mm/sec, μ_{dc} is the decay coefficient and μ_d and μ_s are the dynamic and static friction coefficients, respectively. A summary of the elements of FE based simulation of both crash tests can be seen in the table below.

Table 4-1 Elements of NCDOT and ODOT crash tests

Element Name	**Crash Test 1**	**Crash Test 2**
Vehicle	Ford F-250 Pickup Truck Mass: 4393 lbs Length:16.8 ft Height: 5.95 ft	Chevrolet 2500 Pickup Truck Mass: 4462 lbs Length:18.1 ft Height: 6.0 ft
Barrier	NCDOT F-Type Height: 32 in Length: 10 ft Base Width: 24 in Top Width: 6 in No. of Segments: 20 (200 ft)	ODOT Tall F-Type Height: 42 in Length: 10 ft Base Width: 26 in Top Width: 9 in No. of Segments: 20 (200 ft)
Joints	25 x 760 mm galvanized pins, 3-A36 steel loops	25 x 760 mm galvanized pins, 4-A36 steel loops
Contact Type	Joints: Auto. Single Surface Vehicle-Pavement: Cont. Nodes to Surf. Barrier-Pavement: Cont. Nodes to Surf. Vehicle-Barrier: Auto. Cont. Surf to Surf.	Joints: Auto. Single Surface Vehicle-Pavement: Cont. Nodes to Surf. Barrier-Pavement: Cont. Nodes to Surf. Vehicle-Barrier: Cont. Nodes to Surf.

4.3 Simulation of Original NCDOT F-Type PCB - Ford F-250 Pickup Truck Crash Test

In this segment of our study, we model and simulate the actual crash test of NCDOT barrier with a Ford F-250 pickup truck. The essential elements of the model have been presented in the previous section. In the following, we are presenting the specific features of this model followed by the results.

4.3.1 Finite Element Model and Analyses

The pickup truck and the portable concrete barrier models were obtained from the National Crash Analysis Center (NCAC) and incorporated into the simulation. The mass as well as the actual dimensions specified in the full scale crash tests of both the vehicle and the barrier segments were adjusted and imported in the finite element simulation.

The pickup truck was positioned 25 degrees to the orientation of the barrier article. The vehicle traveling at 62.4 Mph impacted the PCB 1.2 m upstream of the joint between PCB number 7 and PCB number 8 which was mentioned in the full scale crash test. Then we obtained the responses of both the barrier and the vehicle and compared it with original crash test results. The orientation of the barrier segments prior to the test can be seen in Figure 4-3.

The next step of the simulation was the definition of the contact type between the parts of the vehicle and its contacting barrier components. The mesh of the barrier segments and their joints which come into contact with the vehicle during the simulation was finer than the rest of the segments. The reason was to adequately capture the deformation and the structural behavior of the barrier during the crash analysis. However, this modification increased the computation time significantly. Time duration of the analysis was 1.2 seconds which resulted in more than 2 day computation time. On the contrary, it has been understood from the previous analyses that the nonlinear behavior of the model, especially modeling the joints as a combination of bolts, loops and pins requires at least that much long time durations. In addition to the pre-defined contacts of both the barrier and the vehicle, Automatic_Contact_Surface_to_Surface card has been added to the input deck to define the contact between the barrier and the vehicle parts in order to obtain the most accurate and computationally efficient simulation. This is one of the most general types of contacts as it is commonly used for bodies that have arbitrary shapes with relatively large contact areas. Figure 4-4, 4-5 and 4-6 show the finite element model used for this simulation from different views and FE model of the joints can be seen in Figure 4-7 for NCDOT model.

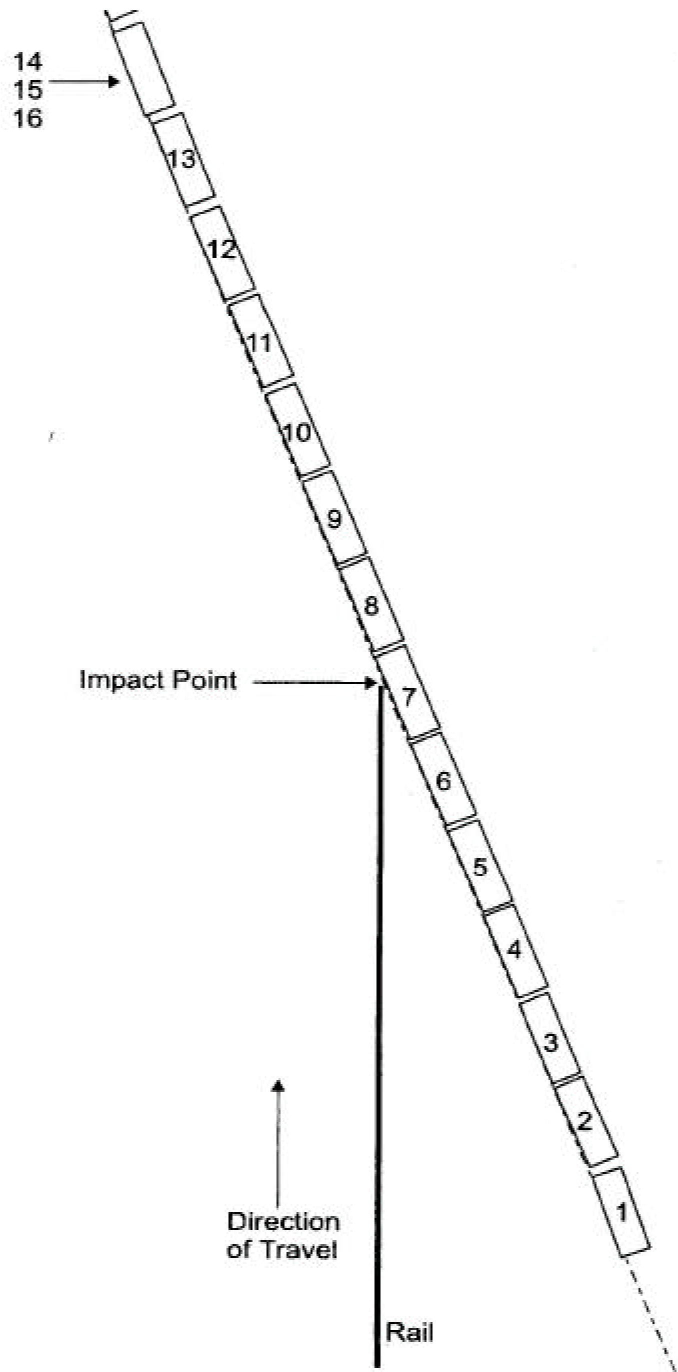

Figure 4-3 Pre-test NCDOT PCB diagram

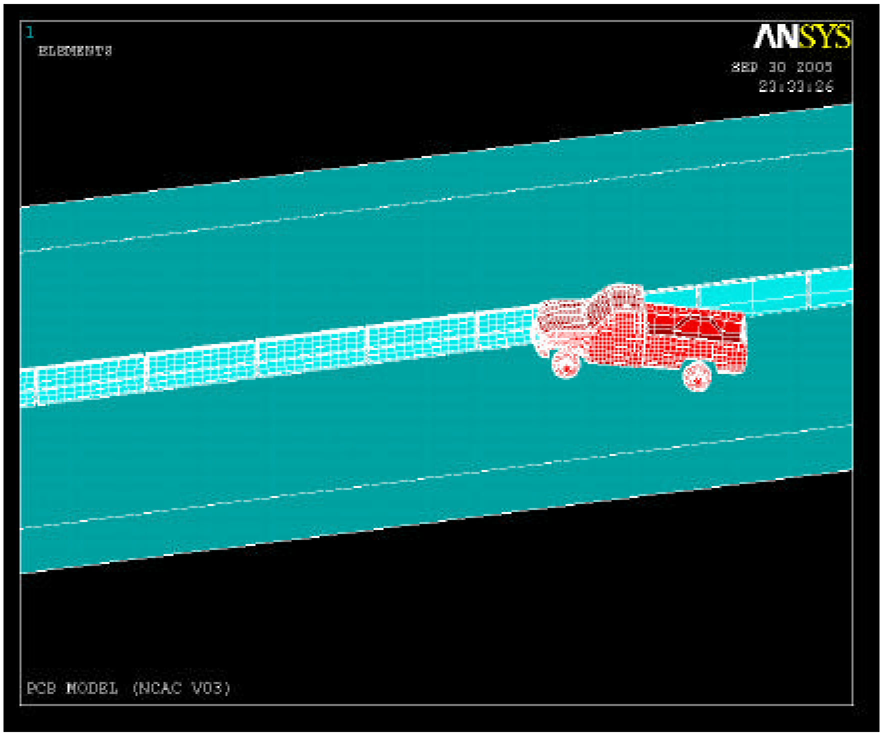

Figure 4-4 Finite element model of the simulation (side view)

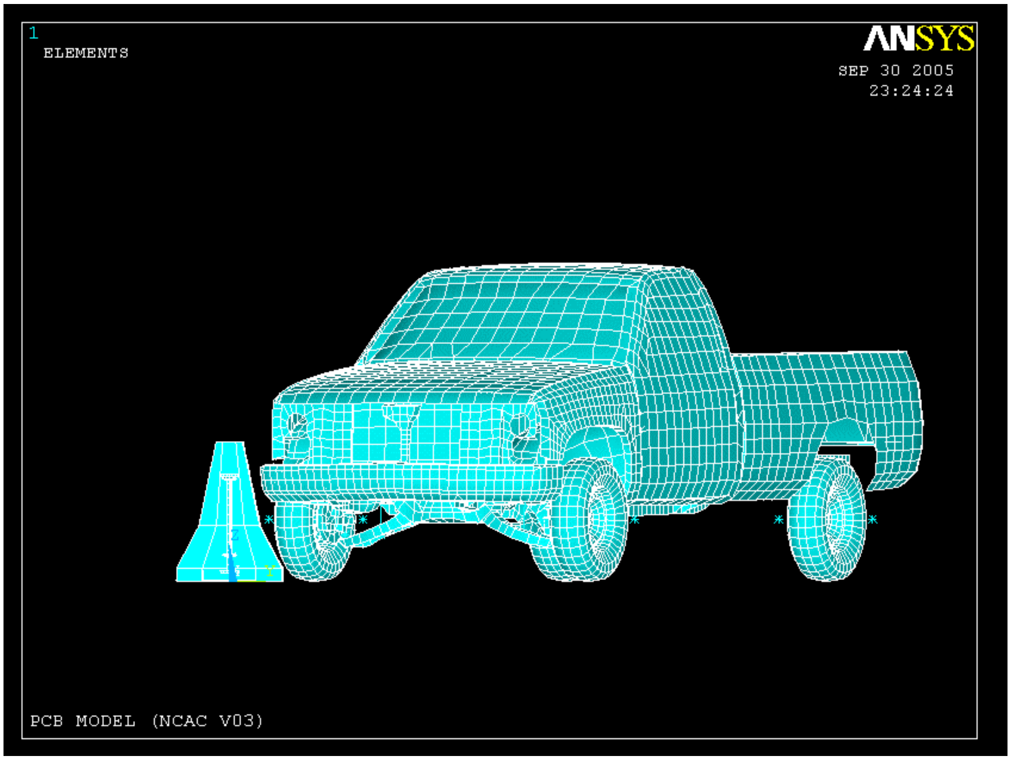

Figure 4-5 Finite element model of the simulation (front view)

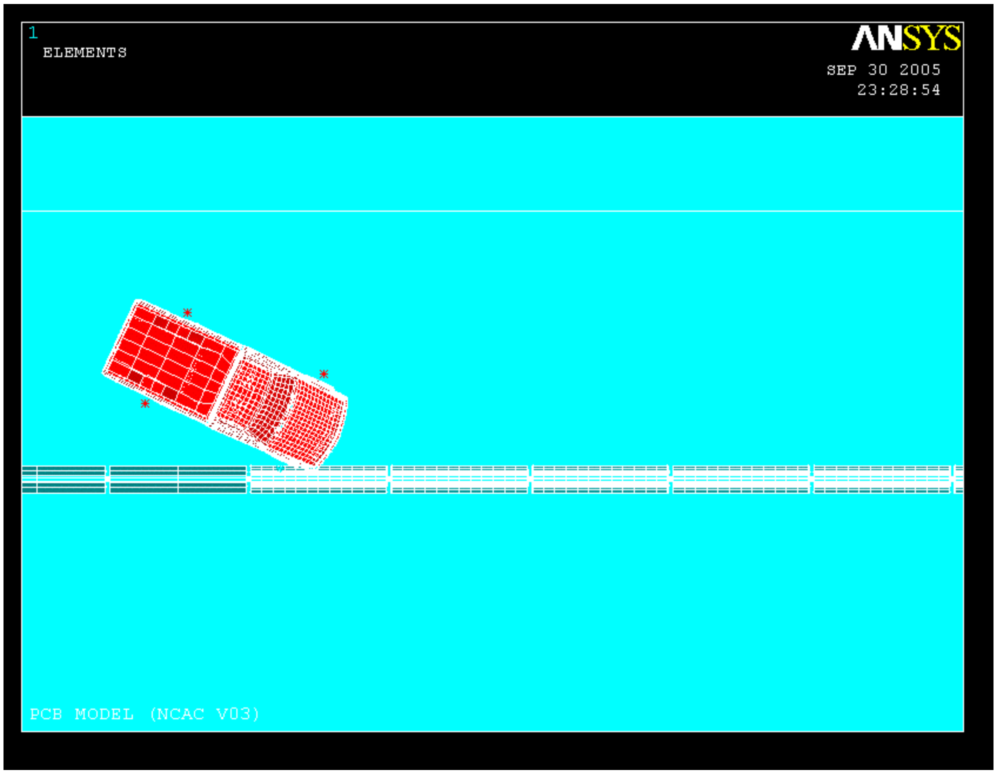

Figure 4-6 Finite element model of the simulation (top view)

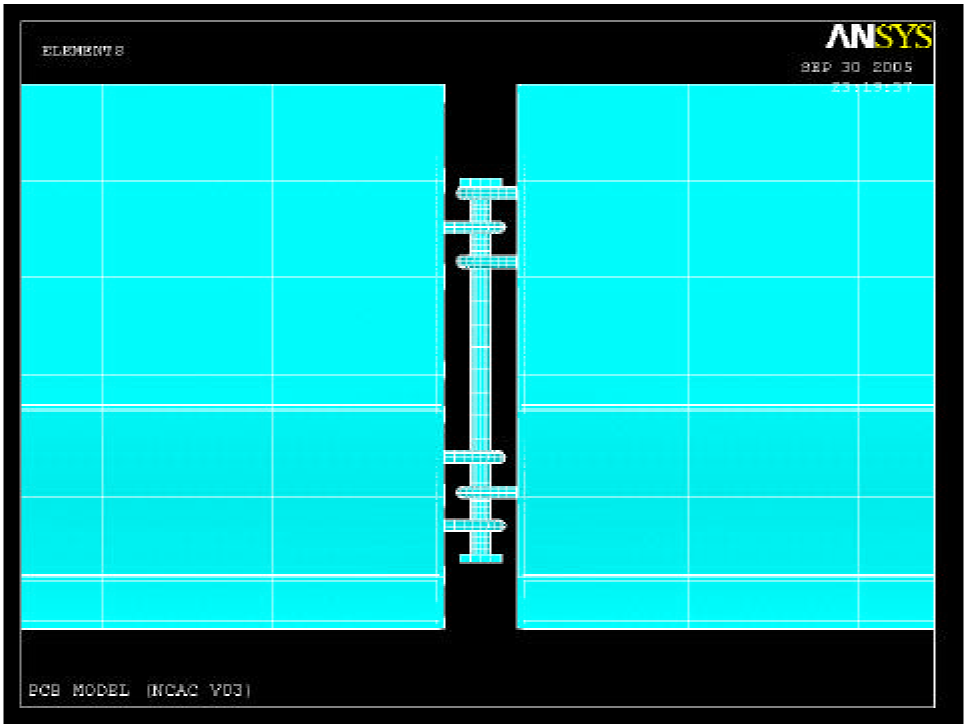

Figure 4-7 Finite element model of joints

Several analyses showed that by assigning μ_d=0.2, μ_s=1.0 and μ_{dc}=0.001 at the contact card between the vehicle and the barrier as well as between the vehicle and the asphalt pavement, the behavior of the components during the whole simulation agreed well with that of full scale crash test. We also used μ_d=0.3, μ_s=1.0 and μ_{dc}=0.001 to model the contact between the barrier and the pavement and after a series of analyses, we decided to stick with this modification. The number of parts, elements and nodes along with their material types can be summarized below;

Table 4-2 Summary of finite element model

	Vehicle			Barrier	
Parameter	Shell	Solid	Beam	Shell	Solid
Element #	10028	437	49	25215	2240
Node #	11060			29144	
Part # (group of elements)	61			160	

4.3.2 Results

At approximately 0.045 seconds after impact, the vehicle began to redirect and the barrier segments began to move. At approximately 0.160 sec. after impact, the vehicle was traveling parallel with the barrier. These times were 0.040 sec and 0.095 sec., respectively in the crash test.

The maximum displacement obtained from the full scale NCDOT crash test was 60.6 inches (1540 mm), Figure 4.8. This study resulted in a maximum displacement of 60 inches (1524 mm) which was measured at the downstream end of segment 7 at joint 7-8. Segment 5 through segment 10 was disturbed with static deflections varying from 0.1 in to 53.4 inches. The graphical comparison of the maximum displacements and their tabular values can be seen in Figure 4-9 and Table 4-3, respectively. None of the segments or pin and loop connections appeared to fail. Figure 4-10 and 4-11 show the Y direction displacement and velocity responses of the NCDOT-PCB, respectively.

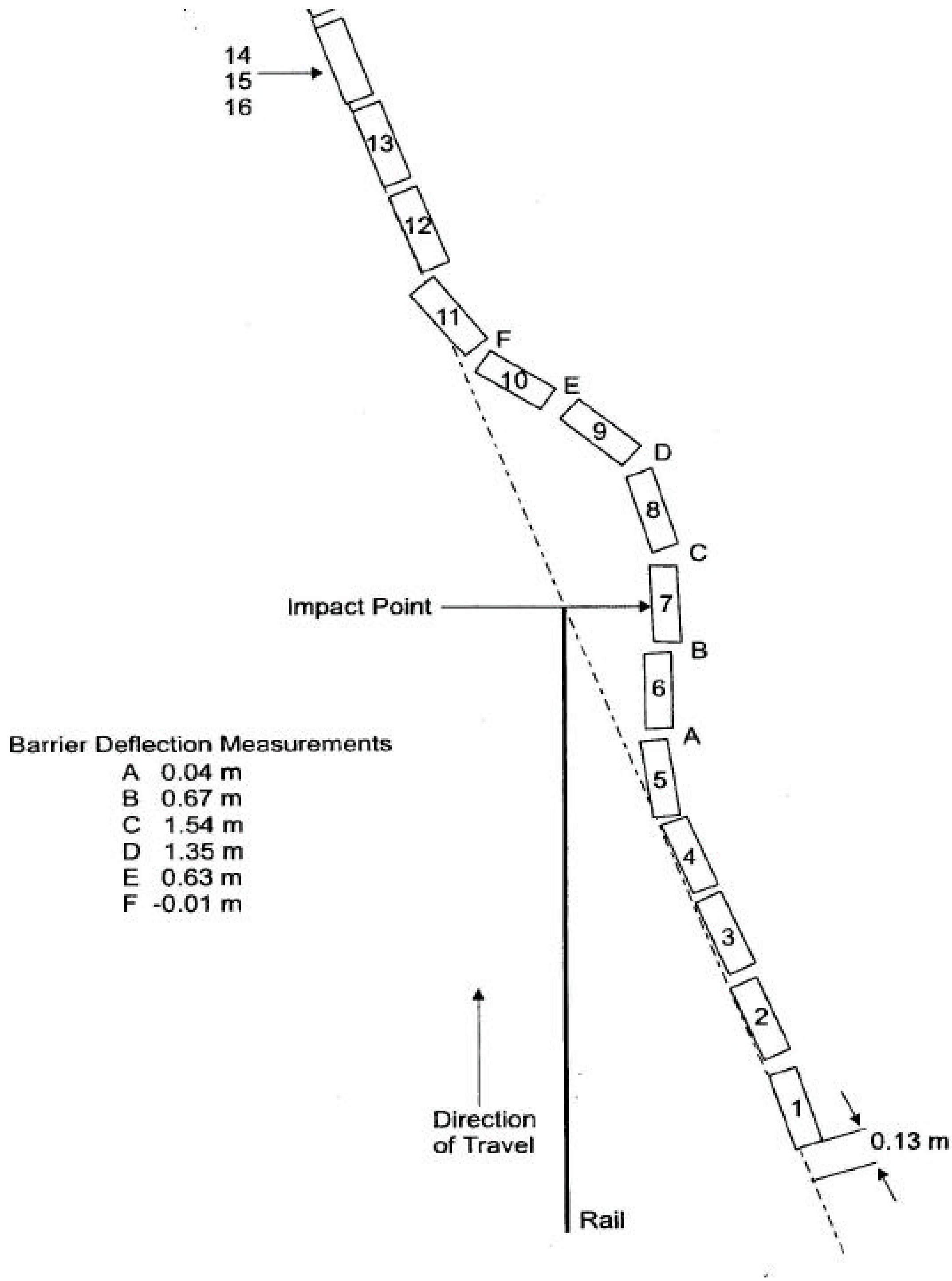

Figure 4-8 Post-test diagram of NCDOT PCBs

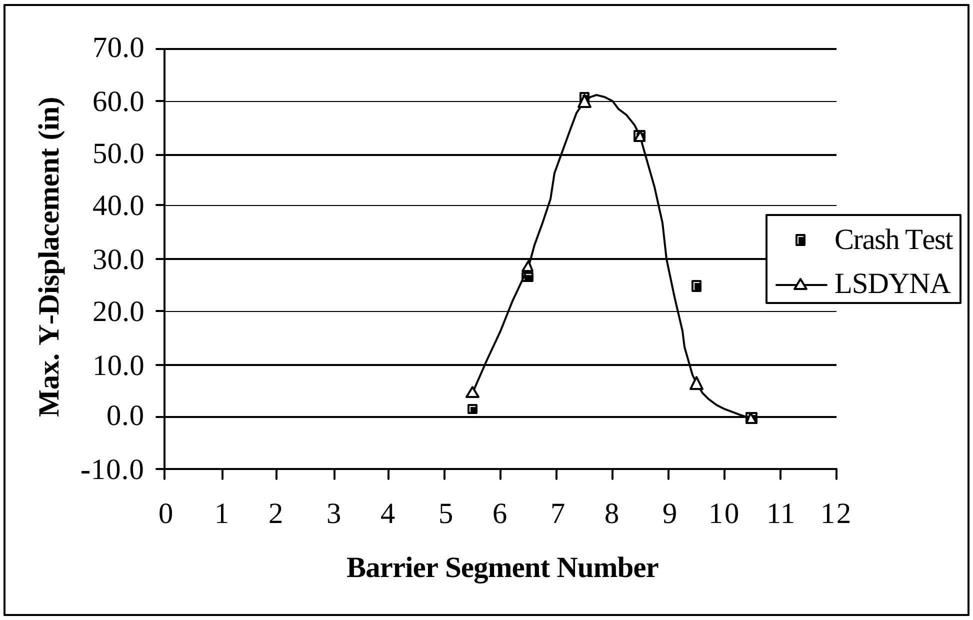

Figure 4-9 Maximum barrier displacements

Table 4-3 Maximum displacement values

	B5-B6	B6-B7	B7-B8	B8-B9	B9-B10	B10-B11
LS-DYNA (in)	4.8	28.7	60.0	53.4	6.4	-0.1
TEST (in)	1.6	26.4	60.6	53.1	24.8	-0.4

As we can see from Figure 4-10, LS-DYNA simulations agreed reasonably well with the crash test results. In Table 4-3, we see that there is some discrepancy between the results for the values obtained between segment 5 and 6 and segment 9 and 10. However, the maximum values and the values at nearby segments agree well. The same input deck was modified for three different impact velocities and the time history results, (Figure 4-10, 4-11), were obtained for these three values. LS-DYNA analyses resulted in a very close maximum displacement with that of obtained in the crash test.

The vehicle sustained moderate damage primarily to the right front. In this perspective, the structural deformation of the right frame rail, right rod ends and right door were experienced the main damage. The vehicle left the barrier orientation with an angle of 12.76 degrees which is less than 60 % of the impact angle of 25 degrees as it is mentioned in NCHRP Report. This was measured as 10 degrees in the crash test.

Figure 4-12 shows the comparison of the results of MSC Model, LS-DYNA and the crash test. MSC Model results have been obtained for two different friction coefficients, 0.2

and 0.35. It can be seen that a friction definition which depends on the relative velocities of the interacting surfaces results in relatively good agreement with the actual crash test.

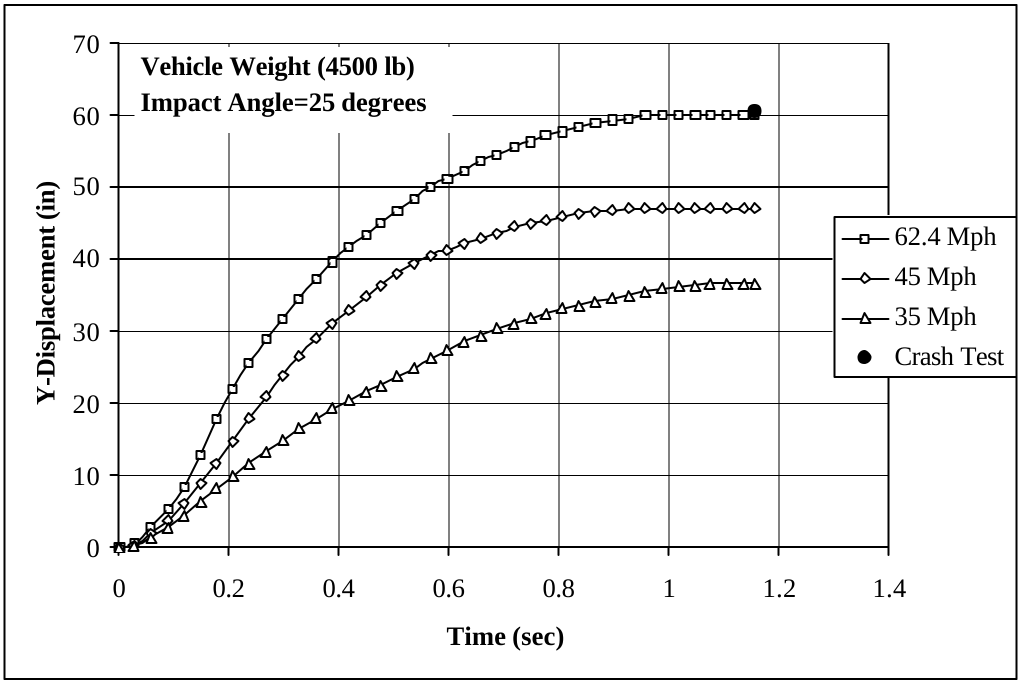

Figure 4-10 Displacement-time history of the node of PCB between segments 7-8 for three different impact velocities

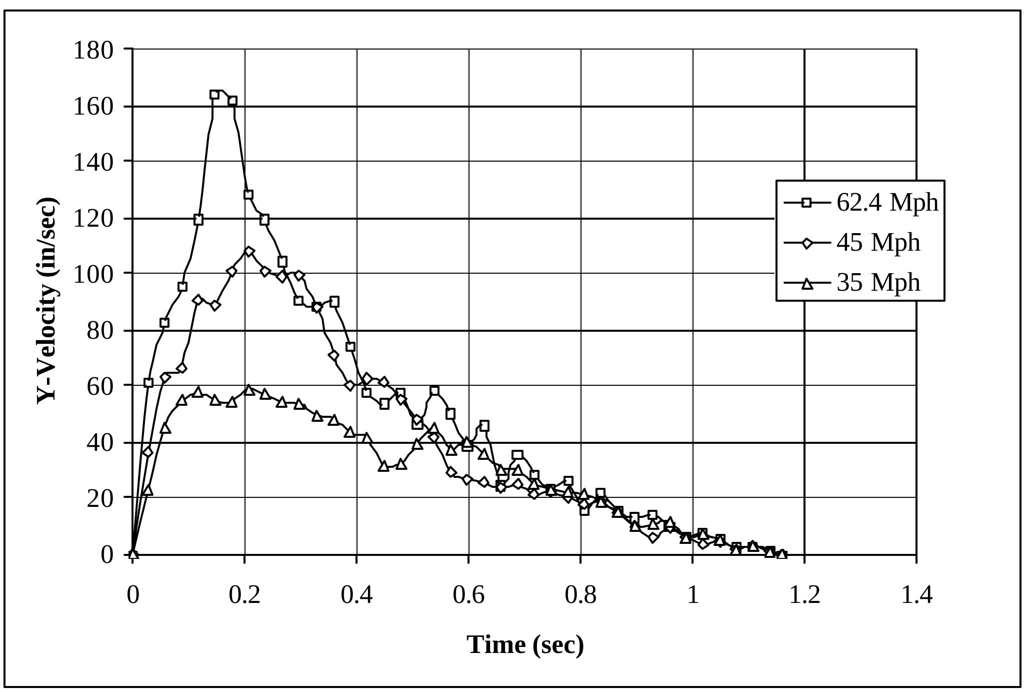

Figure 4-11 Velocity-time history of the node of PCB between segment 7-8 for three different impact velocities

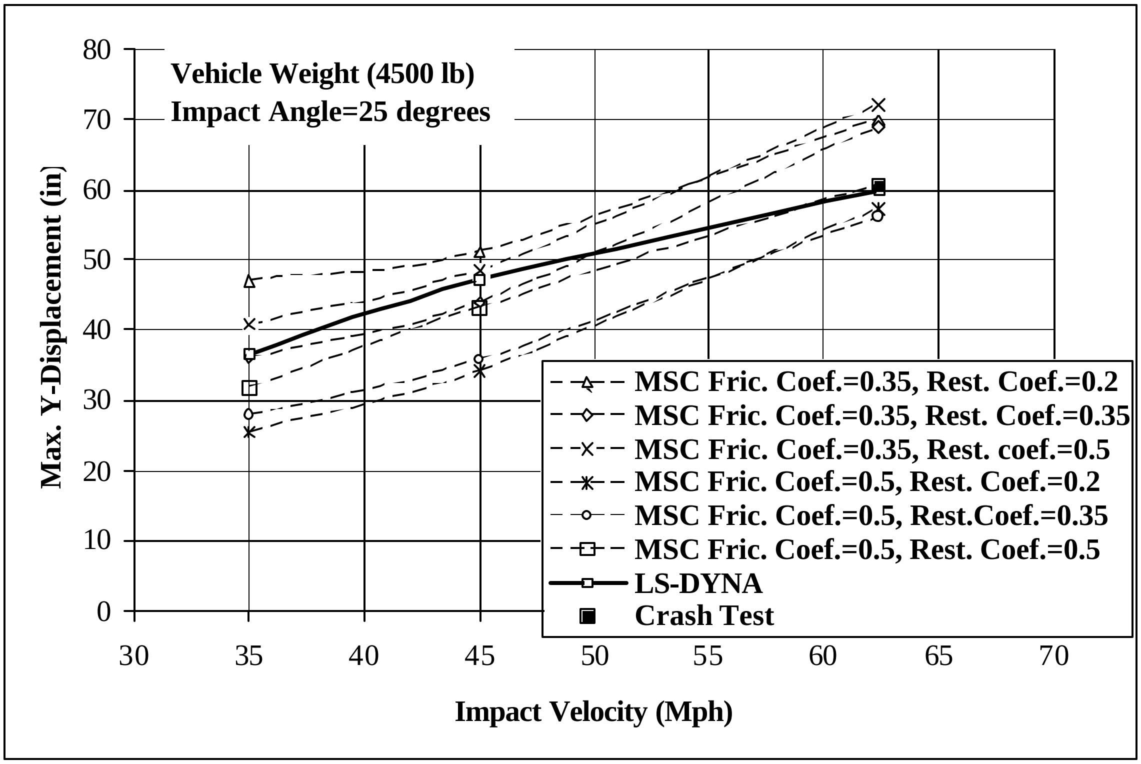

Figure 4-12 Comparison of the results of MSC Model, LS-DYNA and the crash test

The comparison of the behavior of both the barrier and the vehicle during the impact can be seen in Appendix A. The response of the vehicle and the barrier was presented from three different views at the integration times of 0, 0.08, 0.16, 0.24, 0.32, 0.40, 0.48 and 0.54 sec. Also, the overall simulation can be seen in Appendix B.

4.4 Simulation of Original ODOT F-Type PCB - Chevrolet Pickup Truck Crash Test

The second FE model and analysis has been done for the simulation of ODOT PCB and Chevrolet truck. The essential elements of the model have been presented in Section 4.2. In the following, we are presenting the specific features of the second crash model followed by the results.

4.4.1 Finite Element Model and Analyses

In this second simulation, we modeled the original full scale vehicle-barrier impact. For that, we assigned an initial velocity to the Chevrolet 2500 Pickup truck vehicle model whose mass and dimensions were adjusted according to the one that has been used in the full scale crash test. Its weight is 2,024 kg (4,462 lb). The impact occurred between the

ODOT portable concrete barrier and the Chevrolet C2500 pickup truck which was positioned 25 degrees to the orientation of the barrier article. At the point of impact the test vehicle had achieved a speed of 102.38 km/h (63.6 Mph). The mass as well as the actual dimensions specified in the full scale crash tests of the barrier segments were also adjusted and imported in the finite element simulation.

The pickup truck was positioned 25 degrees to the orientation of the barrier article. The vehicle traveling at 62.4 Mph impacted the PCB 1.2 m upstream of the joint between PCB number 7 and PCB number 8 which was mentioned in the full scale crash test. Then we obtained the responses of both the barrier and the vehicle and compared it with original crash test results. The orientation of the barrier segments prior to the test can be seen in Section 2.

In this model, Contact_Nodes_to_Surface type of contact has been the most efficient and accurate definition as far as the contact between the barrier and the vehicle parts is concerned. This is a contact type which is established when a contacting node penetrates a target surface by a limited amount. In this type of contact, the flat or concave surfaces or coarser meshes (barriers) are the targets while the convex surface or the finer mesh (vehicle) is the contact surface (ANSYS/LS-DYNA Manual). The analysis lasted 1.25 seconds which resulted in approximately a 3 day computation time. Figures 4-13 and 4-14 show the finite element model of this simulation from different views. FEM of the joints can be seen in Figure 4-2 and 4-15 for ODOT model.

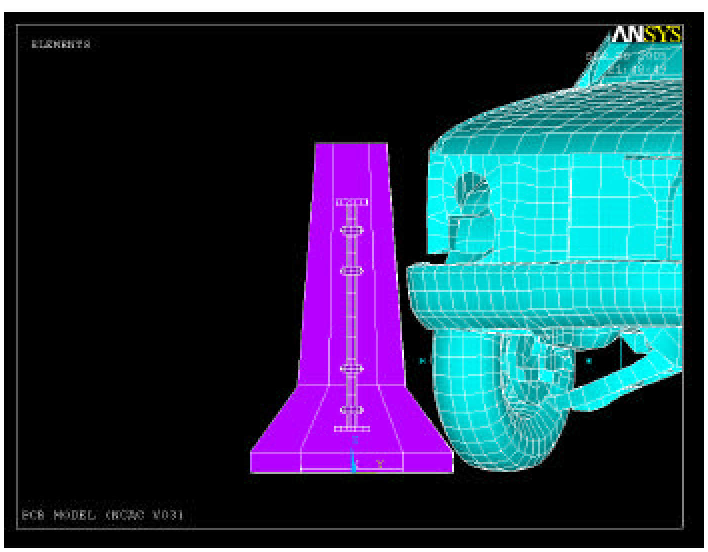

Figure 4-13 Finite element model of the simulation (front view)

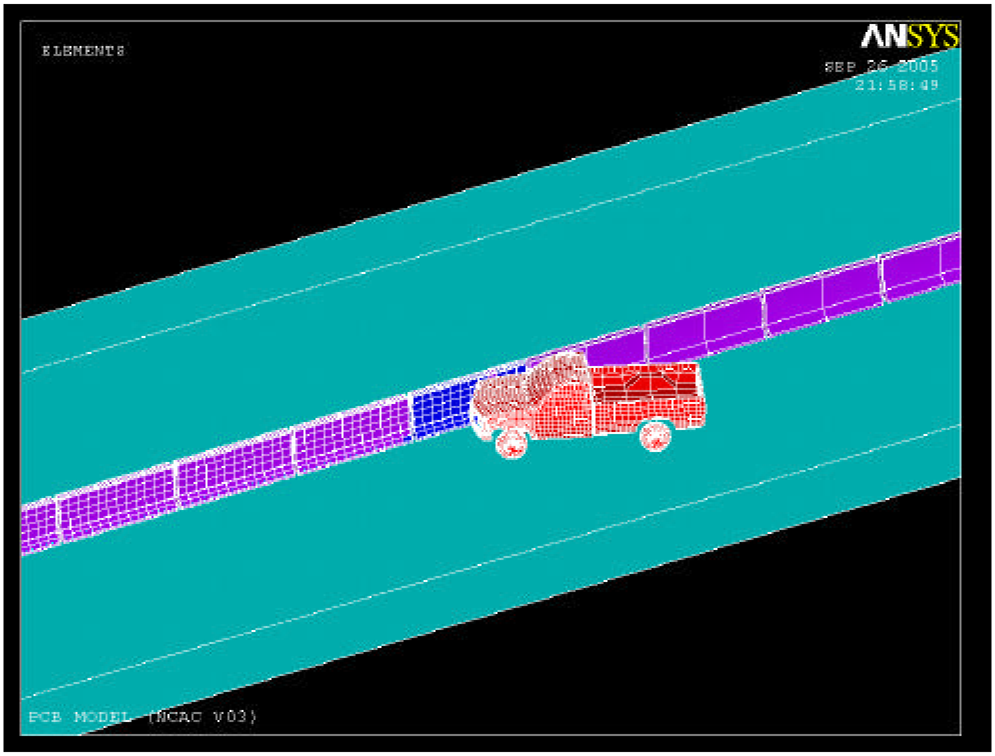

Figure 4-14 Finite element model of the simulation (top view)

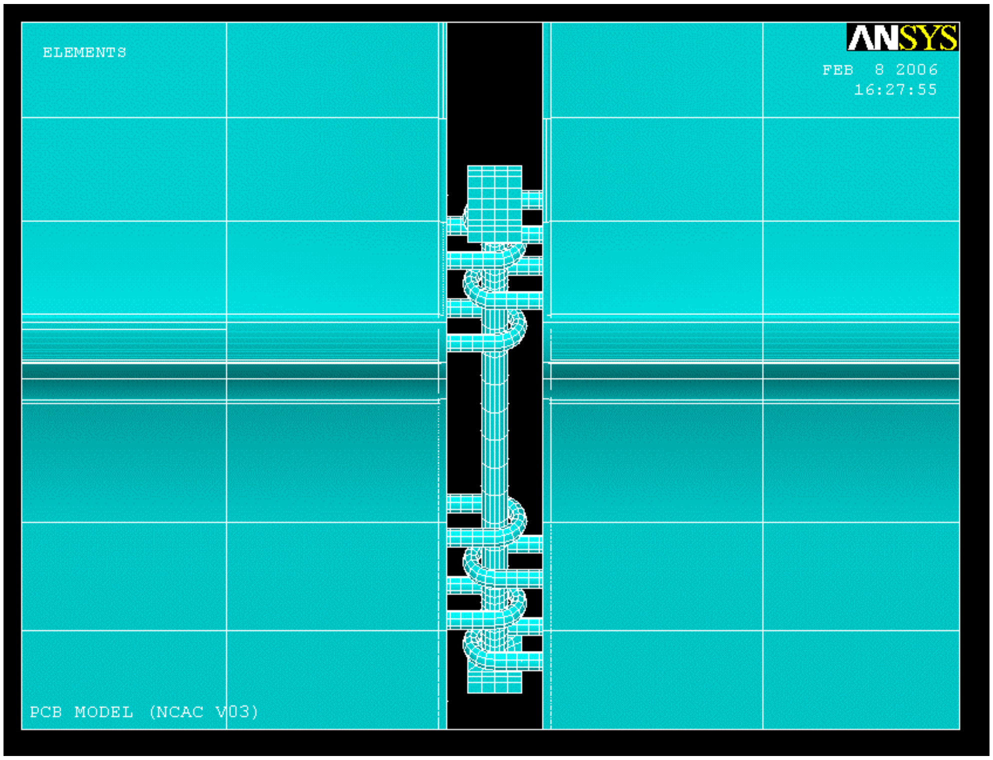

Figure 4-15 Finite element model of joints for ODOT barrier

As we did in the first model study, we again used the same relationship for the friction definition. Several analyses showed that by assigning μ_d=0.3, μ_s=1.0 and μ_{dc}=0.001 at the contact card between the vehicle and the barrier and changing values of μ_d=0.5-0.7, μ_s=1.0 and μ_{dc}=0.001 for the contact between the barrier and the asphalt pavement and μ_d=0.3, μ_s=1.0 and μ_{dc}=0.001 between the vehicle and the asphalt pavement, the behavior of the components during the whole simulation agreed well with that of full scale crash test. The number of parts, elements and nodes can be summarized as below;

Table 4-4 Summary of finite element model

	Vehicle			Barrier	
	Shell	Solid	Beam	Shell	Solid
Element #	10101	447	49	28413	2230
Node #	11250			32442	
Part # (group of elements)	61			160	

4.4.2 Results

At approximately 0.069 seconds after impact, the vehicle began to redirect and after 0.039 sec the barrier segments began to move. At approximately 0.174 sec. after impact, the vehicle was traveling parallel with the barrier. The vehicle remained in physical contact with the longitudinal barrier series for 285 msec. This was measured as 276 msec in the crash test.

The maximum displacement obtained from the full scale ODOT crash test was 32 inches (813 mm). This study resulted in a maximum displacement of 31 inches (787.5 mm) which was measured at the downstream end of segment 10 at joint 10-11. Segment 7 through segment 12 was disturbed with static deflections varying from 0.1 in to 31 inches. None of the segments or pin and loop connections appeared to fail. Figure 4-16 and 4-17 show the Y direction displacement and velocity responses of the ODOT-PCB, respectively.

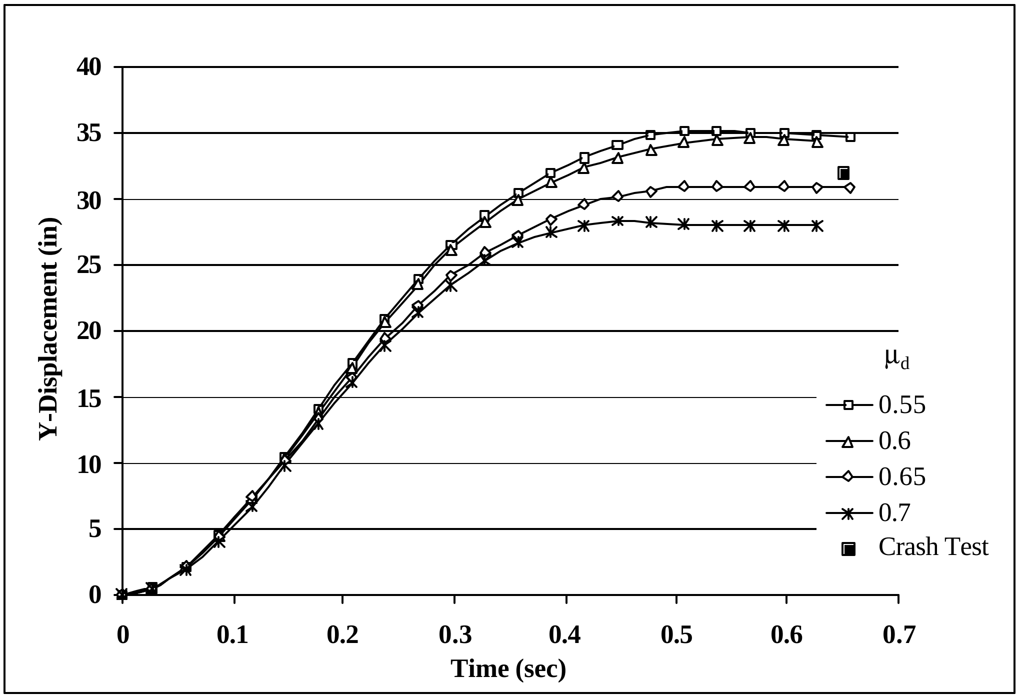

Figure 4-16 Displacement-time history of the node of PCB between segments 10-11 for different friction coefficients

As we can see from Figure 4-16, LS-DYNA results agreed well with the crash test results. Referring the different friction coefficients in that figure we recommend a dynamic friction coefficient of 0.63 between the concrete barrier and the asphalt pavement. LS-DYNA analyses resulted in a very close maximum displacement with that of obtained in the crash test.

The vehicle sustained moderate damage primarily to the right front. The structural deformation of the right frame rail, right rod ends and right door were experienced the main damage. The vehicle left the barrier orientation with an angle of 9.8 degrees which is less than 60 % of the impact angle of 25 degrees as it is mentioned in NCHRP Report. This was measured as 12 degrees in the crash test. The animation of the simulation can be seen in Appendix B.

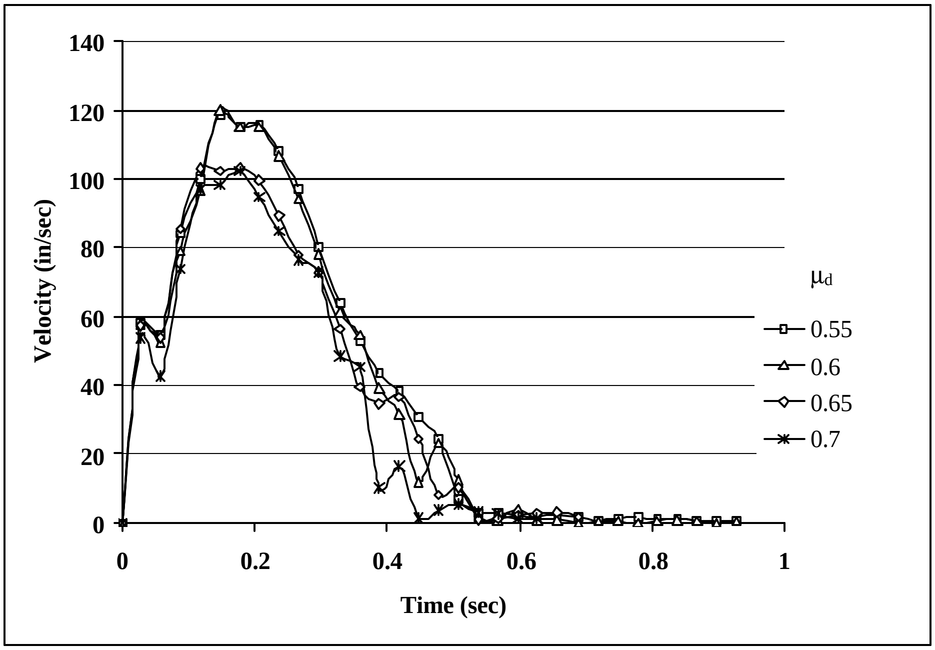

Figure 4-17 Velocity-time history of the node of PCB between segments 10-11 for different friction coefficients

4.5 Rigid Body Assumption for Portable Concrete Barriers

We have presented the finite element results of the vehicle-barrier impact for the two available crash tests. In these simulations, both the vehicle and the barriers are considered deformable. Now, we examine the effect of assuming barriers as rigid bodies. In general, the analyses with rigid body assumption for barriers are found to be reasonably close to those from earlier analyses with deformable barriers. Figure 4-18 shows the displacement-time history results for the ODOT simulation. It can be seen that the rigid body analysis provides a reasonably accurate prediction of the barrier displacement. In fact, the maximum displacement matches the crash test better. This provides us the justification for the use of MSC Working Model (based on the Newtonian rigid body mechanics) for our subsequent analyses and the development of design curves.

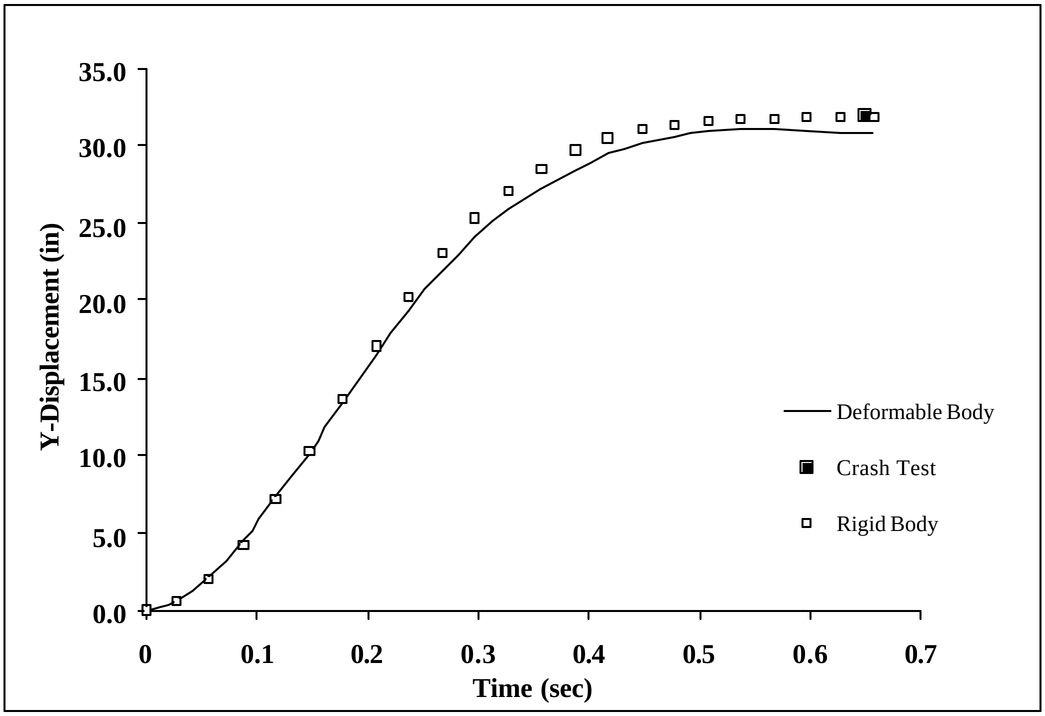

Figure 4-18 Comparison of LS-DYNA and crash test results for two different barrier models

4.6 Summary

In this chapter, we presented the finite element based modeling and simulation of the two crash tests. We introduced the elements of FE models and described each element for both tests. Then, we presented the FE results obtained from ANSYS/LS-DYNA for both crash models. Results agreed reasonably well with the actual crash tests. The maximum barrier displacements obtained from the first analyses are 60 in and 31 in, whereas they were measured as 60.6 in and 32 in at the crash tests. This provides us confidence in the reliability of finite element based simulation of vehicle-barrier impact. Furthermore, a rigid body assumption for barrier in MSC Working Model is reasonable and provides good predictions for the displacement response of the barrier.

5 MSC Working Model Based Study

5.1 Introduction

In this part of our study, we are presenting the results that are obtained from MSC Working Model. MSC Working Model, from MSC Software, is a motion simulation product which is capable of analyzing crash scenarios in a low cost and user friendly way. It allows users to quickly build, run, and refine simulations with pre-defined objects, or imported CAD models in different formats. Working Model measures forces acting on any part of the simulation, and supports contact, collisions, and friction between parts. Simulations also contain non-linearity or user defined events through a built-in equation language.

5.2 Simulation of Original NCDOT F-Type PCB - Ford F-250 Pickup Truck Crash Test

5.2.1 MSC Model

The MSC Working Model for this simulation consists of a pick-up truck vehicle, sets of springs simulating the connection pins and loops between the barrier segments, and the test article barriers. For the tests, the vehicle has the dimensions and center of mass similar to a pick-up truck 1994 Ford F-250 with 6 cylinder engine weighing 1993 kg. The North Carolina Department of Transportation (NCDOT) used an identical truck for its crash test level 3-11. The height to the lower edge of the vehicle bumper was 392 mm and it was 625 mm to the upper edge of the bumper.

The connections between barrier segments are as specified by the NCDOT. High strength ASTM 449 25 x 760 mm galvanized pins and A36 steel loops were replaced by sets of four springs between top side and bottom side of barriers at heights equivalent to the actual connections. According to the NCDOT crash test, none of the connections failed or bent; therefore, all the springs in the model are linear elastic with their spring constant proportional to the maximum elastic force of the weakest point of failure, which is shear in the loops.

The barriers are the test articles. In this model they are similar to the 32 in high F-type portable barrier in segments of 10 ft in length. The base width is 24 in and the barrier tapers to a 6 in width at the top. Twenty of these barrier segments were lined up in order to obtain the 200 ft required by NCHRP Report 350. To validate the model, the parameters were adjusted and calibrated based on the crash test level 3-11 performed by the NCDOT. The used barrier geometry and other properties were mentioned before in the crash tests part. The installation length was 200ft with 20 barrier segments. In the test the pick-up truck hit the barriers at a speed of 62.4 mph at an impact angle of 25 degrees. The maximum deflection obtained in this crash test was 60 inches. The adjusted parameters for the simulation with same characteristics were:

- Coefficient of friction: 0.40
- Coefficient of restitution of vehicle: 0.15
- Weight of the vehicle: 1993 kg

An integration step of 0.001 seconds was used for each simulation run.

5.2.2 Results

Table 5-1 summarizes the results obtained before the validation of this crash modeling. Figures 5-1 shows maximum deflection-impact speed curves (validation charts) for different coefficient of friction (CF) and coefficient of restitution (CR) for NCDOT type of barrier. Also, image of the simulated impact for this type of barrier is shown in Figure 5-2.

Table 5-1 Summary of the NCDOT simulation

Case Study	Coefficient of Friction	Coefficient of Restitution	Maximum Predicted Barrier Deflection	Ratio of Predicted/Measured Deflection
1	0.40	0.25	69.26	1.154
2	0.40	0.15	62.20	1.036
3	0.50	0.25	53.67	0.894
4	0.50	0.15	51.00	0.850

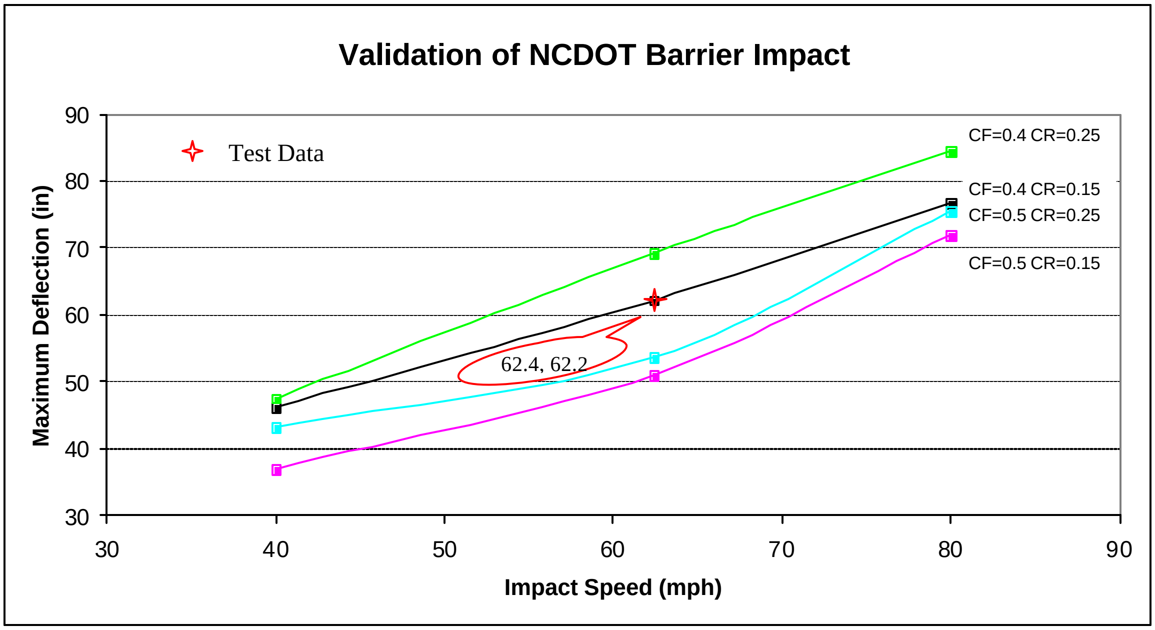

Figure 5-1 Validation of NCDOT crash test

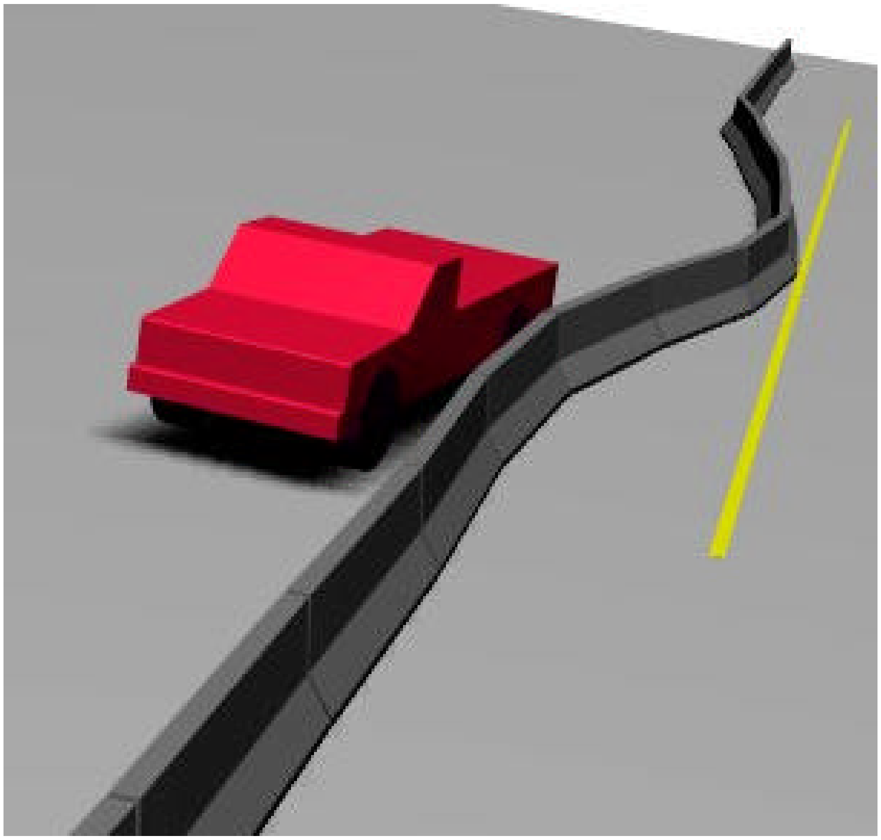

Figure 5-2 MSC model after the crash

Figures from 5-3 to 5-13 illustrate the results of the parametric study. They are presented in terms of the maximum displacement of the barrier segment under constant value of the vehicle weight (4500 lbs) and changing values of the impact speed and impact angle under different friction and restitution coefficients of the analysis. The design aids were developed in terms of two primary parameters, impact angle and impact speed. Four different impact angles were used; 7.5^o, 15^o, 25^o, and 40^o. Four different impact speeds were considered; 35, 45, 65, and 75 Mph. The design aids were all developed for the same spring constant as used in the validation model. However, in order to compare with the finite element analysis, three sets of coefficients of friction and restitution were used, each being 0.2, 0.35, and 0.5. Therefore, for each pair of these coefficients, the maximum deflection of the barrier was shown as a function of impact angle and impact speed in the figures that accompany this report. Sensitivity of the model to the coefficients of friction and restitution are summarized in two of the figures. Finally, typical impacts for 35^o and 60^o are shown for visual aid. After the data shown in the figures are compared with the results of the finite element analysis, further parametric studies were carried out to develop design aids.

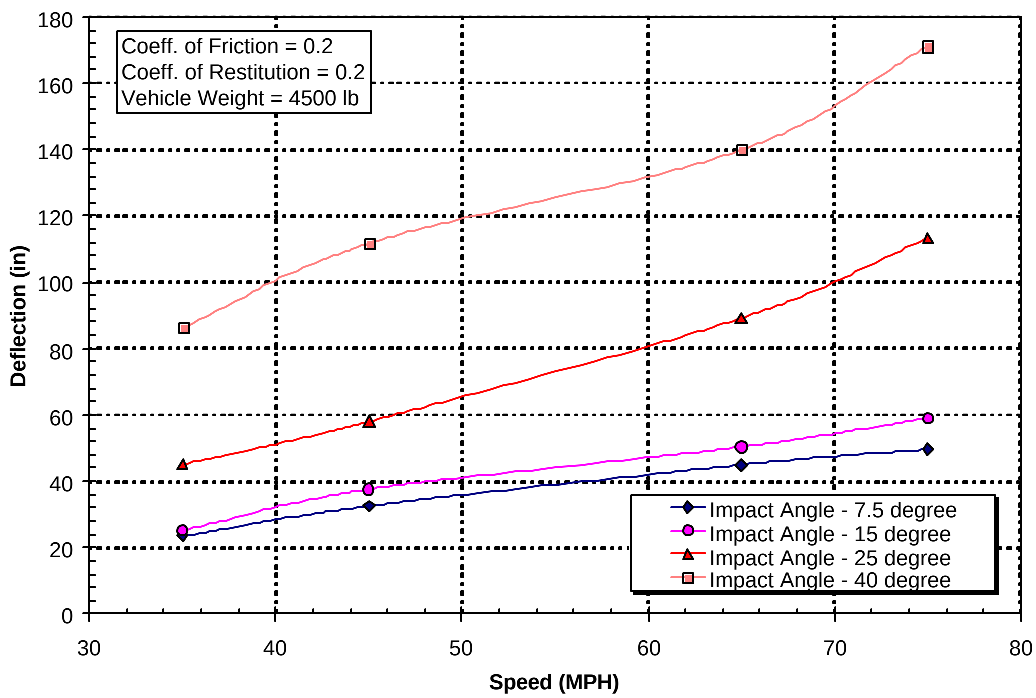

Figure 5-3 a) Deflection-speed curve for m=0.2, e=0.2

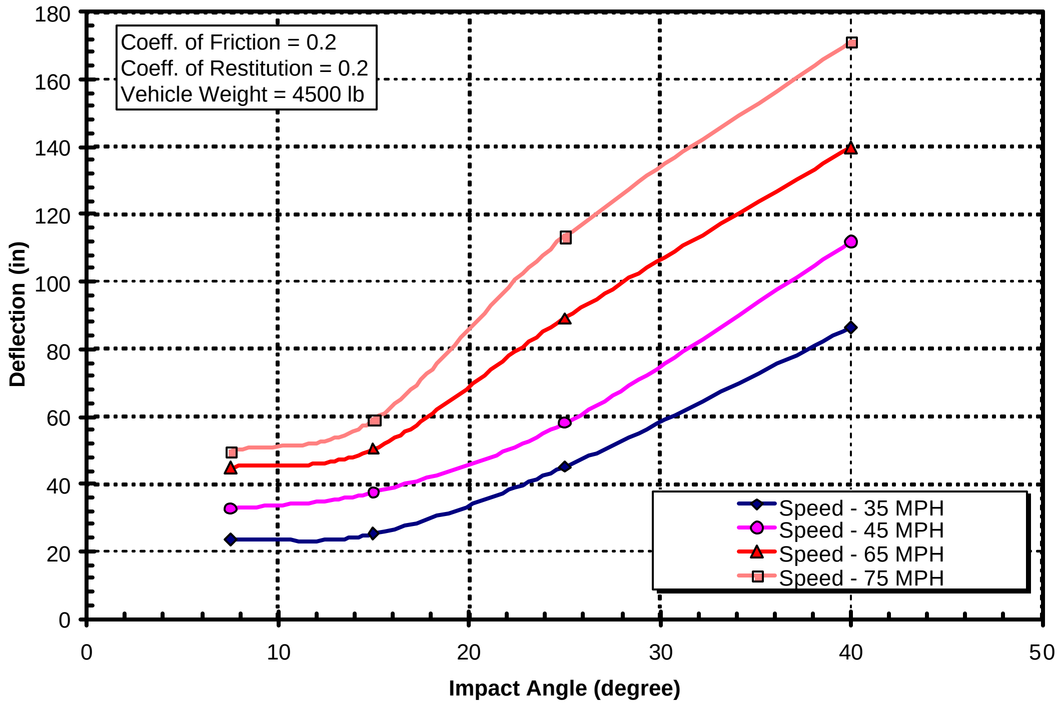

Figure 5-3 b) Deflection-impact angle curve for m=0.2, e=0.2

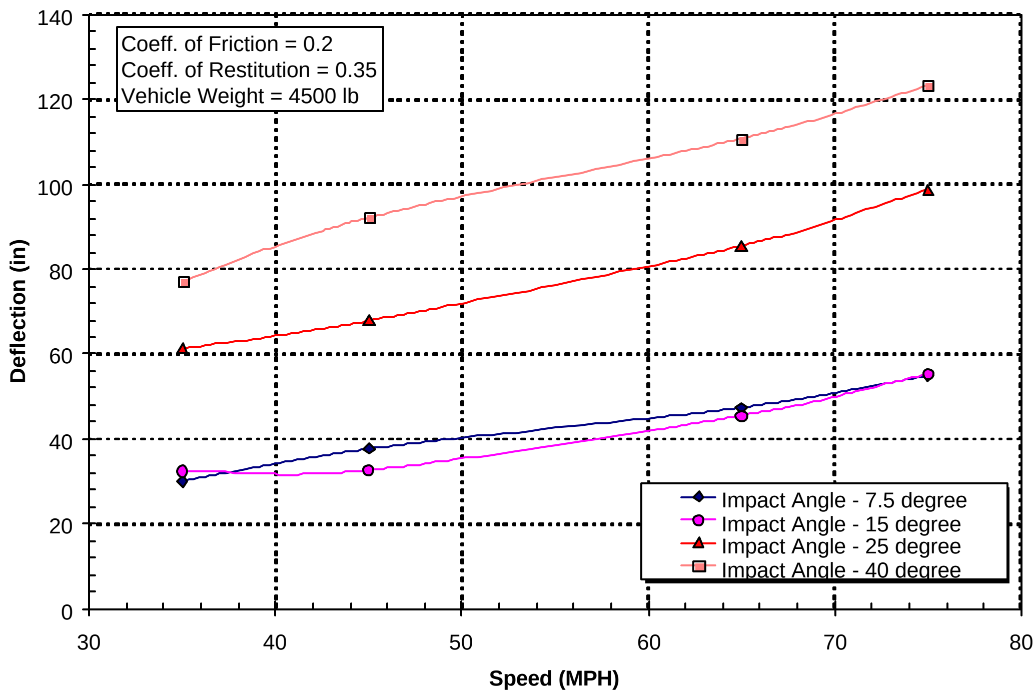

Figure 5-4 a) Deflection-speed curve for m =0.2, e=0.35,

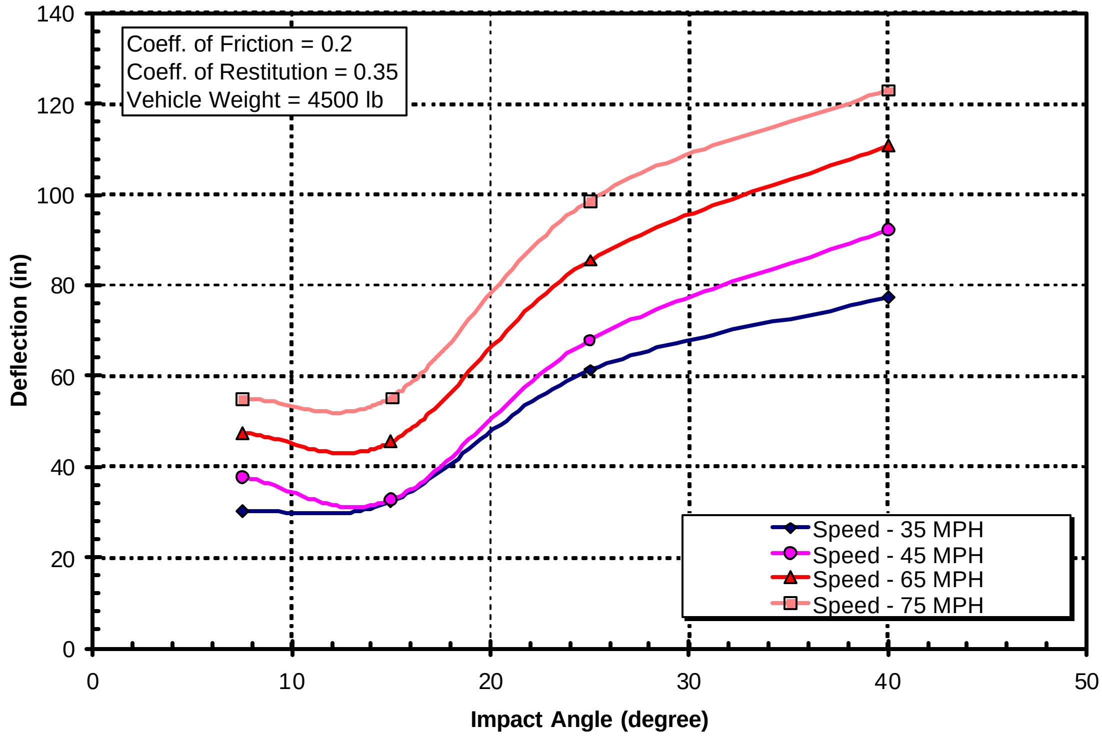

Figure 5-4 b) Deflection-impact angle curve for m =0.2, e=0.35

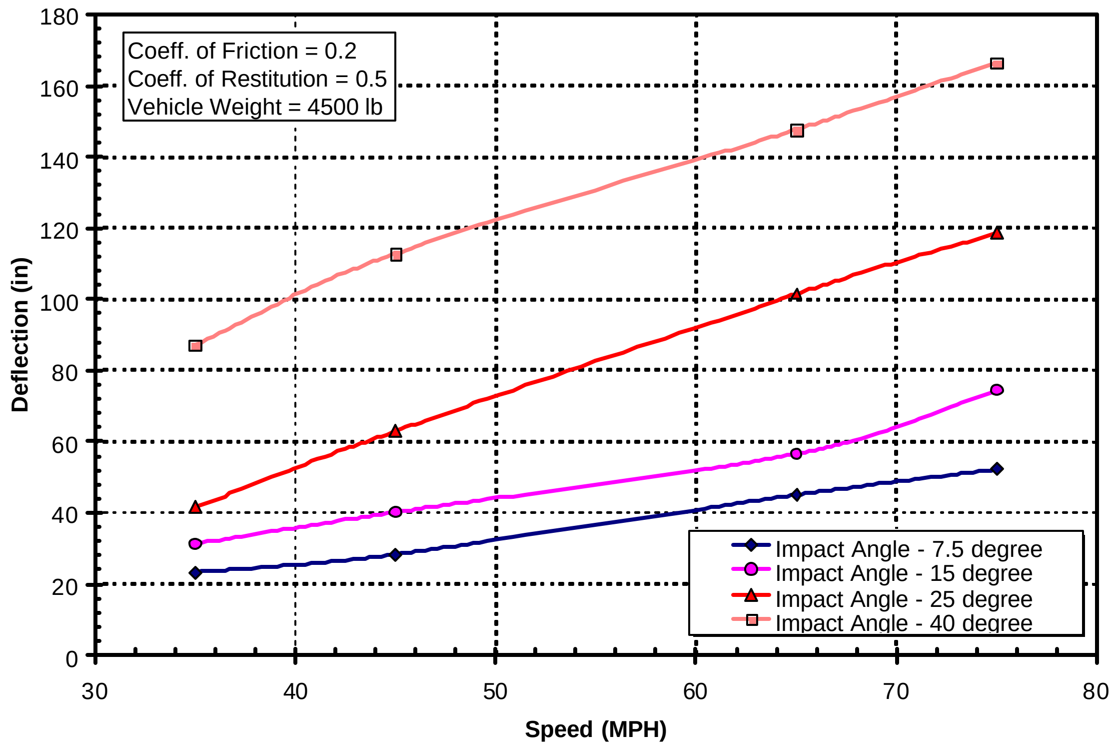

Figure 5-5 a) Deflection-speed curve for m =0.2, e=0.5,

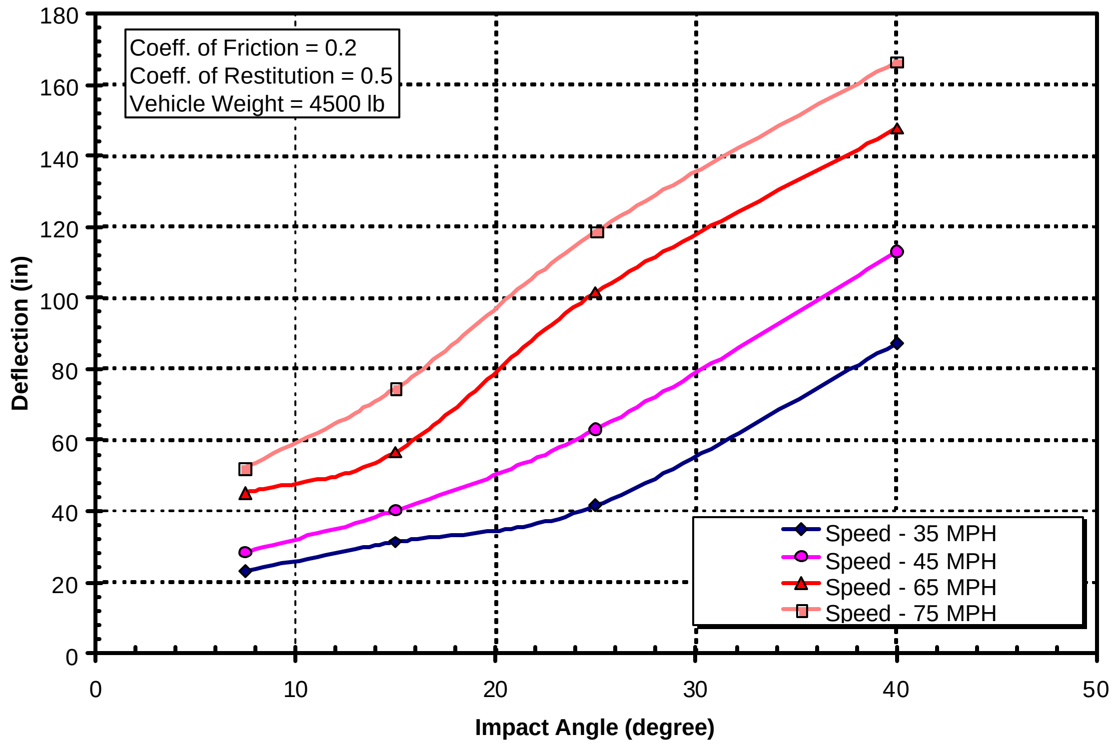

Figure 5-5 b) Deflection-impact angle curve for m =0.2, e=0.5

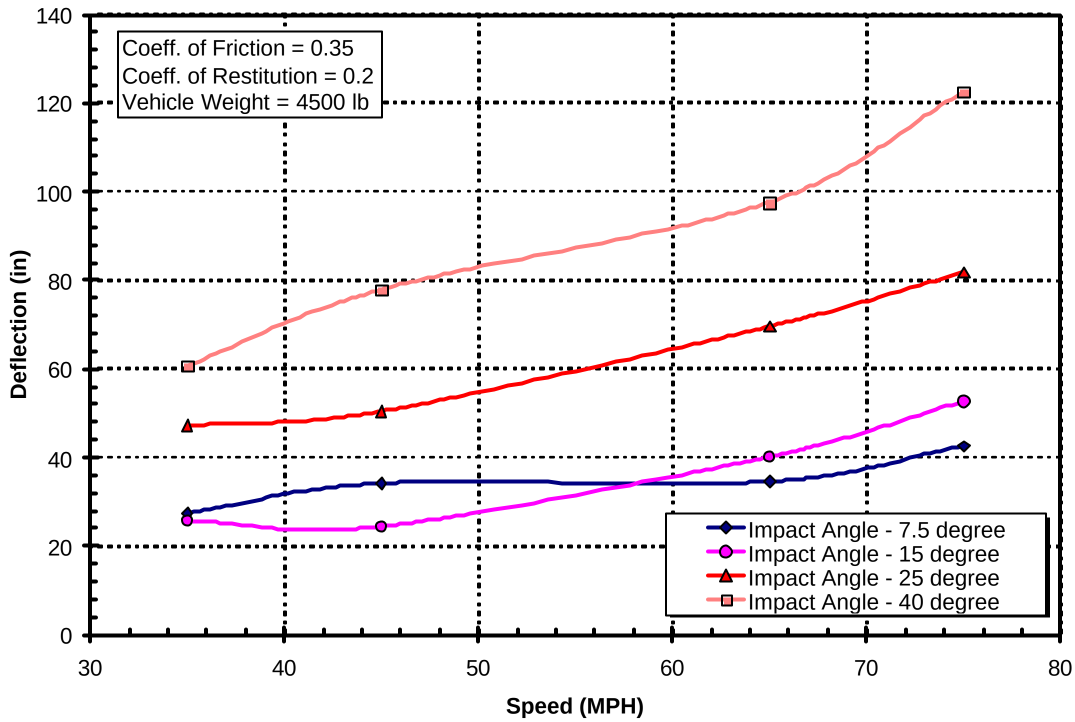

Figure 5-6 a) Deflection-speed curve for m =0.35, e=0.2,

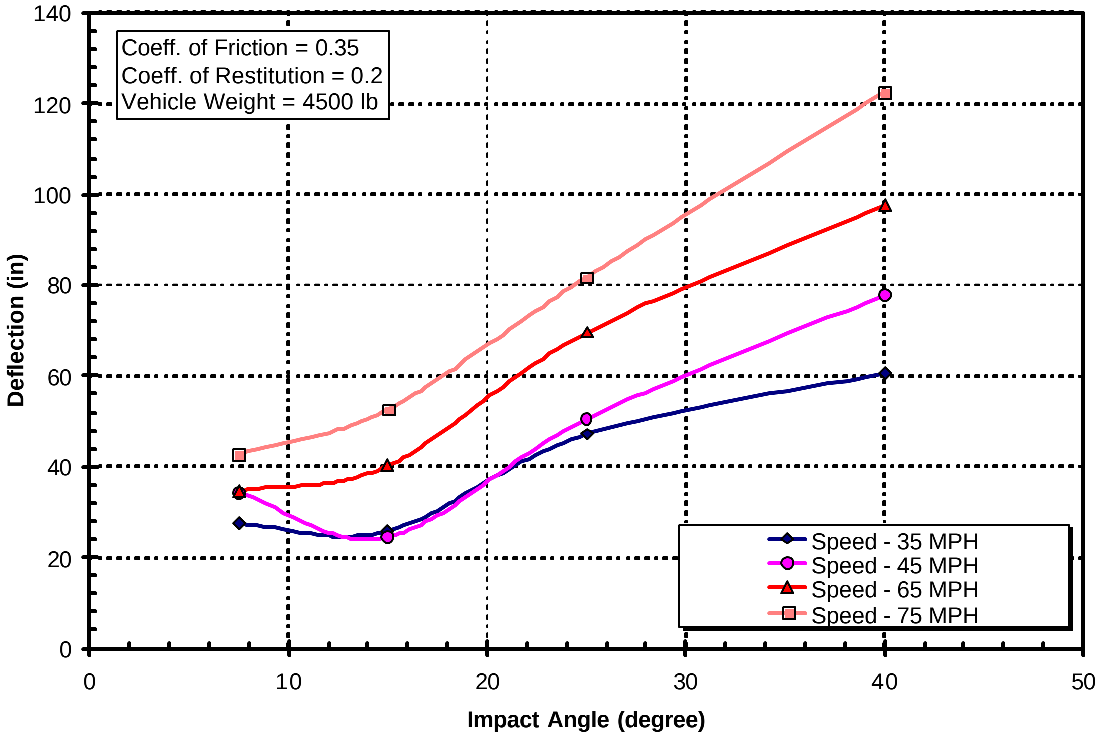

Figure 5-6 b) Deflection-impact angle curve for m =0.35, e=0.2

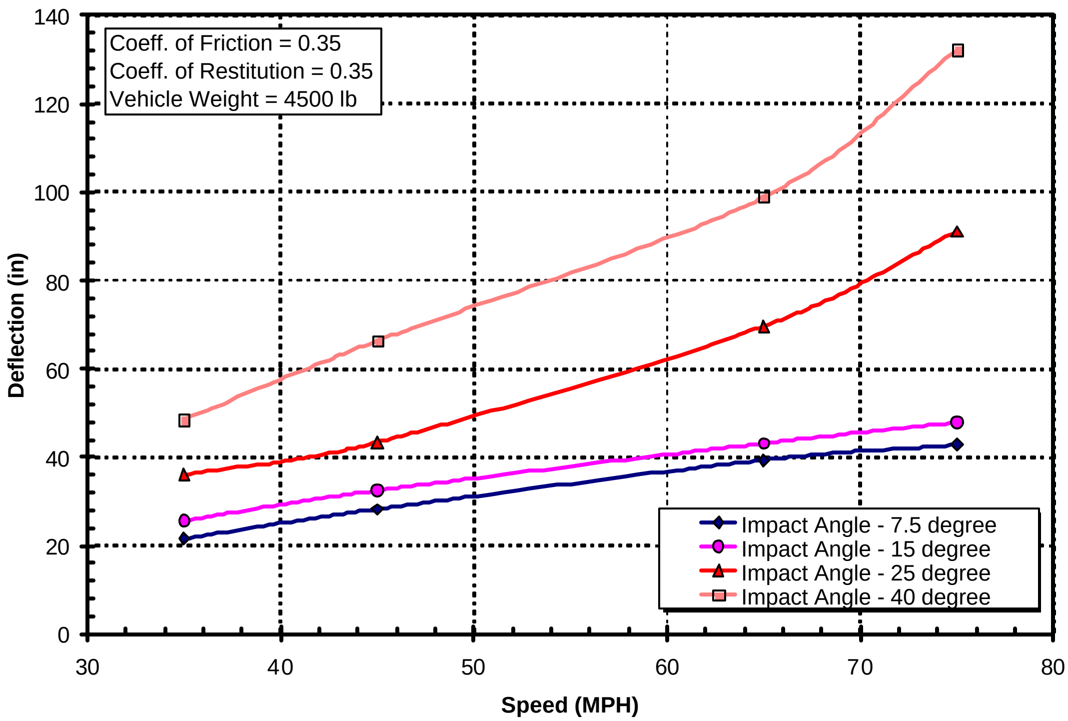

Figure 5-7 a) Deflection-speed curve for m =0.35, e=0.35,

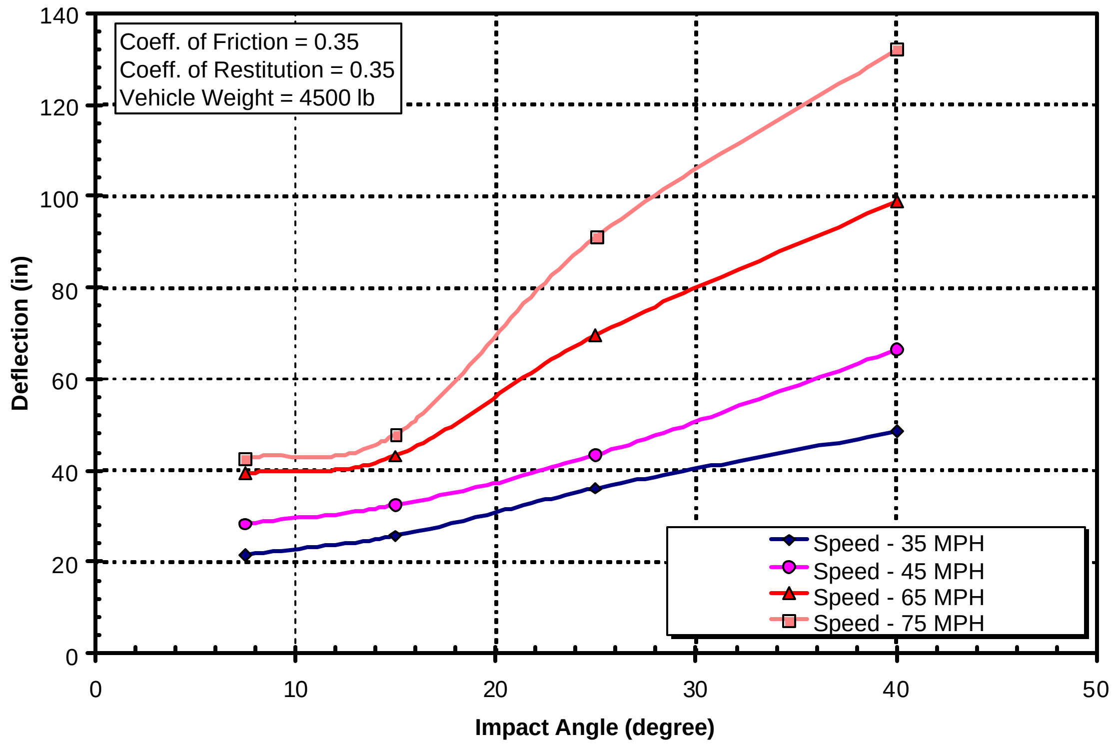

Figure 5-7 b) Deflection-impact angle curve for m =0.35, e=0.35

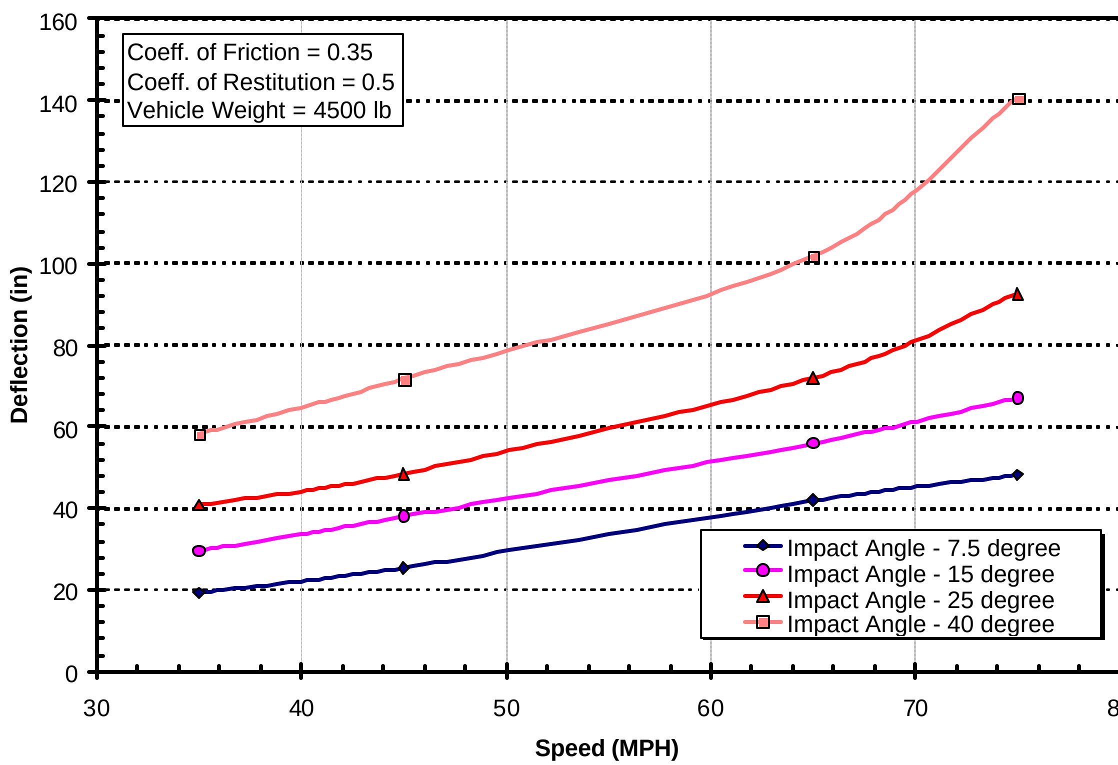

Figure 5-8 a) Deflection-speed curve for m =0.35, e=0.5,

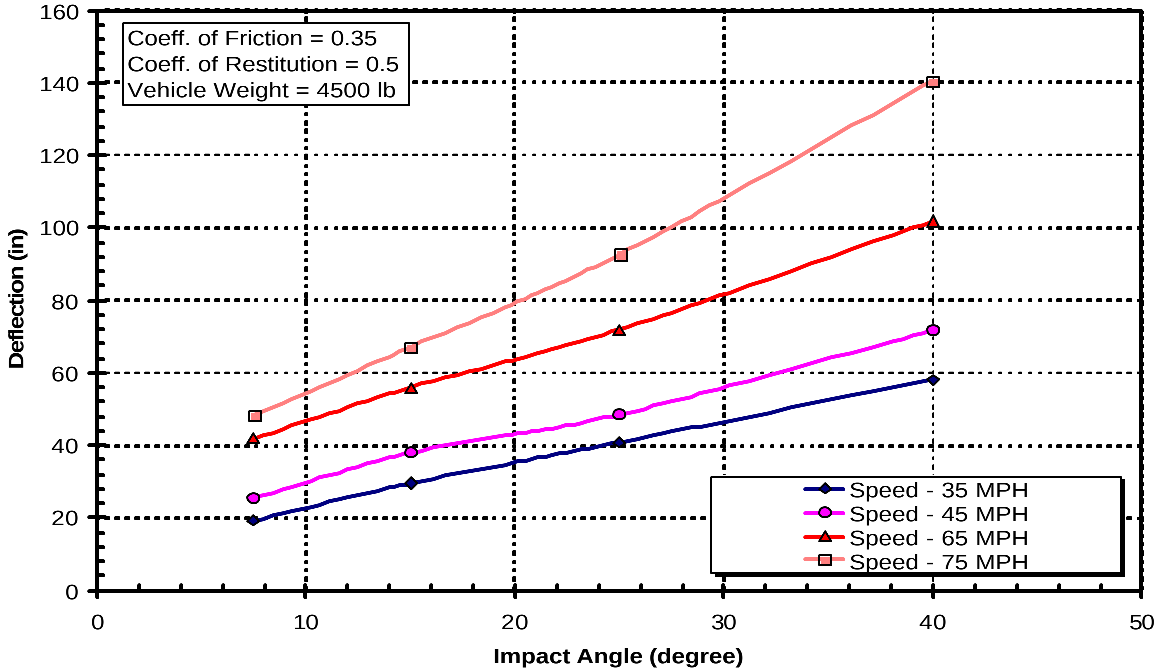

Figure 5-8 b) Deflection-impact angle curve for m =0.35, e=0.5

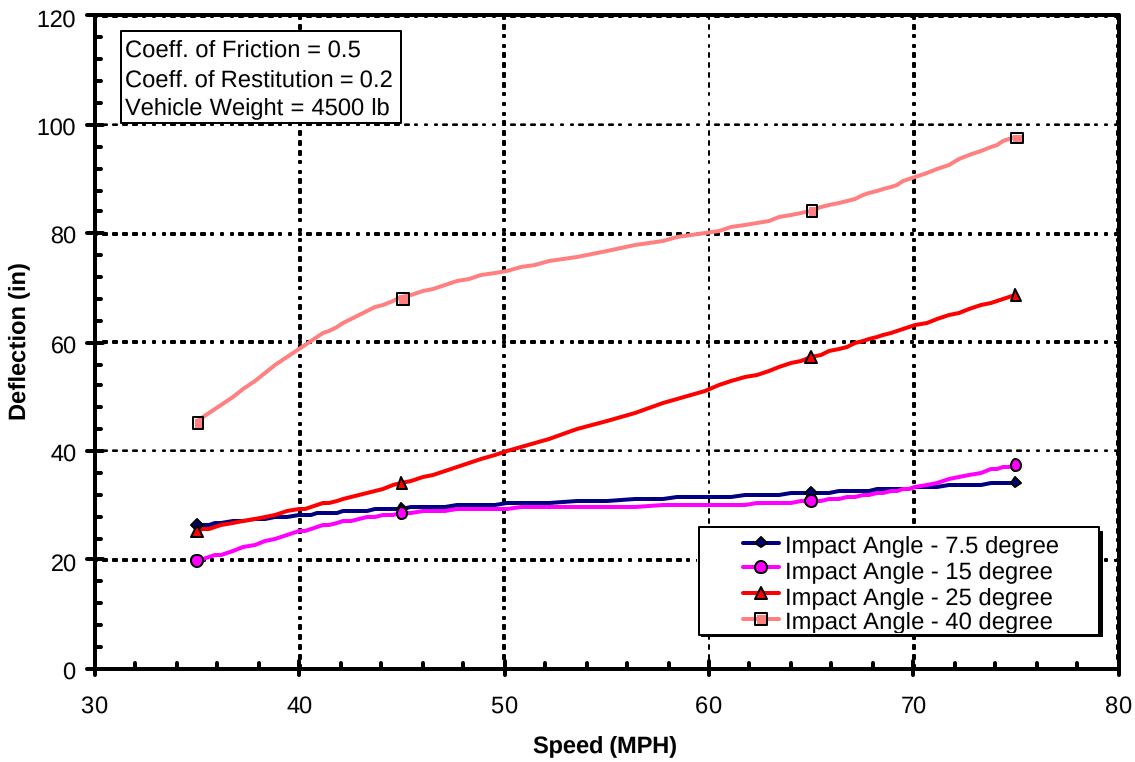

Figure 5-9 a) Deflection-speed curve for m =0.5, e=0.2,

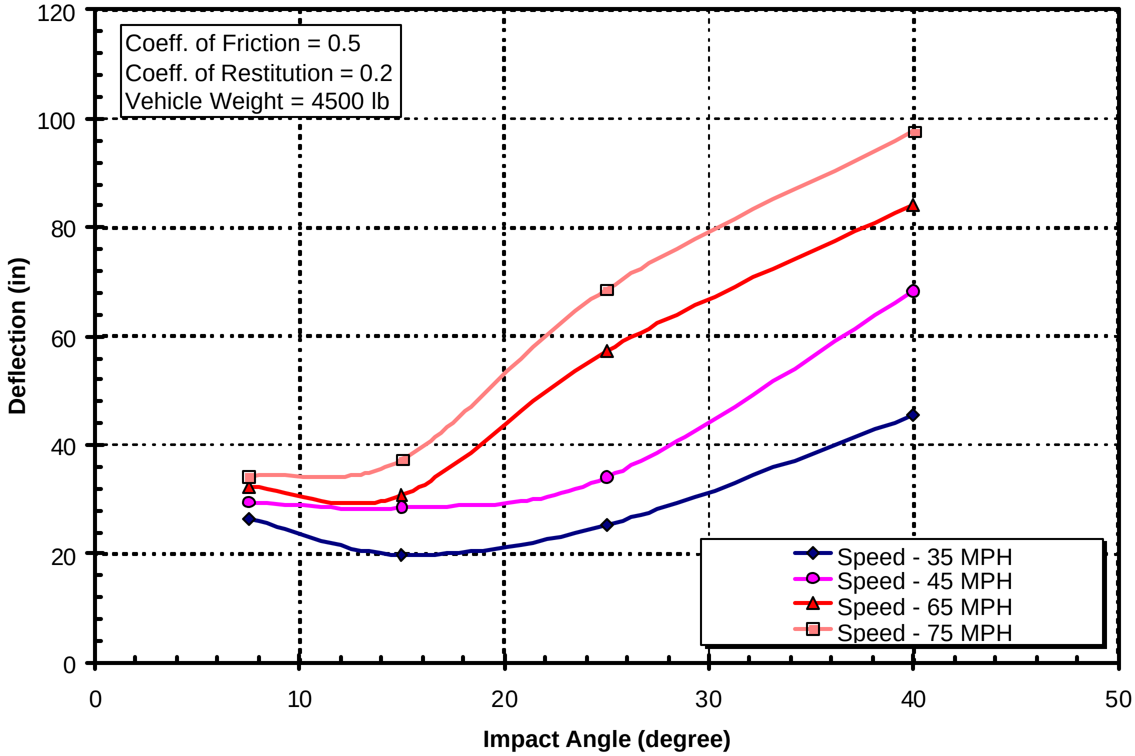

Figure 5-9 b) Deflection-impact angle curve for m =0.5, e=0.2

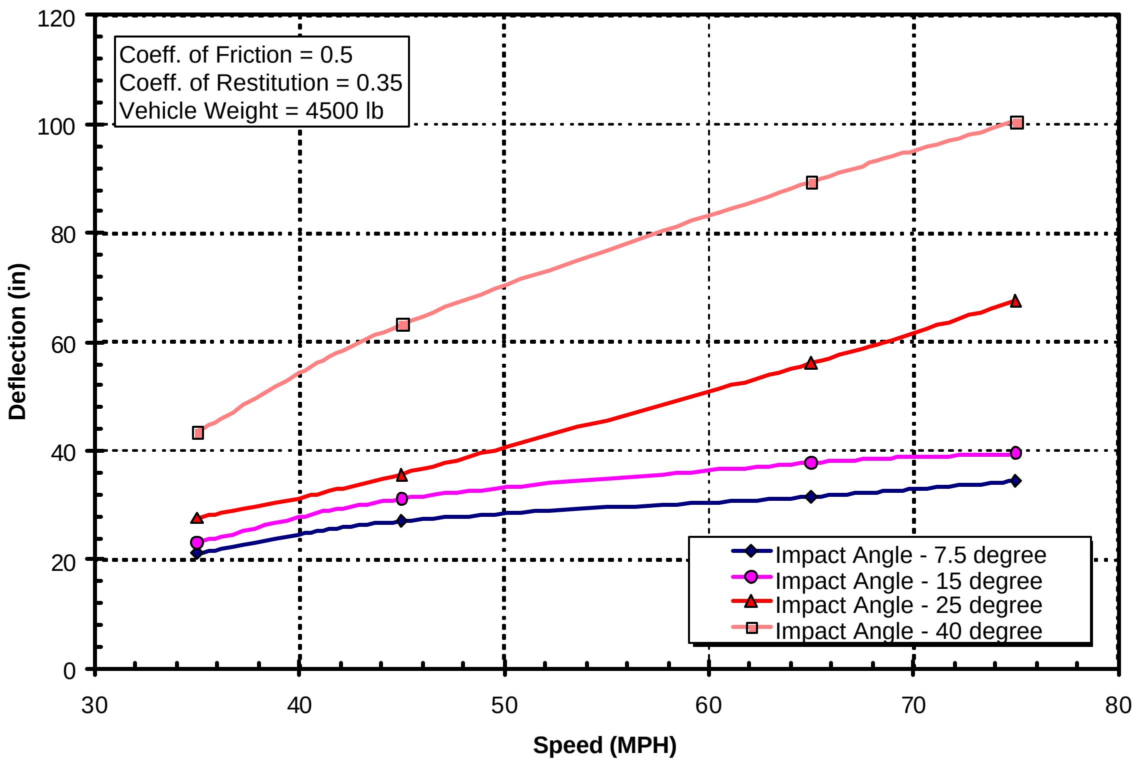

Figure 5-10 a) Deflection-speed curve for m =0.5, e=0.35,

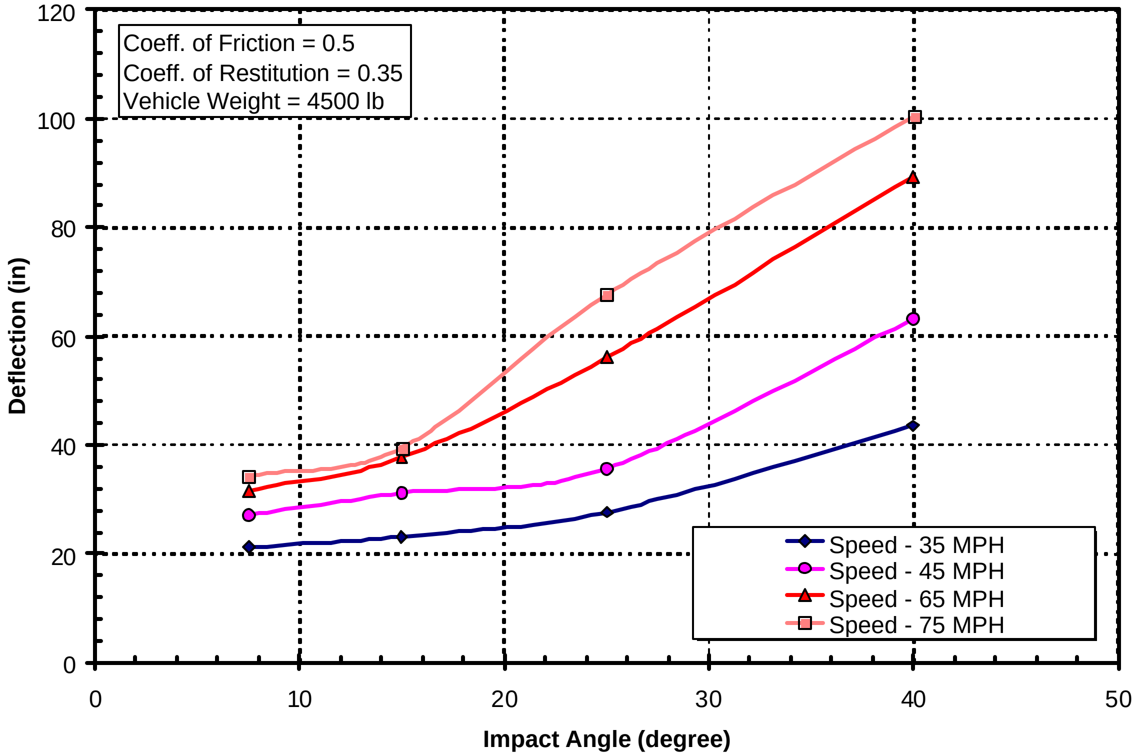

Figure 5-10 b) Deflection-impact angle curve for m =0.5, e=0.35

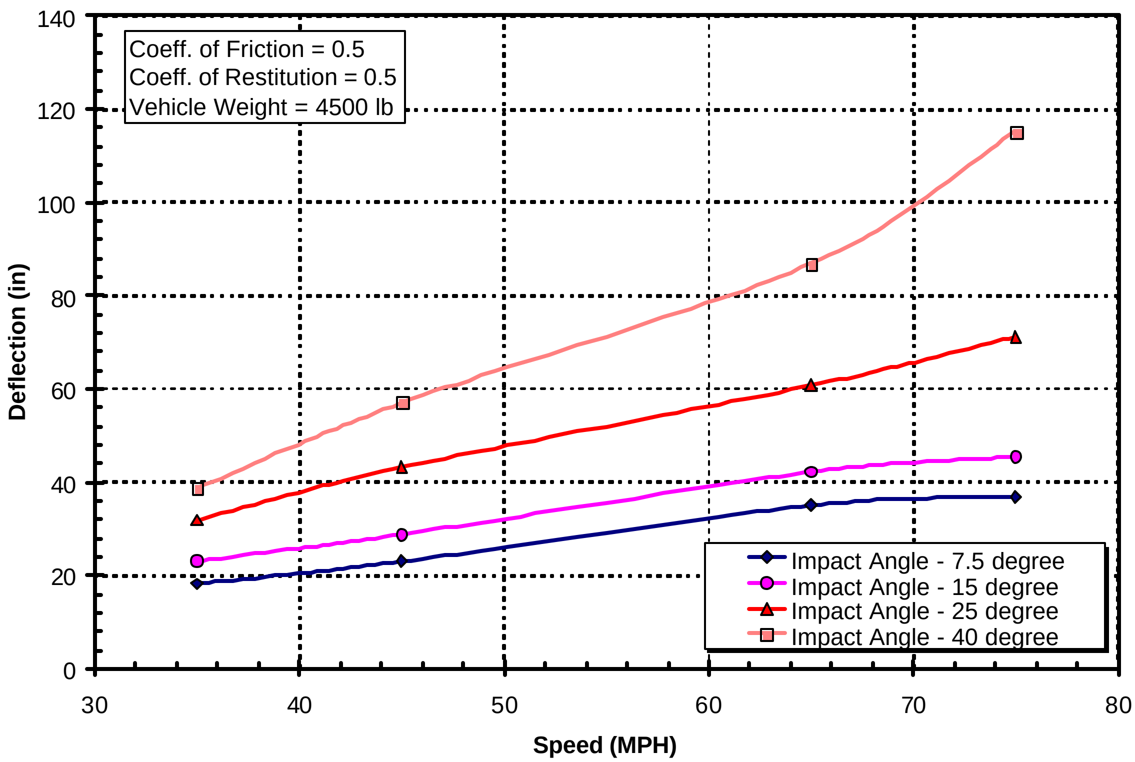

Figure 5-11 a) Deflection-speed curve for m =0.5, e=0.5,

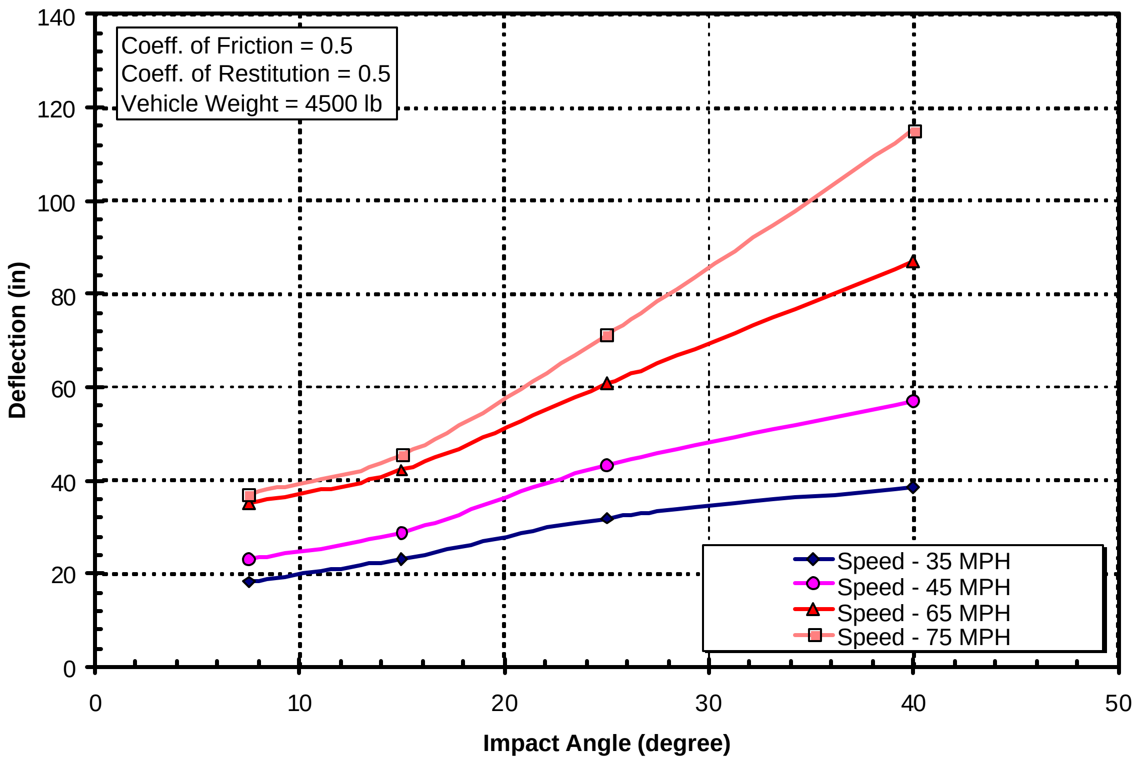

Figure 5-11 b) Deflection-impact angle curve for m =0.5, e=0.5

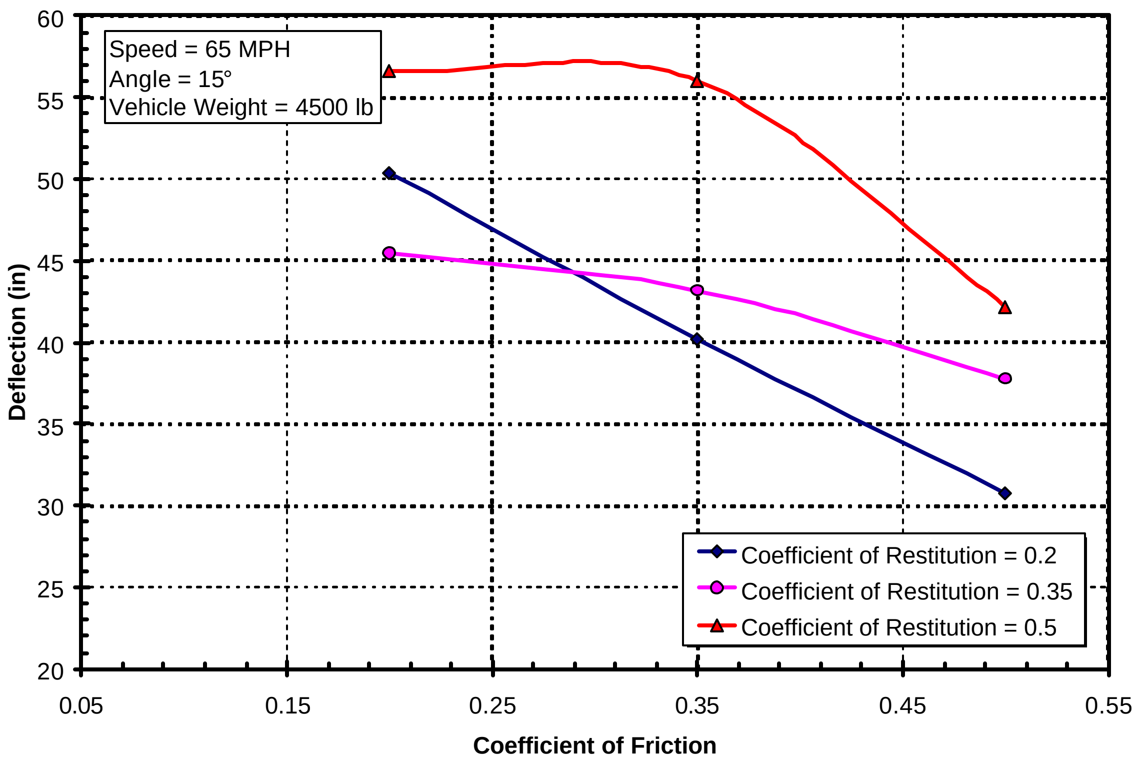

Figure 5-12 Deflection-coefficient of friction relationship

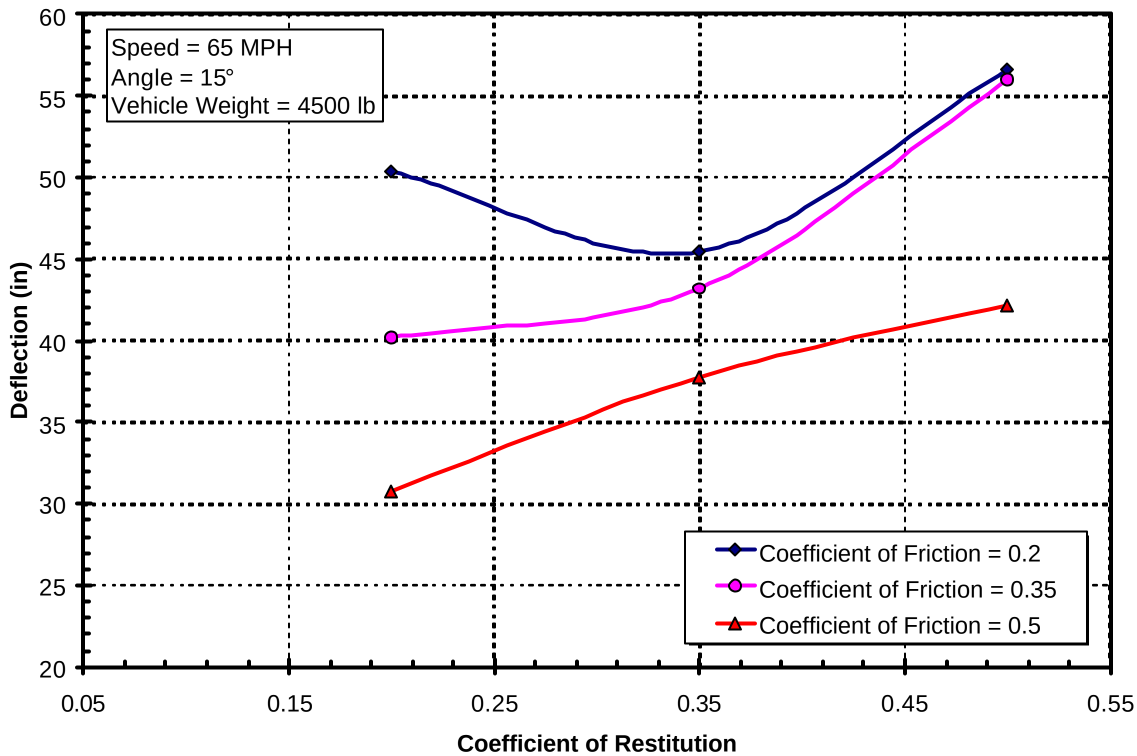

Figure 5-13 Deflection-coefficient of restitution relationship

5.3 Simulation of Original ODOT F-Type PCB - Chevrolet Pickup Truck Crash Test

5.3.1 MSC Model

The MSC Working Model for this simulation again consists of a pick-up truck vehicle, sets of springs simulating the connection pins and loops between the barrier segments, and the test article barriers. For the tests, the vehicle has the dimensions and center of mass similar to a pick-up truck Chevrolet Cheyenne Truck 8 cylinders weighing 4500lb. The Oregon Department of Transportation (ODOT) used an identical truck for its crash test level 3-11 as found in report "Precast Concrete Barrier Crash Testing Final Report SPR 330". The height of the lower end of the bumper is 17.75in and of the upper end are 26.42 in.

The connections between barrier segments are also as specified by the NCDOT. High strength ASTM 449 25 x 760 mm galvanized pins and A36 steel loops were replaced by sets of four springs between top side and bottom side of barriers at heights equivalent to the actual connections. According to the ODOT crash test, none of the connections failed or bent; therefore, all the springs in the model are linear elastic with their spring constant proportional to the maximum elastic force of the weakest point of failure, which is shear in the loops.

The barrier and the vehicle model properties are the same as specified in the crash test. To validate the model, the parameters were adjusted and calibrated based on the crash test level 3-11. The installation length was 200ft with 20 barrier segments. In the test the pick-up truck hit the barriers at a speed of 62.4 mph at an impact angle of 25 degrees. The maximum deflection obtained in this crash test was 32 inches.

The adjusted parameters for the simulation with same characteristics were:

- Coefficient of friction: 0.40
- Coefficient of restitution of vehicle: 0.30
- Weight of the vehicle: 2042 kg

An integration step of 0.001 seconds was used for each simulation run.

5.3.2 Results

Table 5-2 summarizes the results obtained before the validation of this second crash modeling. Then, in Figure 5-14, the validation charts for ODOT type barrier can be seen. This completes the validation of the MSC/Working Model for Oregon Tall F barrier crash test. Figure 5-15 shows the post-impact image of the validation model for a coefficient of restitution of 0.30 and friction of 0.4. The following results in the table below were obtained, using coefficient of frictions of 0.40 and 0.50 and coefficient of restitutions of 0.2 and 0.3. Note that the maximum barrier deflection measured during crash tests was 32 in. The spring constants were adjusted compared to the NC model based on the joint details.

Table 5-2 Summary of the ODOT simulation

Case Study	Coefficient of Friction	Coefficient of Restitution	Maximum Predicted Barrier Deflection	Ratio of Predicted/Measured Deflection
1	0.40	0.2	39.02	1.22
2	0.40	0.3	36.20	1.13
3	0.50	0.2	24.36	0.76
4	0.50	0.3	22.14	0.69

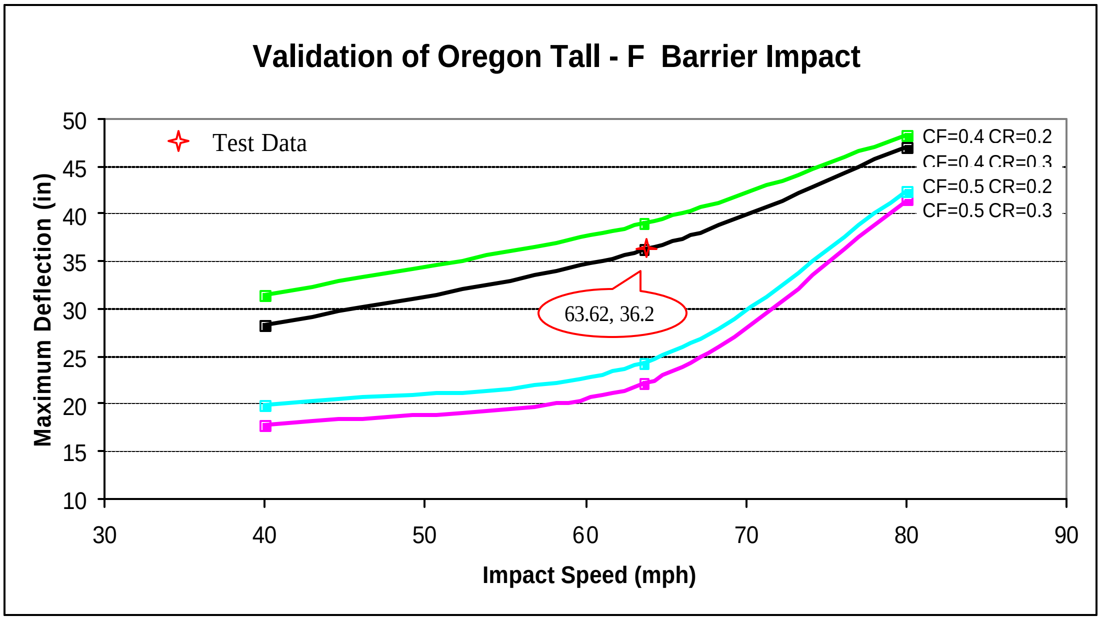

Figure 5-14 Validation of ODOT crash test

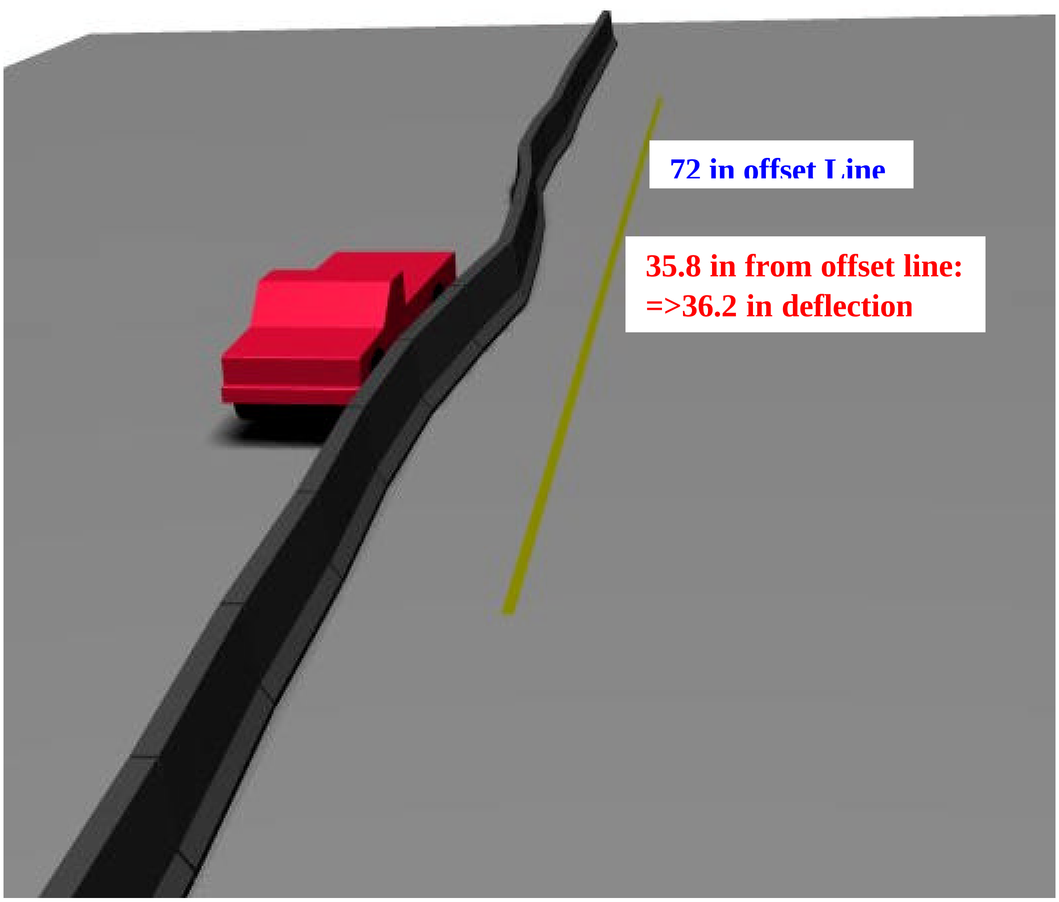

Figure 5-15 Post-Impact Image of Oregon Crash Test Model Using Coefficient of Restitution of 0.3

5.4 Summary

In this segment of our report, we presented the results obtained from MSC Working Model. It has been determined that the analyses of the two crash models resulted in good agreement with the actual crash tests. MSC Model is advantageous to use in this kind of crash scenarios because on one hand, it provides easy to use environment with accurate and detailed results, on the other hand it is cost effective and based on Newtonian Mechanics. The work done by using MSC Working Model is parallel to the work done by using finite elements. After an extensive verification of finite element based study, we went through the actual analysis and simulation of the full scale crash tests by using LS-DYNA and MSC Working Model. Both studies provide reasonably good results; however, as expected, FE based study provides better results. On the other hand, a further analysis done by using finite elements and with a rigid body simplification of the barriers resulted in a better agreement with the ODOT crash test. This shows that the rigid body assumption used in MSC working model is justifiable.

6 Design Curves

6.1 Introduction

The purpose of design curves for the NCDOT is to eliminate the current methodology of using an impact severity formula, which is based on the Kinetic Energy principle and tends to be highly empirical. In addition, the current methodology does not correlate well with the crash test data. Instead, in accordance with NCDOT, here in this study, an attempt is made to develop design charts correlating the deflection of the barrier with the vehicle design speed for two different types of barriers, i.e., NC and OR, and for two different types of pavements, i.e., asphalt and concrete. The charts are developed using the calibrated models discussed in previous chapters.

6.2 Method

Four series of design charts are developed using the MSC Working Model, one for each combination of barrier type (i.e., NCDOT or ODOT barriers) and pavement type (asphalt or concrete). In all design charts, the same vehicle weight of a standard pick-up truck is used. Also, the coefficient of restitution is assumed to be the same as that used in the calibration of each type of barrier, as discussed earlier in Chapter 5. In each design chart, instead of the current practice of using an impact angle, distance from the lane centerline to the face of the barrier is taken as the varying parameter. In order to correlate the offset parameter with the impact angle, a detailed interpolation was made from the table in the current NCDOT design manual. It is assumed that each lane is 12 ft wide, and that there is a 2 ft offset from the face of the barrier to the first lane of traffic. Figures 6-1 through 6-4 show the design charts for the two types of barriers and the two types of pavements in this study. In each chart, curves are shown for offsets from 8 ft to 62 ft varying by 6 ft intervals. The corresponding data sets for each design chart are also shown in Tables 6-1 through 6-4. The tables also feature the impact angles for each combination of offset and design speed.

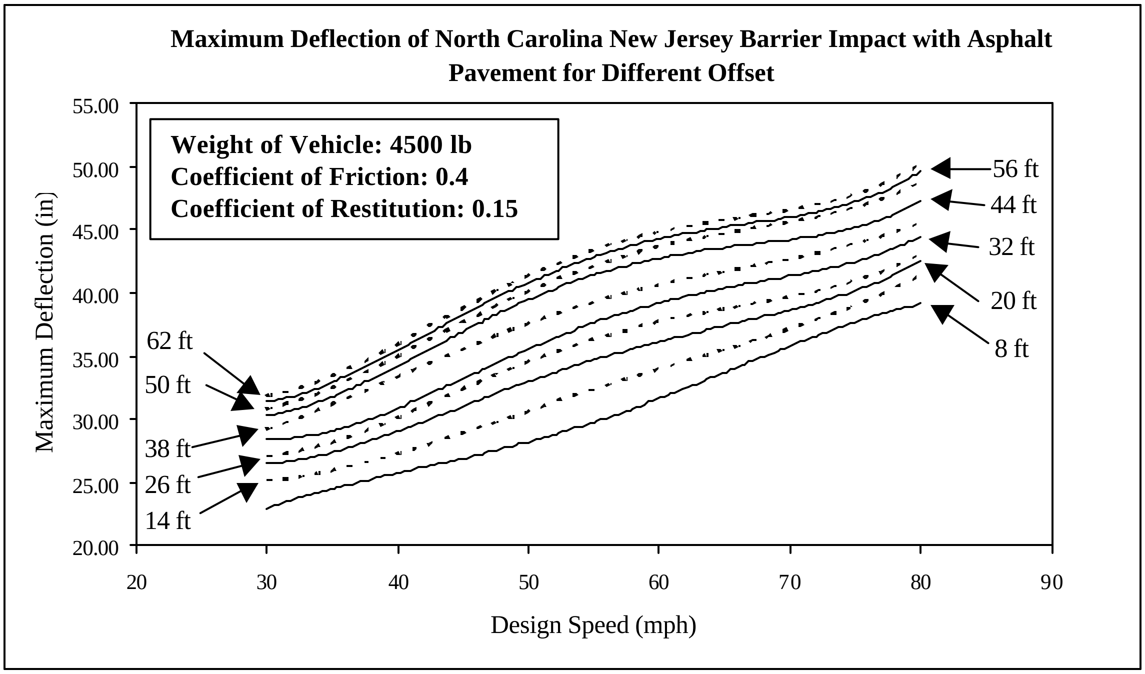

Figure 6-1 NCDOT Barrier impact design curves for asphalt pavement

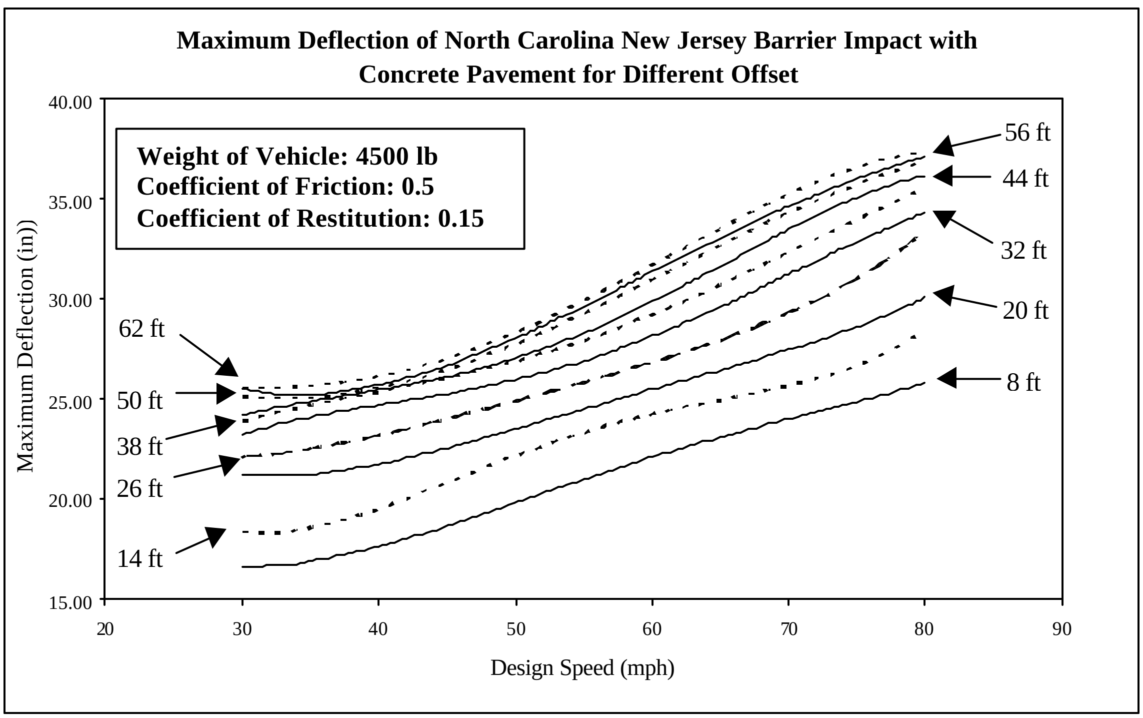

Figure 6-2 NCDOT Barrier impact design curves for concrete pavement

Note: The New Jersey barrier in the titles of above figures (F barrier throughout the report) corresponds to the PCB that has been used in the full scale crash test.

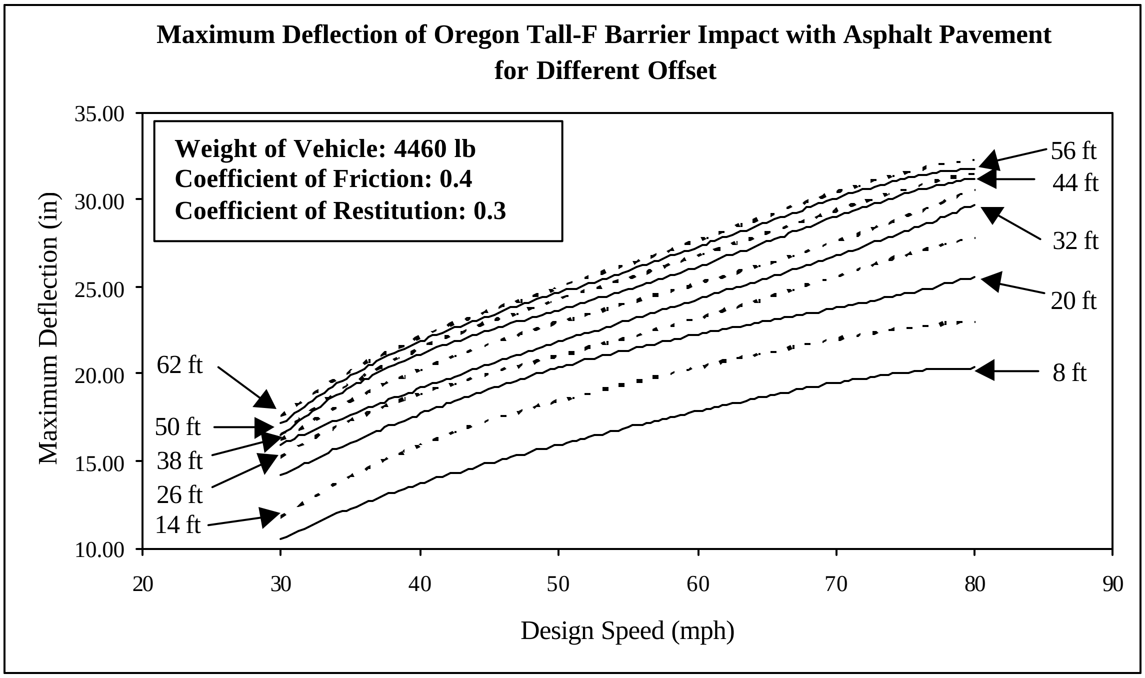

Figure 6-3 ODOT Barrier impact design curves for asphalt pavement

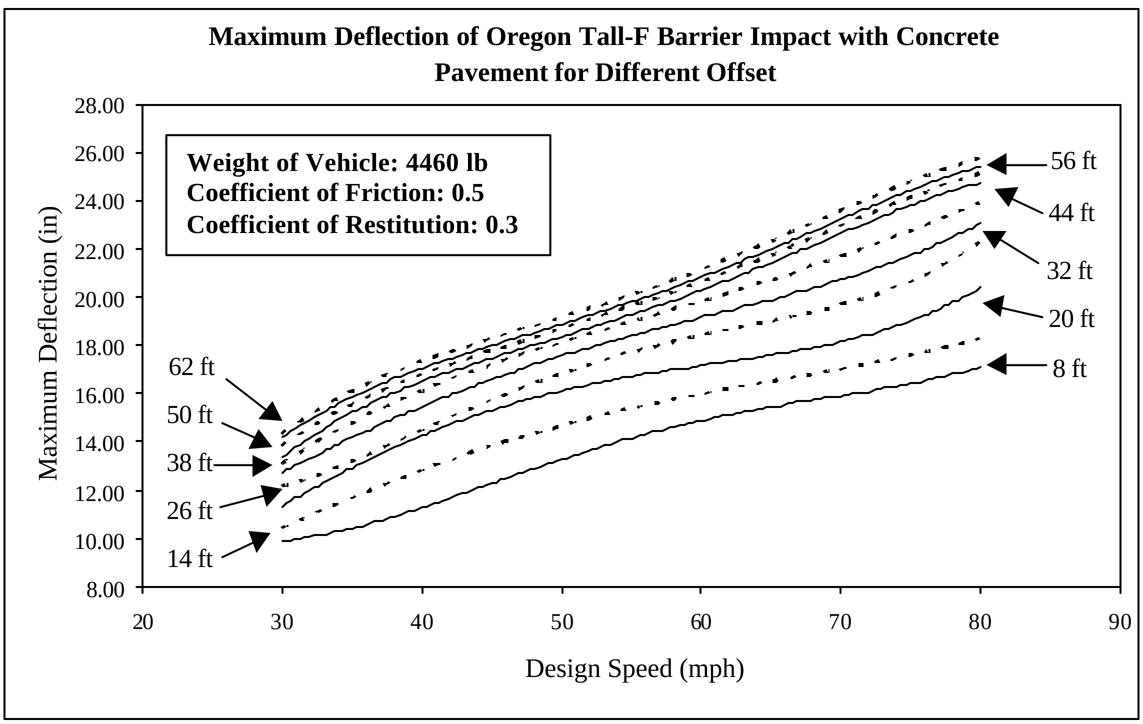

Figure 6-4 ODOT Barrier impact design curves for concrete pavement

Table 6-1 NCDOT Barrier impact design table for asphalt pavement

Impact Angle (degree)/ Maximum Deflection (in)			Design Speed (mph)					
			30	**40**	**50**	**60**	**70**	**80**
Offset (ft)	**8**	**Impact Angle**	11.1	10.4	9.6	8.7	7.7	6.7
		Maximum Deflection	23.00	25.86	28.04	31.86	35.72	39.12
	14	**Impact Angle**	12.7	12.1	11.4	10.5	9.3	8.0
		Maximum Deflection	25.16	27.42	30.43	34.25	37.02	41.45
	20	**Impact Angle**	13.2	12.8	12.2	11.5	10.9	10.3
		Maximum Deflection	26.52	28.94	33.30	35.89	38.77	42.51
	26	**Impact Angle**	13.3	12.9	12.6	12.0	11.3	10.5
		Maximum Deflection	27.14	30.11	34.68	37.62	39.74	43.14
	32	**Impact Angle**	13.3	13.0	12.7	12.4	12.1	11.8
		Maximum Deflection	28.56	30.71	35.99	38.82	41.56	44.38
	38	**Impact Angle**	13.3	13.1	13.0	12.6	12.2	12.0
		Maximum Deflection	29.34	33.23	37.92	40.31	42.89	45.51
	44	**Impact Angle**	13.4	13.2	13.0	12.8	12.7	12.6
		Maximum Deflection	30.45	33.93	40.14	42.12	44.53	47.21
	50	**Impact Angle**	13.4	13.2	13.0	12.9	12.9	12.8
		Maximum Deflection	30.95	34.62	40.92	42.89	46.00	48.70
	56	**Impact Angle**	13.6	13.2	13.0	13.0	12.9	12.9
		Maximum Deflection	31.42	35.24	41.34	43.78	46.27	49.53
	62	**Impact Angle**	13.6	13.2	13.0	13.0	12.9	12.9
		Maximum Deflection	31.87	35.86	41.62	44.56	46.72	50.18

Table 6-2 NCDOT Barrier impact design table for concrete pavement

Impact Angle (degree)/ Maximum Deflection (in)			Design Speed (mph)					
			30	40	50	60	70	80
Offset (ft)	8	Impact Angle	11.1	10.4	9.6	8.7	7.7	6.7
		Maximum Deflection	16.68	17.45	20.21	21.70	24.20	25.74
	14	Impact Angle	12.7	12.1	11.4	10.5	9.3	8.0
		Maximum Deflection	18.43	19.42	22.33	24.05	25.76	28.39
	20	Impact Angle	13.2	12.8	12.2	11.5	10.9	10.3
		Maximum Deflection	21.28	21.70	23.61	25.37	27.51	30.05
	26	Impact Angle	13.3	12.9	12.6	12.0	11.3	10.5
		Maximum Deflection	22.12	23.02	25.22	26.49	29.45	33.27
	32	Impact Angle	13.3	13.0	12.7	12.4	12.1	11.8
		Maximum Deflection	23.24	24.62	26.12	27.98	31.30	34.26
	38	Impact Angle	13.3	13.1	13.0	12.6	12.2	12.0
		Maximum Deflection	23.87	25.36	26.89	29.18	32.32	35.47
	44	Impact Angle	13.4	13.2	13.0	12.8	12.7	12.6
		Maximum Deflection	24.19	25.45	27.04	29.85	33.46	36.12
	50	Impact Angle	13.4	13.2	13.0	12.9	12.9	12.8
		Maximum Deflection	25.11	25.70	27.42	31.24	34.14	36.85
	56	Impact Angle	13.6	13.2	13.0	13.0	12.9	12.9
		Maximum Deflection	25.48	25.80	27.83	31.54	34.51	37.12
	62	Impact Angle	13.6	13.2	13.0	13.0	12.9	12.9
		Maximum Deflection	25.55	26.20	28.16	31.80	35.15	37.34

Table 6-3 ODOT Barrier impact design table for asphalt pavement

Impact Angle (degree)/ Maximum Deflection (in)			Design Speed (mph)					
			30	40	50	60	70	80
Offset (ft)	8	Impact Angle	11.1	10.4	9.6	8.7	7.7	6.7
		Maximum Deflection	10.56	13.51	16.32	17.47	19.68	20.33
	14	Impact Angle	12.7	12.1	11.4	10.5	9.3	8.0
		Maximum Deflection	11.76	15.80	18.70	20.12	22.12	22.98
	20	Impact Angle	13.2	12.8	12.2	11.5	10.9	10.3
		Maximum Deflection	14.25	17.46	20.86	21.76	24.02	25.54
	26	Impact Angle	13.3	12.9	12.6	12.0	11.3	10.5
		Maximum Deflection	15.33	18.53	21.70	22.53	25.92	27.79
	32	Impact Angle	13.3	13.0	12.7	12.4	12.1	11.8
		Maximum Deflection	16.09	18.68	22.80	23.31	27.27	29.60
	38	Impact Angle	13.3	13.1	13.0	12.6	12.2	12.0
		Maximum Deflection	16.23	20.06	23.34	24.78	27.78	30.56
	44	Impact Angle	13.4	13.2	13.0	12.8	12.7	12.6
		Maximum Deflection	16.52	20.87	24.20	25.61	29.29	31.12
	50	Impact Angle	13.4	13.2	13.0	12.9	12.9	12.8
		Maximum Deflection	16.56	21.23	24.72	26.28	29.62	31.43
	56	Impact Angle	13.6	13.2	13.0	13.0	12.9	12.9
		Maximum Deflection	17.19	21.61	25.13	26.79	30.31	31.75
	62	Impact Angle	13.6	13.2	13.0	13.0	12.9	12.9
		Maximum Deflection	17.60	21.81	25.51	27.10	30.68	32.21

Table 6-4 ODOT Barrier impact design table for concrete pavement

Impact Angle (degree)/ Maximum Deflection (in)			Design Speed (mph)					
			30	40	50	60	70	80
Offset (ft)	8	Impact Angle	11.1	10.4	9.6	8.7	7.7	6.7
		Maximum Deflection	9.96	11.08	13.72	14.47	16.13	17.08
	14	Impact Angle	12.7	12.1	11.4	10.5	9.3	8.0
		Maximum Deflection	10.42	12.89	14.56	16.12	16.96	18.31
	20	Impact Angle	13.2	12.8	12.2	11.5	10.9	10.3
		Maximum Deflection	11.35	14.24	16.18	17.13	18.18	20.39
	26	Impact Angle	13.3	12.9	12.6	12.0	11.3	10.5
		Maximum Deflection	12.12	14.51	16.82	18.47	19.66	22.28
	32	Impact Angle	13.3	13.0	12.7	12.4	12.1	11.8
		Maximum Deflection	12.72	15.55	17.42	19.32	20.64	23.08
	38	Impact Angle	13.3	13.1	13.0	12.6	12.2	12.0
		Maximum Deflection	13.08	16.26	17.90	20.08	21.56	23.93
	44	Impact Angle	13.4	13.2	13.0	12.8	12.7	12.6
		Maximum Deflection	13.36	16.52	18.36	20.30	22.63	24.74
	50	Impact Angle	13.4	13.2	13.0	12.9	12.9	12.8
		Maximum Deflection	13.81	16.83	18.66	20.68	22.92	25.15
	56	Impact Angle	13.6	13.2	13.0	13.0	12.9	12.9
		Maximum Deflection	14.19	17.11	18.78	20.94	23.17	25.45
	62	Impact Angle	13.6	13.2	13.0	13.0	12.9	12.9
		Maximum Deflection	14.33	17.36	19.17	21.14	23.58	25.78

Based on the above tables, one can summarize the required barrier offsets, as listed below. It is very important to note that the conditions used for developing the design charts and tables and the following summary need to be the same as those in the crash tests that were used to calibrate the MSC Working Model. For example, wet or dry condition of the pavement may have a significant effect on the deflections. Moreover, the design charts and tables and the following summary are based on the vehicle type used in the crash tests, and could be quite different for heavier vehicles.

1. For North Carolina barriers on asphalt pavements:

    a) For speeds less than 45 mph, with only one lane of traffic, the barrier is not expected to deflect more than 2.5 ft. For roadways with more than one lane of traffic, the barrier could deflect as much as 3.5 ft.

b) For speeds between 45 and 65 mph, with only one lane of traffic, the barrier is not expected to deflect more than 3 ft. For roadways with more than one lane of traffic, the barrier could deflect as much as 4 ft.

c) For speeds greater than 65 mph or conditions different from the crash tests used for calibration of the model, or for a more precise deflection calculation, one may directly consult with the design charts and tables.

2. For North Carolina barriers on concrete pavements:

a) For speeds less than 45 mph, with only one lane of traffic, the barrier is not expected to deflect more than 1.75 ft. For roadways with more than one lane of traffic, the barrier could deflect as much as 2.5 ft.

b) For speeds between 45 and 65 mph, with only one lane of traffic, the barrier is not expected to deflect more than 2 ft. For roadways with more than one lane of traffic, the barrier could deflect as much as 3 ft.

c) For speeds greater than 65 mph or conditions different from the crash tests used for calibration of the model, or for a more precise deflection calculation, one may directly consult with the design charts and tables.

3. For Oregon Tall-F barriers on asphalt pavements:

a) For speeds less than 45 mph, with only one lane of traffic, the barrier is not expected to deflect more than 1.5 ft. For roadways with more than one lane of traffic, the barrier could deflect as much as 2.25 ft.

b) For speeds between 45 and 65 mph, with only one lane of traffic, the barrier is not expected to deflect more than 1.75 ft. For roadways with more than one lane of traffic, the barrier could deflect as much as 2.5 ft.

c) For speeds greater than 65 mph or conditions different from the crash tests used for calibration of the model, or for a more precise deflection calculation, one may directly consult with the design charts and tables.

4. For Oregon Tall-F barriers on concrete pavements:

    a) For speeds less than 45 mph, with only one lane of traffic, the barrier is not expected to deflect more than 1.25 ft. For roadways with more than one lane of traffic, the barrier could deflect as much as 1.75 ft.

    b) For speeds between 45 and 65 mph, with only one lane of traffic, the barrier is not expected to deflect more than 1.5 ft. For roadways with more than one lane of traffic, the barrier could deflect as much as 2 ft.

    c) For speeds greater than 65 mph or conditions different from the crash tests used for calibration of the model, or for a more precise deflection calculation, one may directly consult with the design charts and tables.

Typically, crash tests are conducted for a minimum length of 200 ft of the barriers. As such, regardless of the length of the work zone, a minimum straight length of 200 ft is enforced, i.e., 100 ft on either side of the work zone, excluding tapers. A separate study was carried out using the MSC Working Model to investigate the effect of length of the barrier chain on the maximum deflection of the barriers. Figures 6-5 and 6-6 show the effect of barrier length on the two types of barriers, using all data from the crash tests. The length of barrier chain was varied from 80 ft to 320 ft with 40 ft intervals, since the length of each segment of barrier is 20 ft. The data indicates that the 200 ft is a threshold for stabilizing the barrier deflections, as the curves begin to asymptote around 200 ft length. Therefore, no change in the straight length of need is anticipated. Figure 6-7 schematically shows the length of need.

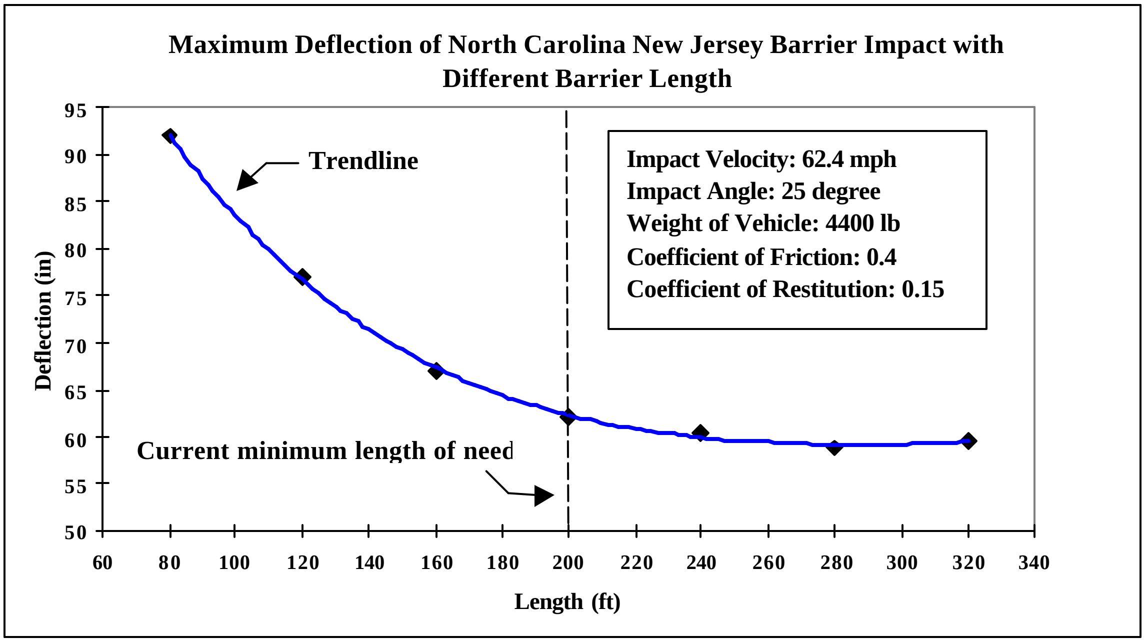

Figure 6-5 Effect of barrier length on the maximum deflection of NCDOT barrier

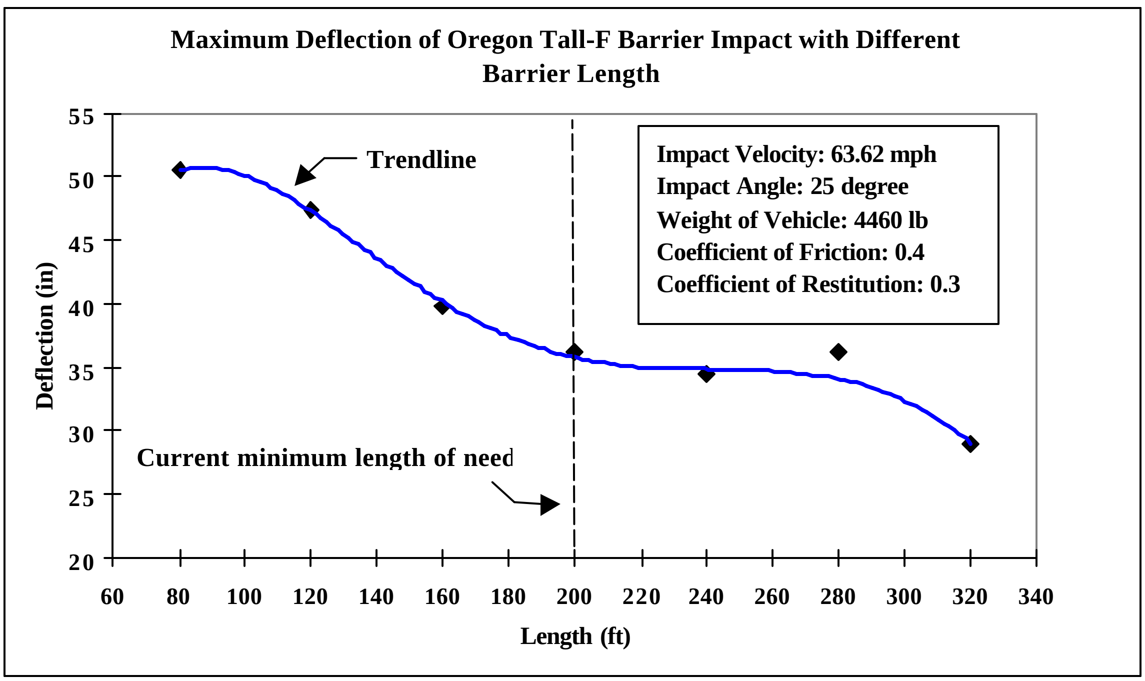

Figure 6-6 Effect of barrier length on the maximum deflection of ODOT barrier

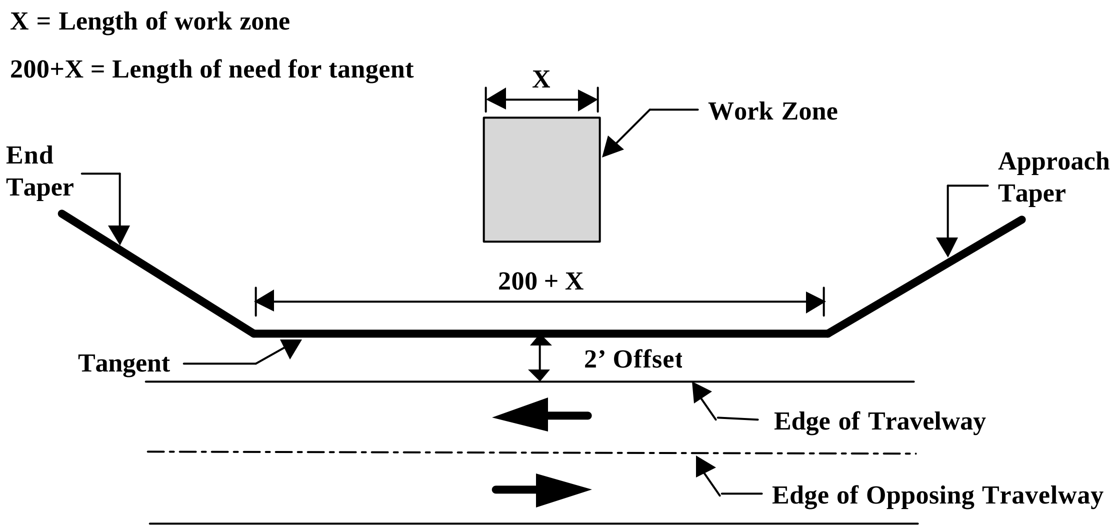

Figure 6-7 Length of Need and Layout of Barriers

7 Summary and Conclusions

In this study the problem of vehicular impact on barriers are thoroughly investigated. The two available crash tests are modeled and impact response simulated through a finite element based program, ANSYS/LS-DYNA. On the basis of the insight gained through these detailed numerical analyses and calibration of essential model parameters, a simpler program, MSC Working Model, is used to perform a comprehensive study of the barriers' response under vehicular impact. This leads to the development of a set of design curves for assessing the barrier displacement and related design variables.

The finite element based modeling and simulation was found to be a very useful tool to study the impact problem under consideration. In addition, the finite element software, ANSYS/LS-DYNA, is found to be an effective tool with adequate capabilities and useful features. Some basic benchmark problems were solved analytically and numerically. The comparison of the results showed a good agreement. Then, with a sense of confidence in ANSYS/LS DYNA, we moved to the actual modeling and simulation of the two crash tests. As far as the maximum displacements of the barrier segments are concerned, for both of the crash simulations, results obtained from finite element study agreed well with the crash tests. Besides, overall behavior of the vehicles and the barriers during the simulations for both of the crash models compared reasonably well with those from the crash tests. Also, from additional studies of the simulation of two crash tests, it was found that the concrete barriers can be treated as rigid bodies. This provided the justification to use the simpler program of MSC Working Model for further analyses and the development of design curves.

The design curves here are developed on the basis of a detailed study of collision between vehicle and the barriers and therefore these are recommended to replace the existing empirical method currently used by NCDOT.

It is very important to note that the conditions used for developing the design charts and tables and the following summary results need to be the same as those in the crash tests that were used to calibrate the models in this study. For example, wet or dry condition of the pavement may have a significant effect on the deflections. Moreover, the design charts and tables and the following summary results are based on the vehicle type used in the crash tests, and could be quite different for heavier vehicles.

1. For North Carolina New Jersey barriers on asphalt pavements:

    a) For speeds less than 45 mph, with only one lane of traffic, the barrier is not expected to deflect more than 2.5 ft. For roadways with more than one lane of traffic, the barrier could deflect as much as 3.5 ft.

    b) For speeds between 45 and 65 mph, with only one lane of traffic, the barrier is not expected to deflect more than 3 ft. For roadways with more than one lane of traffic, the barrier could deflect as much as 4 ft.

    c) For speeds greater than 65 mph or conditions different from the crash tests used for calibration of the model, or for a more precise deflection calculation, one may directly consult with the design charts and tables.

2. For North Carolina New Jersey barriers on concrete pavements:

    a) For speeds less than 45 mph, with only one lane of traffic, the barrier is not expected to deflect more than 1.75 ft. For roadways with more than one lane of traffic, the barrier could deflect as much as 2.5 ft.

    b) For speeds between 45 and 65 mph, with only one lane of traffic, the barrier is not expected to deflect more than 2 ft. For roadways with more than one lane of traffic, the barrier could deflect as much as 3 ft.

    c) For speeds greater than 65 mph or conditions different from the crash tests used for calibration of the model, or for a more precise deflection calculation, one may directly consult with the design charts and tables.

3. For Oregon Tall-F barriers on asphalt pavements:

    a) For speeds less than 45 mph, with only one lane of traffic, the barrier is not expected to deflect more than 1.5 ft. For roadways with more than one lane of traffic, the barrier could deflect as much as 2.25 ft.

b) For speeds between 45 and 65 mph, with only one lane of traffic, the barrier is not expected to deflect more than 1.75 ft. For roadways with more than one lane of traffic, the barrier could deflect as much as 2.5 ft.

c) For speeds greater than 65 mph or conditions different from the crash tests used for calibration of the model, or for a more precise deflection calculation, one may directly consult with the design charts and tables.

4. For Oregon Tall-F barriers on concrete pavements:

    a) For speeds less than 45 mph, with only one lane of traffic, the barrier is not expected to deflect more than 1.25 ft. For roadways with more than one lane of traffic, the barrier could deflect as much as 1.75 ft.

    b) For speeds between 45 and 65 mph, with only one lane of traffic, the barrier is not expected to deflect more than 1.5 ft. For roadways with more than one lane of traffic, the barrier could deflect as much as 2 ft.

    c) For speeds greater than 65 mph or conditions different from the crash tests used for calibration of the model, or for a more precise deflection calculation, one may directly consult with the design charts and tables.

8 References

1. ANSYS Inc., (2004) "ANSYS 8.1 User's Guide"

2. Appel, H., Lutter, G., Sigmund, T., (1994), "Crash tests for passenger cars and their relationship to the actual accident occurrence", Nuclear Engineering and Design , 150, pp. 473-481.

3. Araujo, M., Mirmiran, A. and Rahman, S., (2003), "Traffic barrier deflections under vehicular impact" The report to Department of North Carolina State University

4. Cagliostro, D. J., Mandell, D. A., Schwalbe, L. A., Adams, T. F. and Chapyak, E. J., (1990), MESA 3D, calculations of armor penetration by projectiles with combined obliquity and yaw." Int. J. Imp. Eng., Vol. 10, pp. 351-360.

5. Consolazio, G. R., Chung, J. H., Kurtis, R. G., (2001), "Development of a low profile work zone barrier using impact finite element simulation" University of Florida Research Report.

6. Dienes, J. K., Walsh, J. M., (1973), "The theory of impact: general principles and the method of calculation in Eulerian coordinates", In High-velocity impact phenomena, pp. 48-111, Mir, Moscow.

7. Eskandarian, A., Marzougui D., Gaith A., and Bedewi, N.E., (1995), "Computer simulation of roadside hardware using LS-DYNA3D", Presented at the International IEMS Conference, Cocoa beach, FL.

8. Felippa, C. A., (1978), "Iterative procedures for improving penalty function solutions of algebraic systems", Int. J. Numer. Meth. Engng., **12**, 821-836.

9. Glocker, C., (2004), "Concepts for modeling impacts without friction", Acta Mechanica Vol. 168, pp. 1-19.

10. Huang, M., (2002), "Vehicle crash mechanics", CRC Press LLC N.W. Florida

11. Hughes, G., (1984), "Hard missile impact on reinforced concrete", Nuclear Engineering and Design, pp. 23-35.

12. Hunek, I. (1993), “On a penalty formulation for contact-impact problems”, Computer & Structures Vol. 48, No. 2, pp. 193-203.

13. Jewel, J., Weldon, G., (1999), “Compliance crash testing of K-rail used in semi-permanent installations”, State of California Department of Transportation Engineering Service Center Technical Report, FHWA/CA/OR-99/07.

14. Kan, C.D., Qi, G.Z, and Yang, J.C.S., (1990), “Error analysis of linear and non-linear system identification”, Proceedings of 8th International Modal Analysis Conference, Kissimmee, Florida, Published by IMSL/SME, vol. II, pp 1403-1409.

15. Kirkpatrick, S. W., (2000), “Development and validation of high fidelity vehicle crash simulation models”, Computer Applications for Crash, Optimization and Simulation Research Technical Paper.

16. Kistler, L. S., Waas, A. M., (1998), “Experiment and analysis on the response of curved laminated composite panels subjected to low velocity impact”, Int. Jour. Impact Eng. Vol. 21, No. 9, pp. 711-736.

17. Lin, Y.Y., and Kan, C.D., (1998), “Crash simulation on parallel multiprocessors”, Proceedings of Fifth International LS-DYNA3D Conference, Detroit, MI, section N, paper # 3.

18. Lin, Y.Y., and Kan, C.D., (2000), “A performance study of LS-DYNA on vehicle crash simulation”, Proceedings of 6th International LS-DYNA Users Conference 2000, pp17-17 to 17-24, April, 2000, Detroit, Michigan.

19. Livermore Software Technology Corporation., (2001), “LS-DYNA Keyword User’s Manual Version 960”, Vol. 1.

20. Livermore Software Technology Corporation.,, (2001), “LS-DYNA Keyword User’s Manual Version 960”, Vol. 2.

21. Livermore Software Technology Corporation.,, (2001), “LS-DYNA Keyword User’s Manual Version 970”

22. Livermore Software Technology Corporation, (2002), “LS-PREPOST - V.1.0, User’s Manual”

23. Livermore Software Technology Corporation, (1998). “LSDYNA Theoretical Manual.”

24. Logan, R. W., Tokarz F. J., (1993), “Overview of crash and impact analysis at Lawrence Livermore national laboratory”, ASME Winter Annual Meeting SERAD Emerging Technology Session New Orleans, LA.

25. Nour-Omid, B., Wriggers, P., (1986), “A two-level iteration method for solution of contact problems”, Computer Methods in Applied Mechanics & Engineering. 54, pp. 131-144.

26. MacDonald D. J. and Kirk A. R., (2001), “Precast concrete barrier crash testing final report”, Oregon Department of Transportation

27. Marklund, P. O., Nilsson, L., (2001), “Optimization of a car body component subjected to side impact”, Struc. Multidis. Optim. Vol. 21, pp. 383-392.

28. Marzougui, D.H., Eskandarian, A., Bahouth, G.T., Taylor, H., (2000), “Evaluation of portable concrete barriers using finite element simulation”, Journal of the Transportation Research Board, Transportation Research Record 1729-Paper No. 00-0501.

29. Marzougui, D., Kan, C.D., and Eskandarian, A., (2000), “Evaluation of safety performance of roadside hardware using computer simulation”, Proceedings of ACSE, Austin, Texas.

30. Marzougui, D., Kan, C.D., Eskandarian, A., and Meczkowski, L., (1999), “Finite element simulation and analysis of portable concrete barrier using LS-DYNA”, Proceedings of the Second European LS-DYNA Users Conference 1999, section I, paper #3, pp I19-I26, Gothenburg, Sweden.

31. McDevitt, Charles, F., (2000), “Basics of Concrete Barriers,” Public Roads. Turner-Fairbank Highway Research Center, Federal Highway Administration, McLean, VA. Vol.63, No.5.

32. McGlaun, J.M., Thompson, S. L. and Elrick, M.G., (1990), “CTH: a three dimensional shock wave physics code”, Int. J. Imp. Eng., Vol. 10, pp.351-360.

33. Merzhievsky, L. A., Resnyansky, A. D., (1995), "The role of numerical simulation in the study of high-velocity impact", Int. Journal Impact Eng. Vol. 17, pp. 559-570.

34. Mirmiran, A., Rahman, S., Rizkalla, S., (2002), "Research proposal traffic barrier deflections under vehicular impacts to NCDOT.

35. Mizzi, J. P., Jezequel, L., (1992), "Identification of a crash model", Journal of Sound and Vibration, Vol. 159, No. 1, pp. 57-83.

36. MSC/Working Model Manual, Version 5.0, The MacNeal-Schwendler Corporation, 1999

37. Rahman, M. S., Xu, Q., (2002), "Portable concrete barriers", North Carolina State University Department of Civil Engineering Research Project Report.

38. Ross, H.E. Jr., Sicking, D.L., Zimmer R.A., Michie J. D., (1993), "Recommended Procedure for the Safety Performance Evaluation of Highway Features", National Cooperative Highway Research Program Report 350: Transportation Research National Academy Press Washington D.C.

39. Tabiei, A. Wu, J., (1997), "Roadmap for crashworthiness finite element simulation of roadside structures", Department of Aerospace Engineering and Engineering Mechanics, University of Cincinnati.

40. Tornambe, A., (1996), "Modelling and controlling one-degree-of-freedom impacts" IEE Proc. Control Theory Appl. Vol. 143, No.1, pp. 85-90.

41. Tornambe, A. (1996), "Modelling and controlling one-degree-of-freedom impacts under elastic and plastic deformations" IEE Proc. Control Theory Appl. Vol. 143, No.5, pp. 470-476.

42. Wilkins, M. L., (1967), "Calculation of elasto-plastic flows", pp. 212-263, Mir, Moscow

43. Wriggers, P., Miehe, C., (1994), "Contact constraints within coupled thermo-mechanical analysis - A finite element model", Computer Methods in Applied Mechanics & Engineering. **113**, pp. 301-319

44. Wriggers, P., Vu Van, T. and Stein, E., (1990), "Finite element formulation of large deformation impact-contact problems with friction", Computers & Structures Vol. 37, No. 3, pp. 319-331

45. www.nafems.org, "Computational Simulations for Safer Roads."

46. www.ncac.gwu.edu "National Crash Analysis Center"

47. Yonten, K., Manzari, M. T., Eskandarian, A., Marzougui, D., (2002), "An evaluation of constitutive models of concrete in LS-DYNA finite element code", 15th ASCE Engineering Mechanics Conference, Columbia University, New York.

48. Zaouk, A. K., Nabih, E. B., Cing Dao, K., Hnasjoerg, S., (2002), "Evaluation of a multi-purpose pickup truck model using full scale crash data with application to highway barrier impacts" Technical report for FHWA/NHTSA National Crash Analysis Center.

49. Zaouk, A. and Marzougui, D., (2001), "Development and validation of a US side impact moveable deformable barrier FE model", Third European LS-DYNA Conference, Paris, France, June.

50. Zaouk, A. K., Nabih, E. B., Cing Dao, K., Marzougui, D., (1996), "Development and evaluation of a C-1500 pickup truck model for roadside hardware impact simulation" Technical report for FHWA/NHTSA National Crash Analysis Center.

APPENDICES

APPENDIX A:

COMPARISON OF FINITE ELEMENT RESULTS AND CRASH TESTS FOR NCDOT SIMULATION

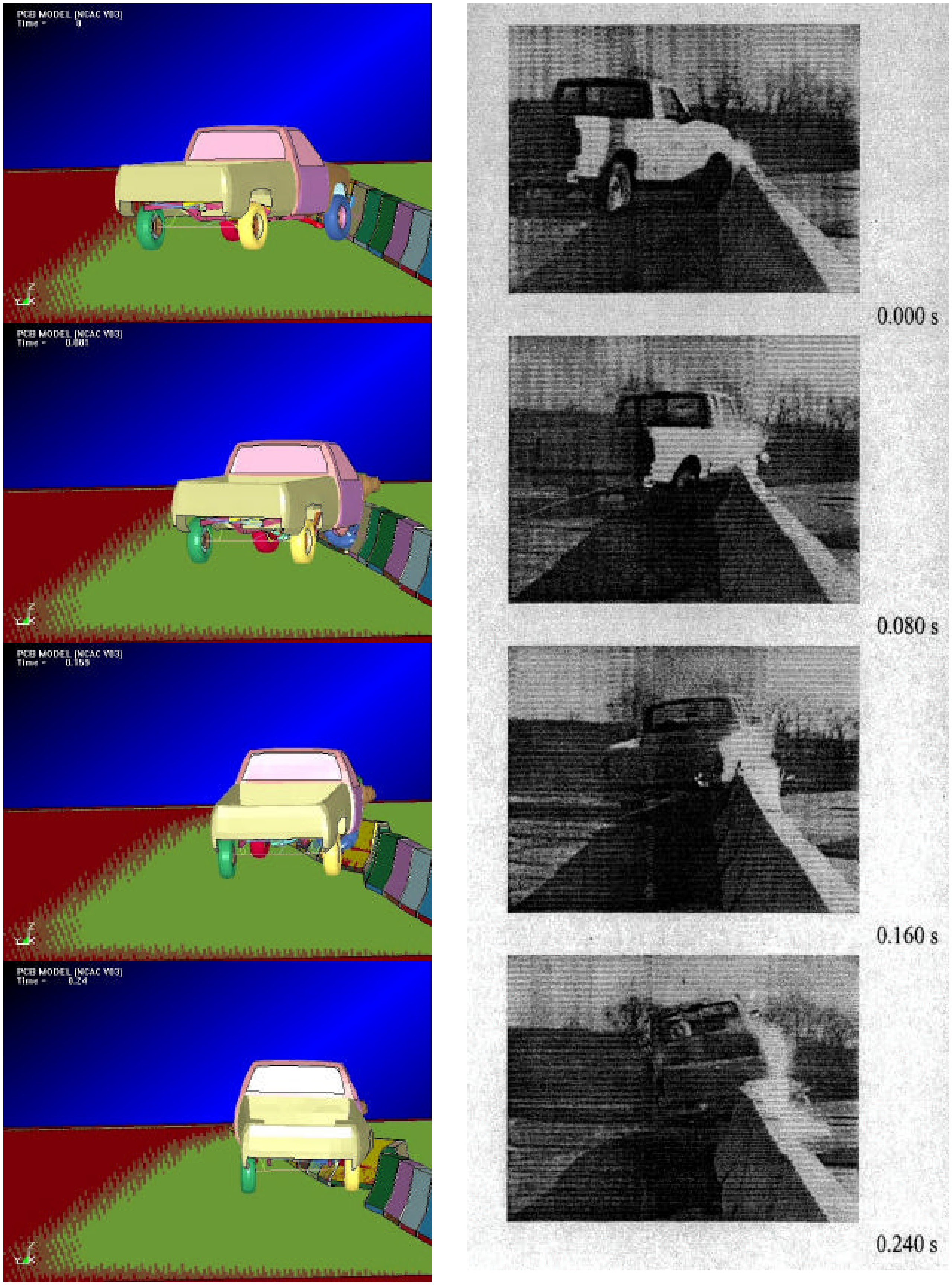
0.000 s
0.080 s
0.160 s
0.240 s

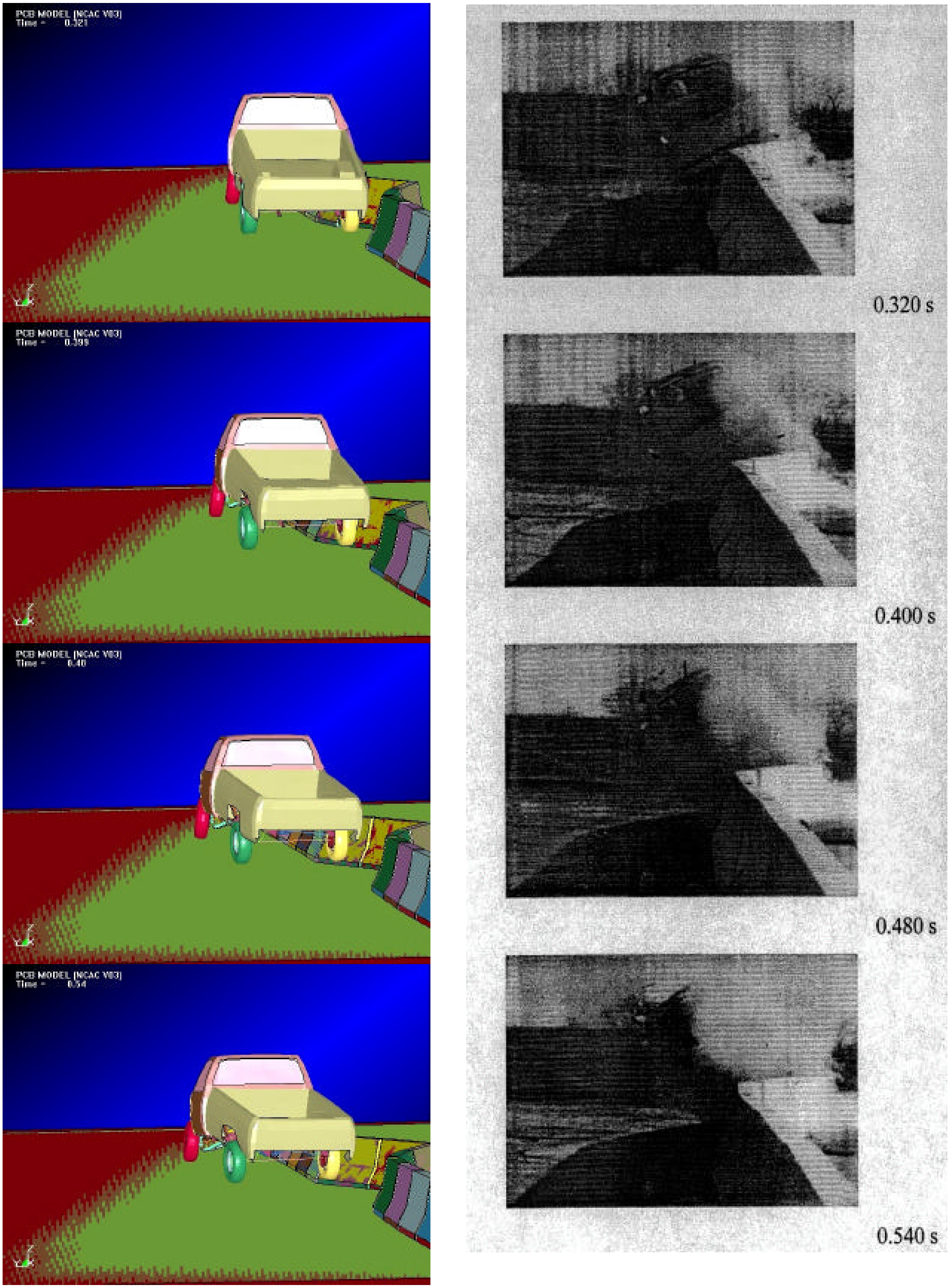
0.320 s
0.400 s
0.480 s
0.540 s

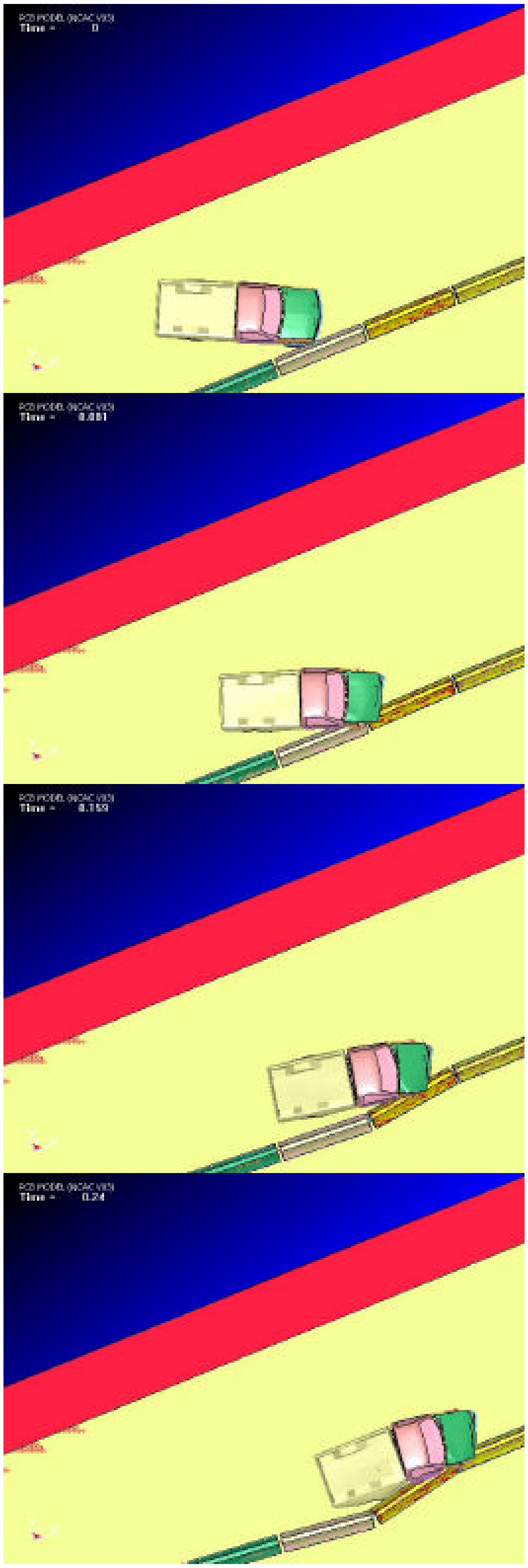

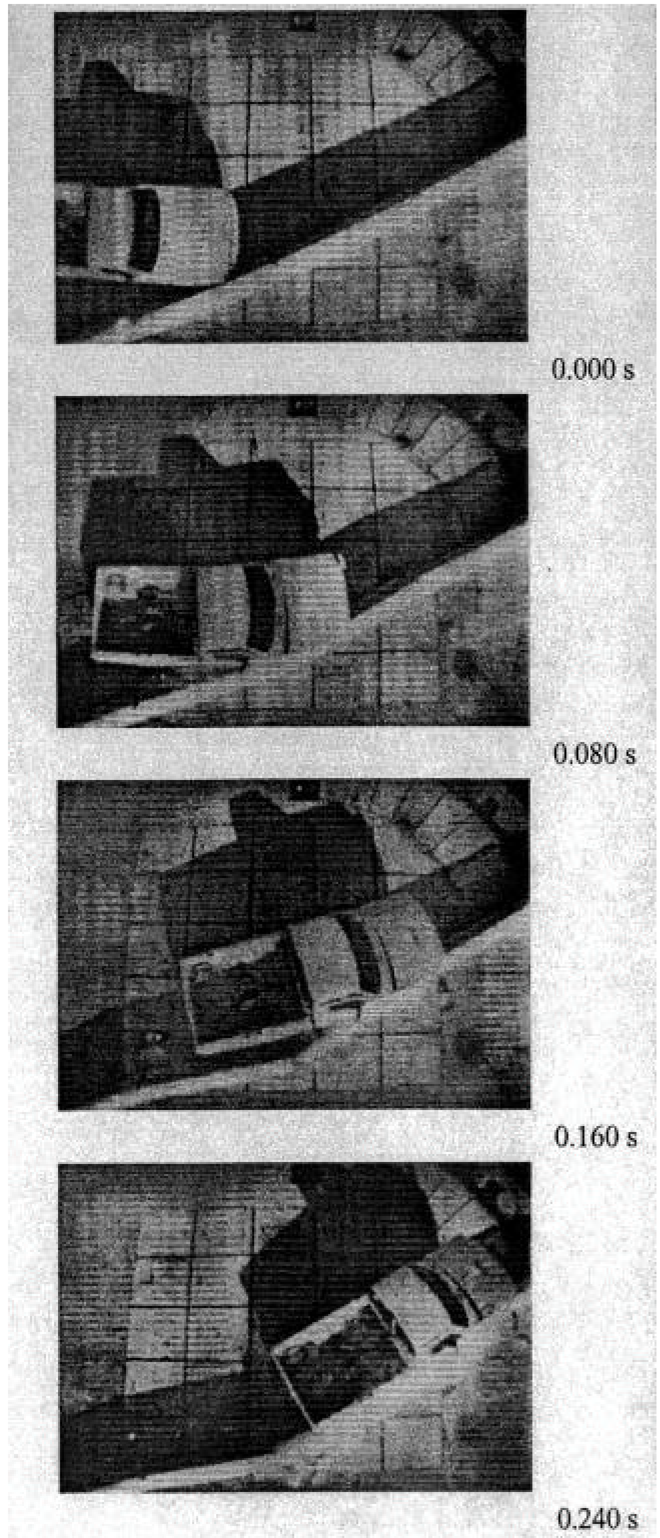
0.000 s
0.080 s
0.160 s
0.240 s

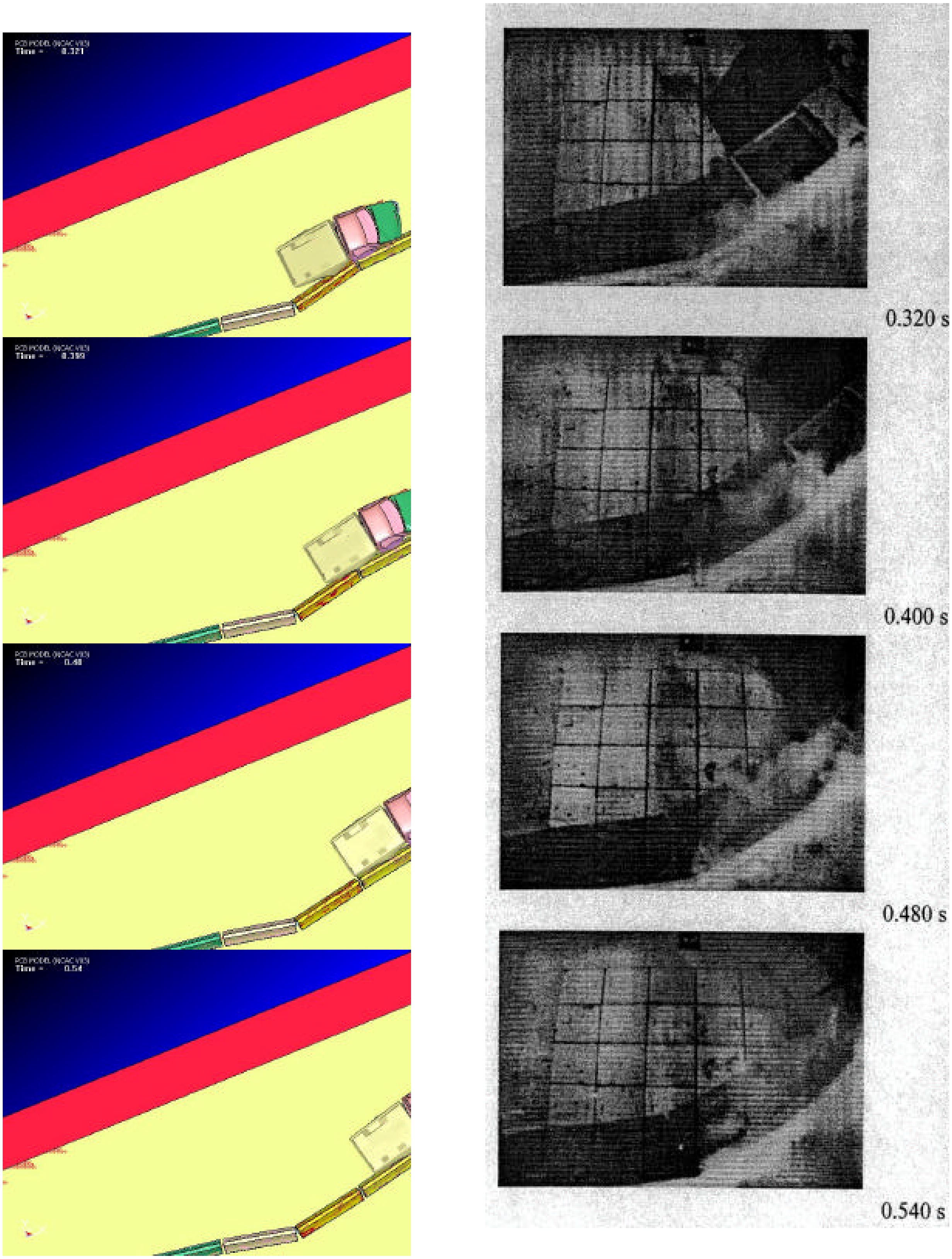
0.320 s
0.400 s
0.480 s
0.540 s

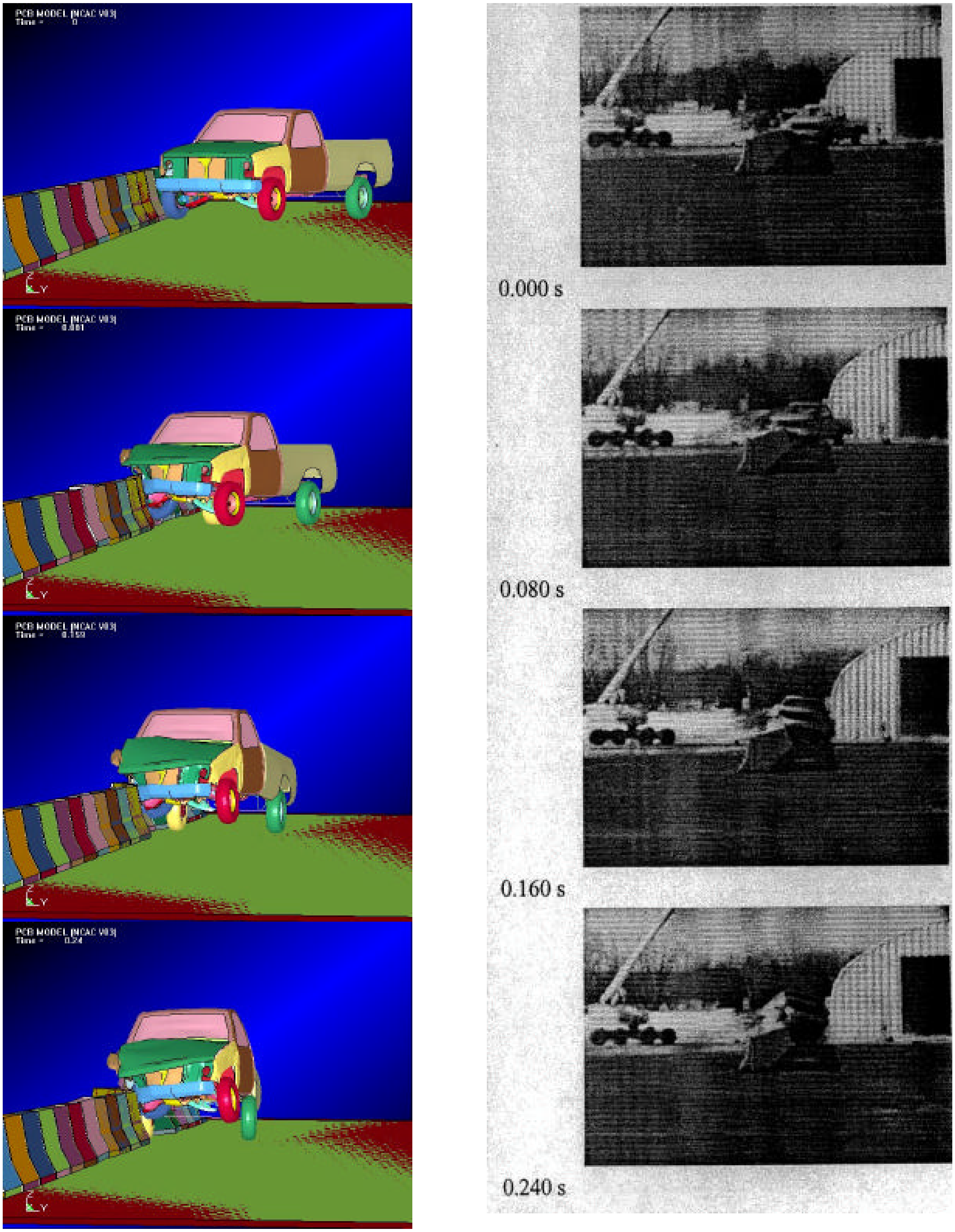
0.000 s
0.080 s
0.160 s
0.240 s

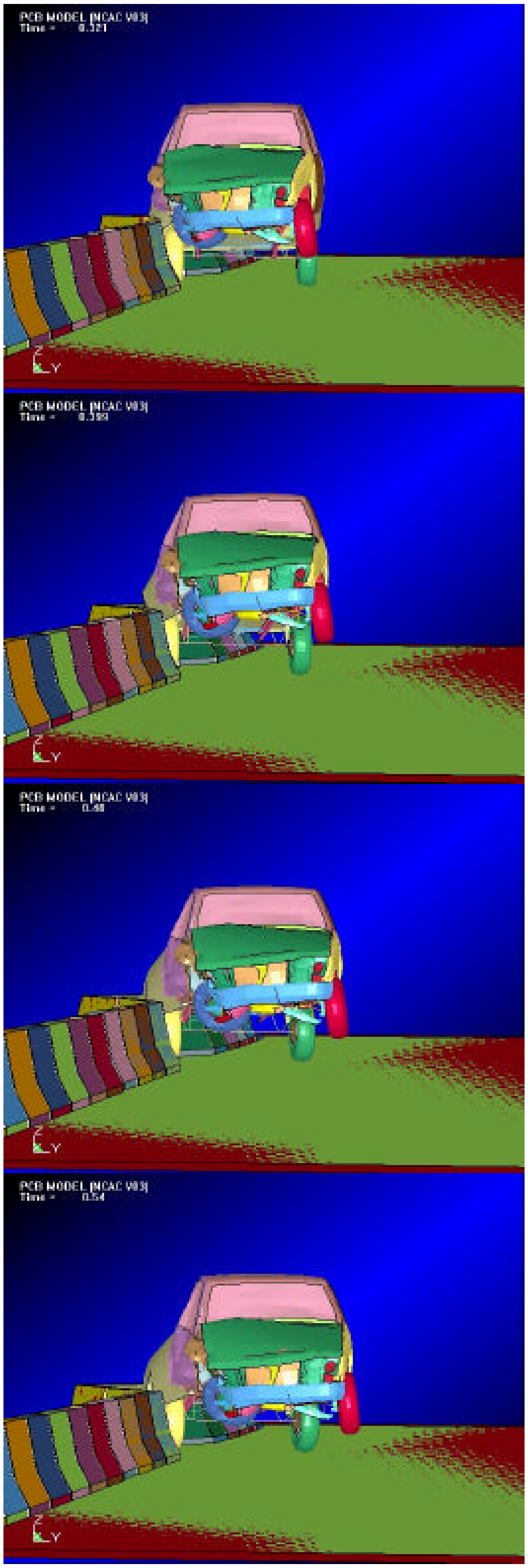

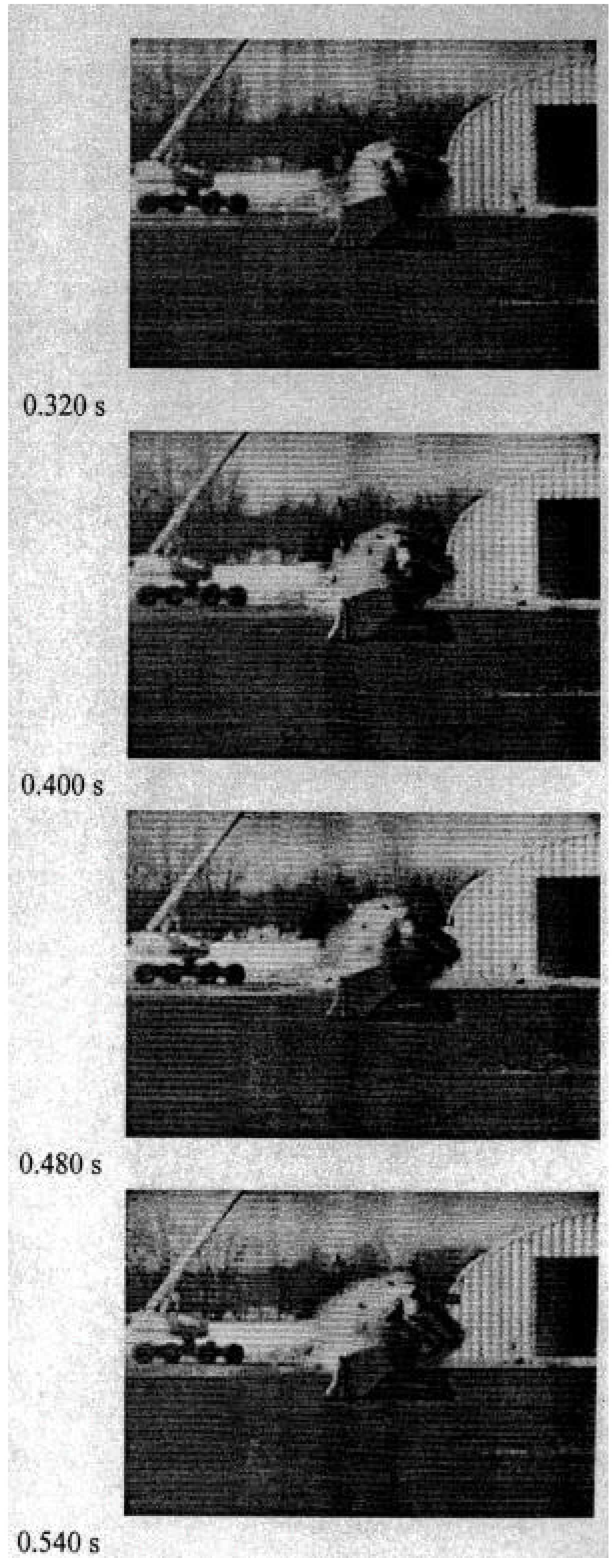
0.320 s
0.400 s
0.480 s
0.540 s

APPENDIX B:
ANIMATIONS OF THE FINITE ELEMENT SIMULATIONS OF CRASH TESTS

SIMULATION OF ORIGINAL NCDOT F-TYPE PCB - FORD F-250 PICKUP TRUCK CRASH TEST

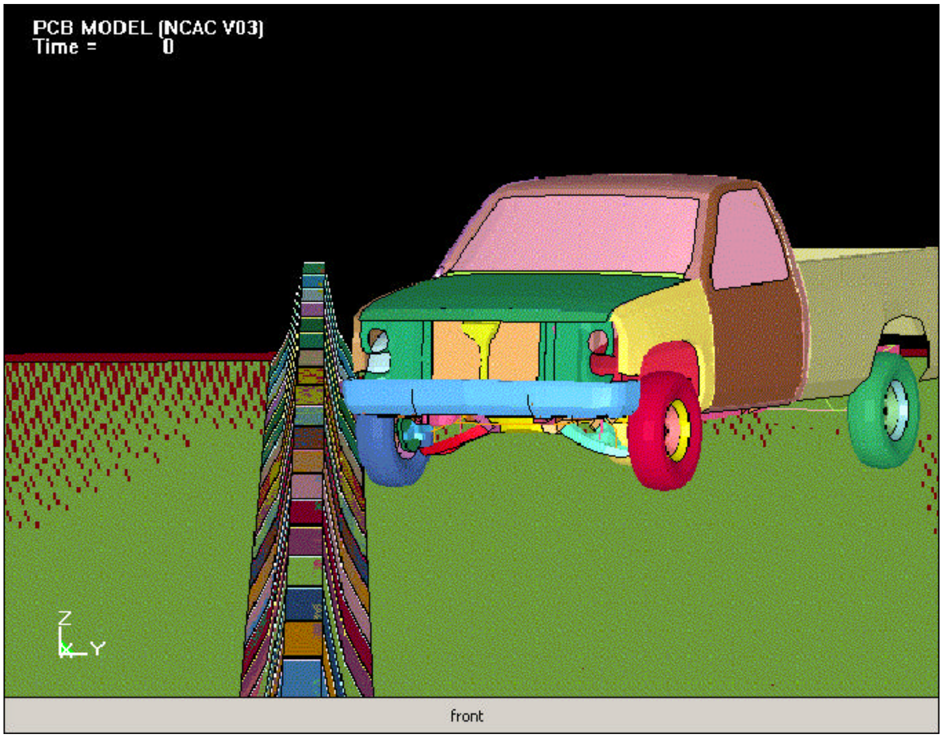

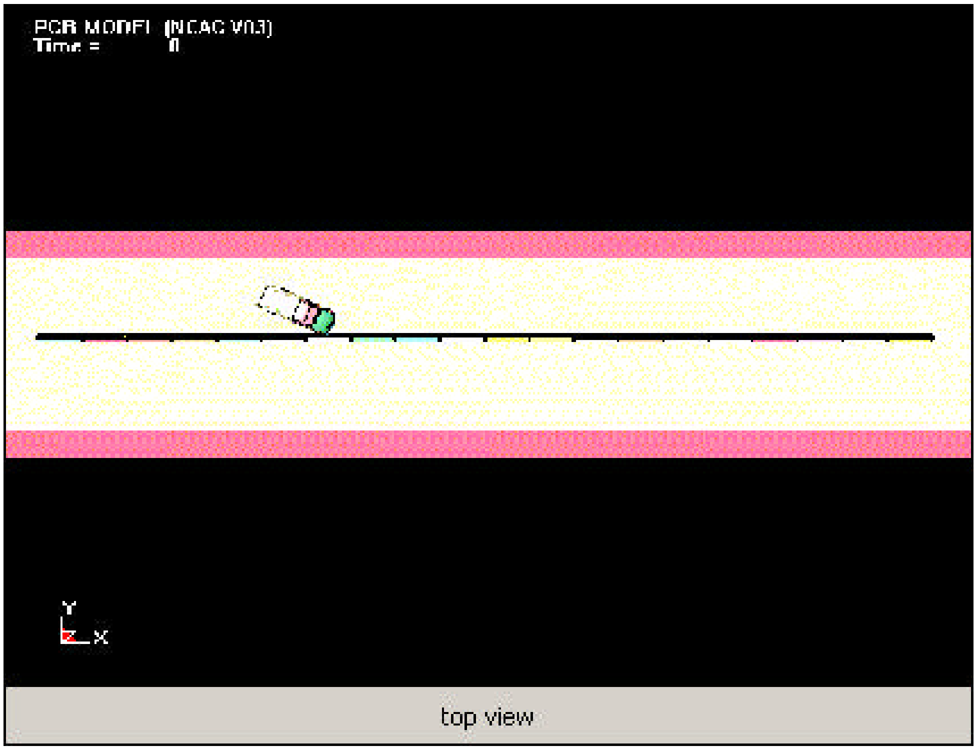

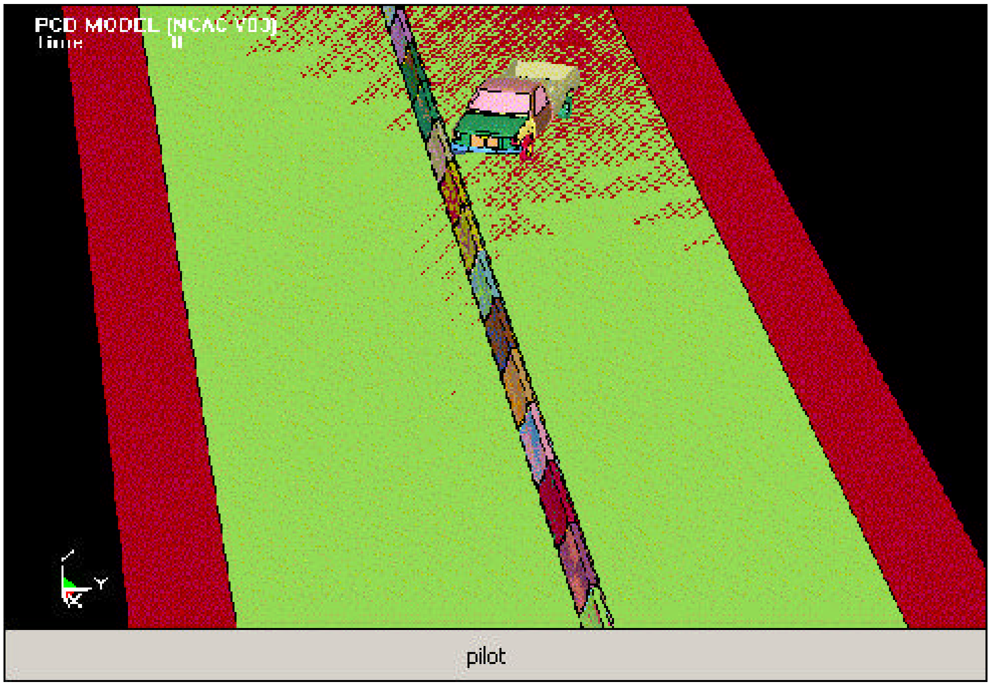
PCB MODEL (NCAC V03)
Time = 0
Y
X
pilot

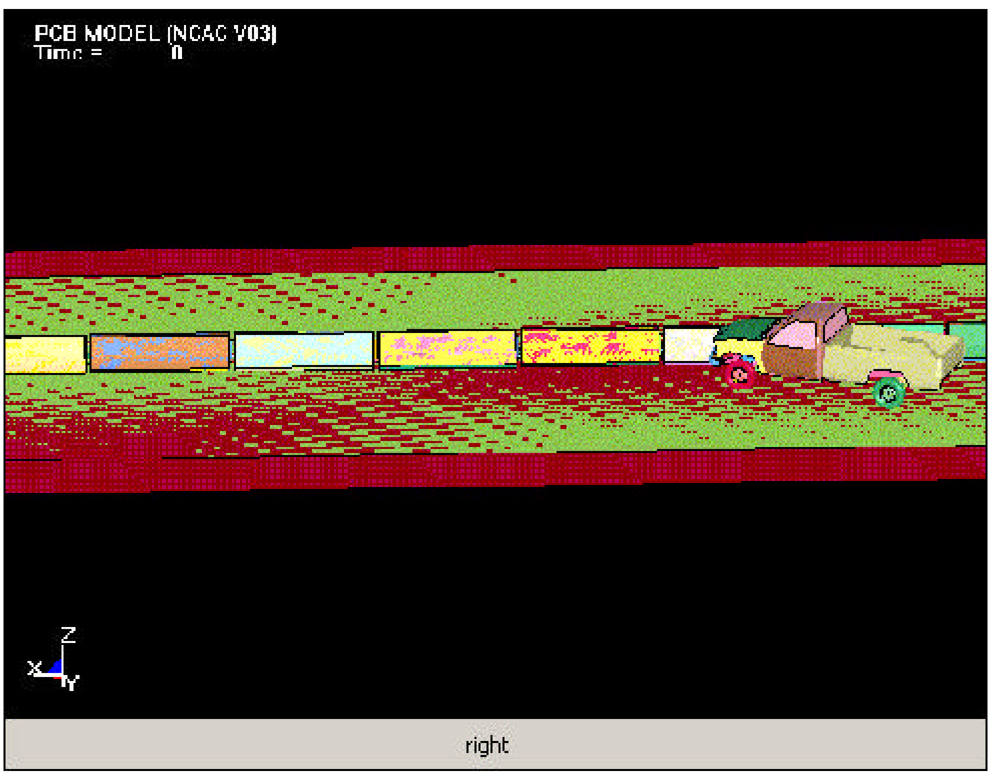
PCB MODEL (NCAC V03)
Time = 0
Z
X
Y
right

SIMULATION OF ORIGINAL ODOT F-TYPE PCB - CHEVROLET C2500 PICKUP TRUCK CRASH TEST

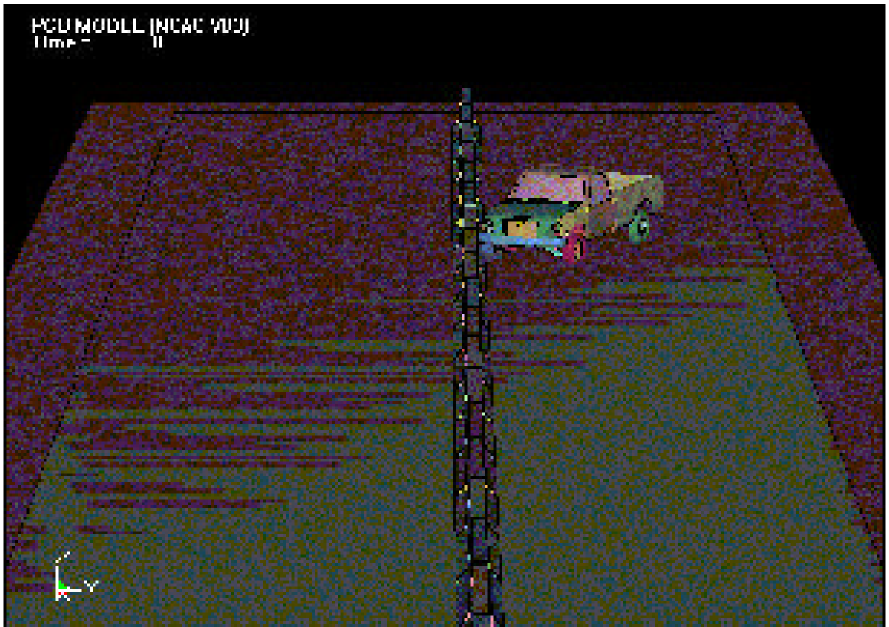

Front View

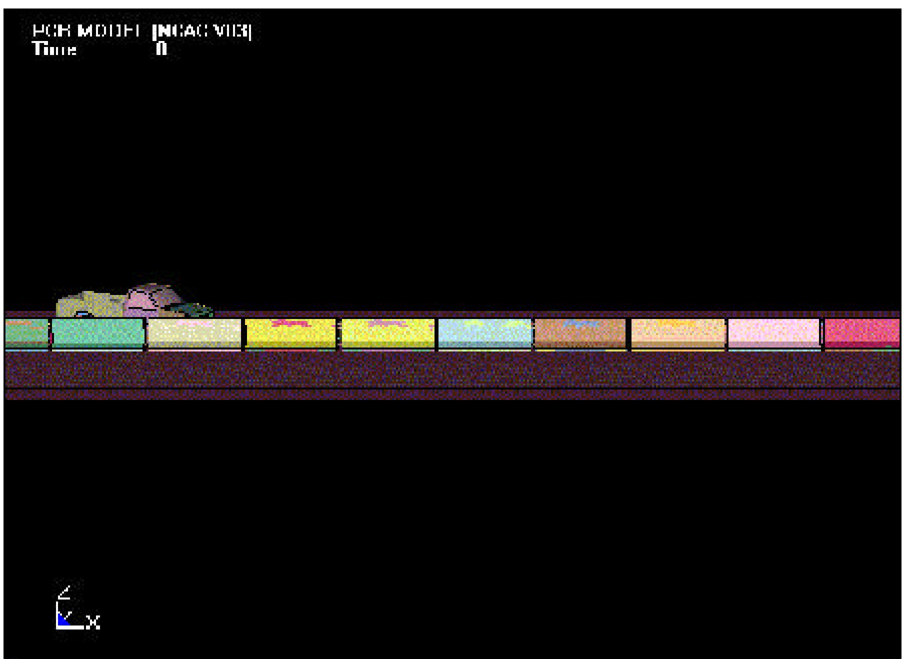

Left View

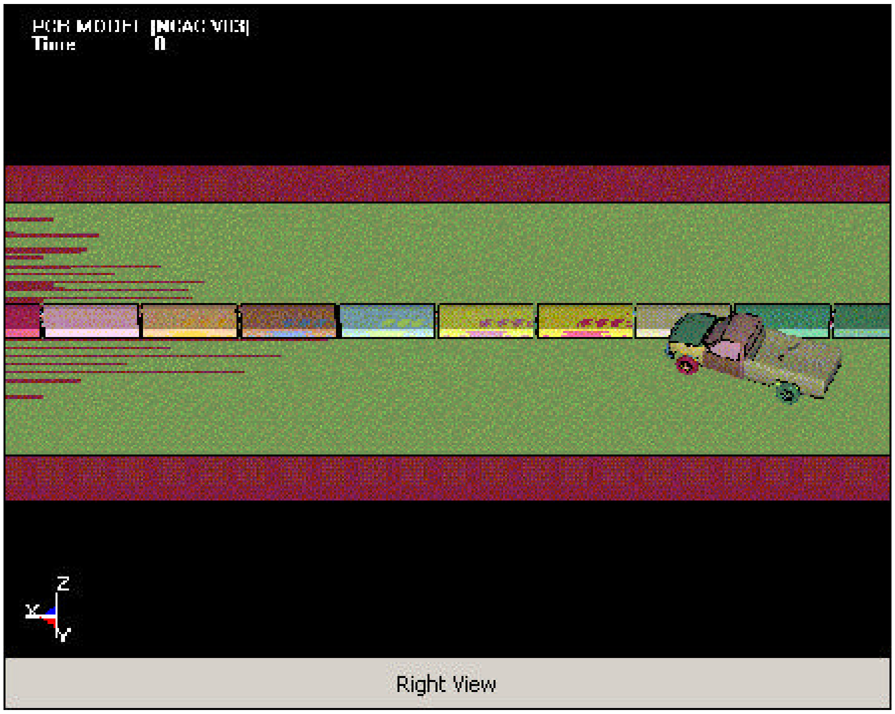
PCB MODEL [NCAC V03]
Time 0
Right View

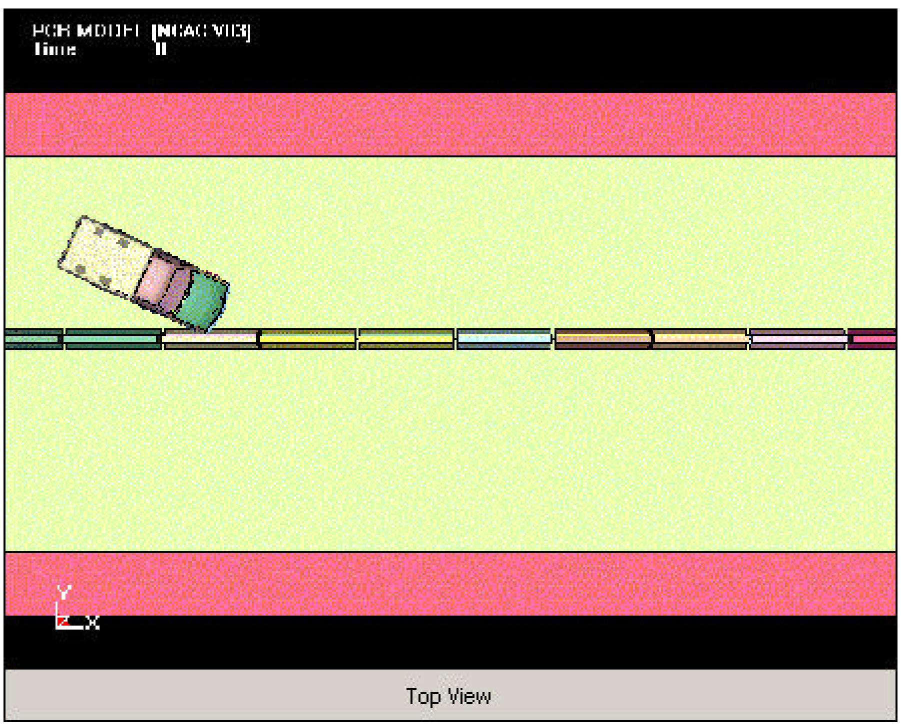
PCB MODEL [NCAC V03]
Time 0
Top View